AD-A090 799 JOHNS HOPKINS UNIV BALTIMORE MD DEPT OF MATERIALS SC--ETC F/G 14/2
ULTRASONIC AND ACOUSTIC EMISSION DETECTION OF FATIGUE DAMAGE.(U)
JUL 80 S R BUXBAUM, C L FRIANT, S E FICK F44620-76-C-0081
UNCLASSIFIED AFOSR-TR-80-1069 NL

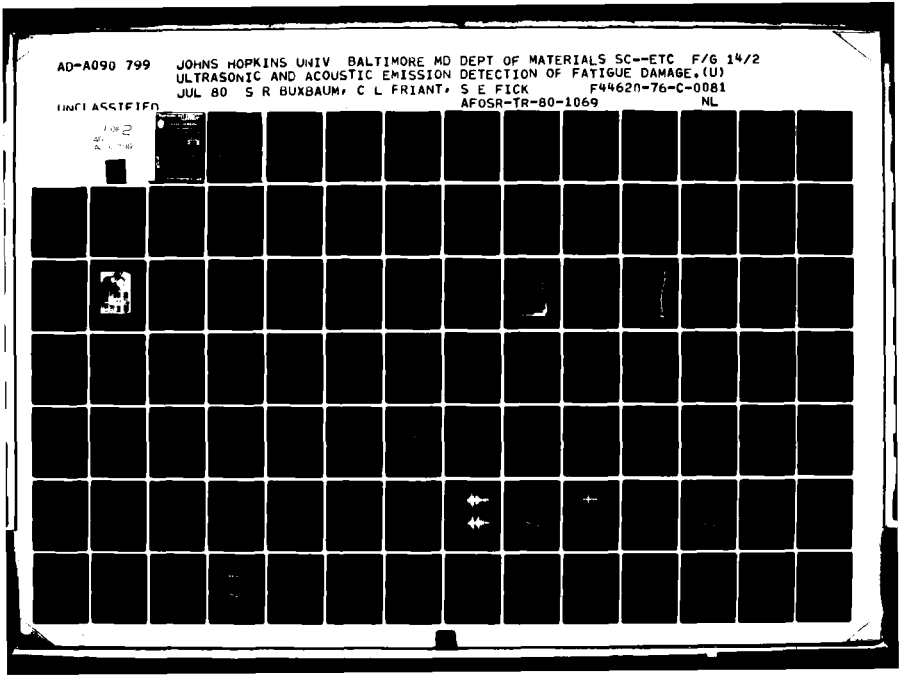

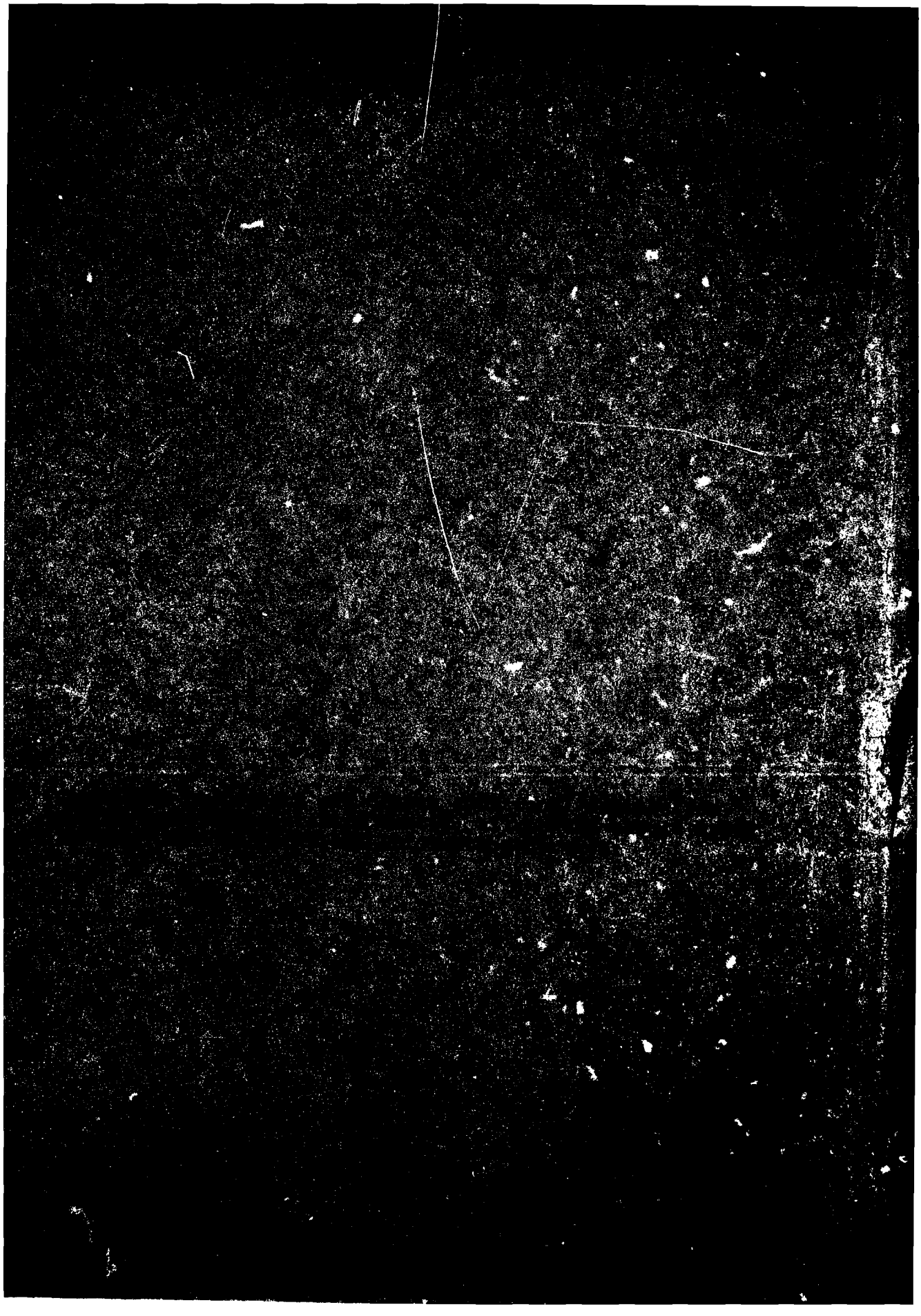

UNCLASSIFIED

SECURITY CLASSIFICATION OF THIS PAGE (When Data Entered)

REPORT DOCUMENTATION PAGE

READ INSTRUCTIONS BEFORE COMPLETING FORM

REPORT NUMBER	2. GOVT ACCESSION NO.	3. RECIPIENT'S CATALOG NUMBER
AFOSR-TR-80-1069	AD-A090 799	

4. TITLE (and Subtitle)

ULTRASONIC AND ACOUSTIC EMISSION DETECTION OF FATIGUE DAMAGE

5. TYPE OF REPORT & PERIOD COVERED: FINAL rept. MAR. 1, 1976 - MAY 31, 1980

6. PERFORMING ORG. REPORT NUMBER: 1 Mar 76 - 31 May 80

7. AUTHOR(s)

S. R. BUXBAUM, C. L. FRIANT, S. E. FICK, R. E. GREEN, Jr.

8. CONTRACT OR GRANT NUMBER(s): F44620-76-C-0081

9. PERFORMING ORGANIZATION NAME AND ADDRESS

JOHNS HOPKINS UNIVERSITY
MATERIALS SCIENCE & ENGINEERING DEPT.
BALTIMORE, MARYLAND 21218

10. PROGRAM ELEMENT, PROJECT, TASK AREA & WORK UNIT NUMBERS: 2307 B2, 61102F

11. CONTROLLING OFFICE NAME AND ADDRESS

AIR FORCE OFFICE OF SCIENTIFIC RES/NA
BUILDING 410, BOLLING AIR FORCE BASE
WASHINGTON, D.C. 20332

12. REPORT DATE: July 1980

13. NUMBER OF PAGES: 109 (12) 120

14. MONITORING AGENCY NAME & ADDRESS (if different from Controlling Office)

(10) Sanford R. Buxbaum
Carl Lee Friant
Steven E. Fick
Robert E. Green, Jr.

15. SECURITY CLASS. (of this report): UNCLASSIFIED

15a. DECLASSIFICATION/DOWNGRADING SCHEDULE

16. DISTRIBUTION STATEMENT (of this Report)

APPROVED FOR PUBLIC RELEASE; DISTRIBUTION UNLIMITED

17. DISTRIBUTION STATEMENT (of the abstract entered in Block 20, if different from Report)

18. SUPPLEMENTARY NOTES

19. KEY WORDS (Continue on reverse side if necessary and identify by block number)

ULTRASONIC ATTENUATION
ACOUSTIC EMISSION
NONDESTRUCTIVE TESTING
FATIGUE
EDDY CURRENT
METALLOGRAPHY

New

411 193

20. ABSTRACT (Continue on reverse side if necessary and identify by block number)

This report is a summary of research activities performed under Air Force Office of Scientific Research Contract No.F44620-76-C-0081 for the period March 1, 1976 through May 31, 1980. The primary purpose of the research was to optimize existing ultrasonic and acoustic emission techniques and to investigate new ones for early detection of fatigue damage in aluminum alloys used in aircraft construction. Ultrasonic attenuation

DD FORM 1473 EDITION OF 1 NOV 65 IS OBSOLETE

UNCLASSIFIED

measurements made simultaneously with fatigue tests on aluminum alloy bar, and sheet specimens gave warning of crack formation and imminent fracture much earlier than conventional ultrasonic methods. An ultrasonic pulse-echo system was used during fatigue cycling to record conventional A-scan waveforms as well as to monitor ultrasonic attenuation. In addition, acoustic emission signals were recorded simultaneously with the ultrasonic measurements on each test specimen using two different acoustic emission systems. The correlation of evidence of cumulative fatigue damage and acoustic emission data was approached by the use of long term true-rms averaging of the system output and frequency domain analysis of acoustic emission signals recorded at selected intervals throughout the test. The integrity of the data was verified by independent electronic testing of the instrumentation. Visual and in situ eddy current inspection, and optical and scanning electron microscopy were used to correlate acoustic emission and ultrasonic attenuation data to the physically deformed microstructure.

Ultrasonic and Acoustic Emission Detection of Fatigue Damage

FINAL TECHNICAL REPORT

(March 1, 1976 - May 31, 1980)

Air Force Office of Scientific Research

Contract No. F44620-76-C-0081

July 1980

Presented by: S. R. Buxbaum, C. L. Friant, S. E. Fick
and R. E. Green, Jr.
The Johns Hopkins University
Baltimore, MD 21218

Submitted to: Air Force Office of Scientific Research/NA
Building 410
Bolling Air Force Base, D.C. 20332

TABLE OF CONTENTS

Ultrasonic and Acoustic Emission Detection of Fatigue Damage

S. R. Buxbaum, C. L. Friant, S. E. Fick, and R. E. Green, Jr.
Materials Science & Engineering Department
The Johns Hopkins University
Baltimore, Maryland 21218

ABSTRACT

This report is a summary of research activities performed under Air Force Office of Scientific Research Contract No. F44620-76-C-0081 for the period March 1, 1976 through May 31, 1980. The primary purpose of the research was to optimize existing ultrasonic and acoustic emission techniques and to investigate new ones for early detection of fatigue damage in aluminum alloys used in aircraft construction. Ultrasonic attenuation measurements made simultaneously with fatigue tests on aluminum alloy bar, and sheet specimens gave warning of crack formation and imminent fracture much earlier than conventional ultrasonic methods. An ultrasonic pulse-echo system was used during fatigue cycling to record conventional A-scan waveforms as well as to monitor ultrasonic attenuation. In addition, acoustic emission signals were recorded simultaneously with the ultrasonic measurements on each test specimen using two different acoustic emission systems. The correlation of evidence of cumulative fatigue damage and acoustic emission data was approached by the use of long term true-rms averaging of the system output and frequency domain analysis of acoustic

emission signals recorded at selected intervals throughout the test. The integrity of the data was verified by independent electronic testing of the instrumentation. Visual and in situ eddy current inspection, and optical and scanning electron microscopy were used to correlate acoustic emission and ultrasonic attenuation data to the physically deformed microstructure.

LIST OF ILLUSTRATIONS

INTRODUCTION

Under the sponsorship of the Air Force Office of Scientific Research, Contract No. F44620-76-C-0081, a study has been made of various methods of nondestructively detecting the onset of fatigue damage in aluminum alloys by use of ultrasonic, acoustic emission, and electromagnetic techniques. This report is a summary of the progress made in these areas since the research was initiated in 1976. A systematic comparison of techniques involving the detection of reflected ultrasonic surface and body waves, and techniques involving the measurement of ultrasonic attenuation and acoustic emission showed that, for the early detection of fatigue damage, the reflection techniques are surpassed by those involving ultrasonic attenuation and acoustic emission[1].

Initially, ultrasonic attenuation measurements were made simultaneously with fatigue tests on aluminum rectangular bar specimens. These measurements gave warning of crack initiation and imminent fracture much earlier that conventional body wave reflection techniques. This behavior was exhibited by defect-free specimens as well as specimens initially containing induced latent defects. Our previous reports[2-7] have documented the success of ultrasonic attenuation methods of detecting fatigue damage.

Acoustic emission was chosen for investigation because of its complementarity to the other techniques under study and because of its applicability to fatigue testing of aluminum [6-32]. Inititally the acoustic emission experiments of this

research were combined with tensile tests. Since uniaxial tensile loading causes an easily-described deformation and introduces less mechanical noise into the specimen than does fatigue(cyclic) loading, it was assumed that acoustic emission signals resulting from tensile deformation might be more readily characterized. Tensile tests were performed on various aluminum alloys in order to compare acoustic emission monitoring with ultrasonic attenuation monitoring as indicators of microstructural alterations due to tensile deformation. Both ultrasonic attenuation and acoustic emission measurements were made simultaneously during tensile elongation of "dogbone" shaped test specimens of 1100-H, 6061-T6, 2024-T3, and 7075-T651 aluminum. The results of these experiments showed that for all four alloys acoustic emissions above the background level occur almost exclusively before yield and reach maximum activity at approximately 3% strain. Ultrasonic attenuation changes occurred after yield, with periods of most rapid change appearing just after yield and at the beginning of load drop.

After the responses of acoustic emission and ultrasonic attenuation in aluminum subjected to simple uniaxial tension had been studied, and some correlations found, the research was focused on the more complex case of fatigue loading. Acoustic emission and ultrasonic attenuation measurements were performed simultaneously during fatigue testing of specimens of aluminum alloys possessing compositions and geometries typical of actual

aircraft components. The purpose of these measurements was to determine the range of applicability of the two methods to the testing of actual aircraft parts. Acoustic emission measurements were successfully made only after steps were taken to eliminate the excessive noise caused by the fatigue machine.

In the meantime, fatigue tests were run on 7075-T6 aluminum specimens in the forms of plain sheets and sheets embodying fasteners in patterns similar to those of rivets in aircraft. Ultrasonic attenuation measurements were continuously monitored during the fatigue cycling of these specimens. The specimen thickness(1/16") necessitated the use of a modified Lucite wedge to appropriately "launch" the ultrasonic waves inside the sheet specimen. Results of this study on 7075-T6 aluminum sheet specimens indicated that continuous monitoring of the change in ultrasonic attenuation provides warning of fatigue damage with approximately 10% of the fatigue life remaining.

The next set of fatigue tests involved bar-shaped specimens of 7075-T651 and 7075-W(solution treated) aluminum. The true root-mean-square(rms) voltage output of an acoustic emission system loaned by the Admiralty Materials Laboratory (now Admiralty Marine Technology Establishment) was continuously recorded, as was the ultrasonic attenuation signal. Both signals provided early warning of fatigue damage at about 80% of the fatigue life for the 7075-T651 specimens and even earlier

for the solution-treated specimens. Additionally, differences observed in the acoustic emission signals indicated that the microscopic deformation mechanisms generating acoustic emission during tensile deformation of 7075 aluminum are not the same as those causing fatigue deformation.

In the most recent experiments, the rectangular bar shaped speciments were modified to a "T" shape. This was done to incorporate in situ eddy current scanning for verification of the presence of surface breaking fatigue cracks while still permitting simultaneous ultrasonic attenuation monitoring and acoustic emission monitoring by two separate commercial units during fatigue testing. Various alloys, heat treatments, and surface preparations were tested to study their effect on acoustic emission and ultrasonic attenuation response. Different bending stress amplitudes were used to study the effect on ultrasonic attenuation and acoustic emission behavior.

Several changes were made in the experimental set-up to improve both system flexibility and ultrasonic attenuation and acoustic emission sensitivity to fatigue damage. Set-point and rate-of-rise cutoff circuits were installed to stop the fatigue test when predetermined ultrasonic attenuation criteria were met. One ultrasonic attenuation system was electronically multiplexed to accomodate two fatigue tests(ultrasonic attenuation changes were sufficiently slow to allow time-sharing). It was found that a change in specimen temperature could have

a significant effect on the attenuation so the temperature of each specimen was monitored continuously during the test.

Unlike ultrasonic attenuation measurements, acoustic emission measurements are adversely affected by extraneous machine noise. For this reason, the test specimen was acoustically isolated. Independent electronic testing of acoustic emission transducers and amplifiers was necessary to determine how acoustic emission bursts were "colored" by the detection system. Using knowledge of acoustic emission system frequency response, time and frequency domain analysis assisted in discrimination between acoustic emission signals generated by various structural defects and the signals caused by extraneous noise sources during fatigue cycling. This type of analysis was also used to characterize burst emissions from specimens containing a fatigue crack under both static and dynamic loading. With a fatigue crack present, the capability of monitoring acoustic emissions from selected portions of the load cycle proved beneficial in separating emissions due to crack propagation from those due to crack wall rubbing. Finally, the acoustic emission and ultrasonic attenuation data were compared with the physically deformed microstructure near cracks in partially failed specimens, and fracture surfaces in failed specimens using optical and scanning electron microscopy.

ULTRASONIC ATTENUATION

Background

It has been well established that the continuous monitoring of ultrasonic attenuation can serve to assess evolving fatigue damage in aluminum and its alloys [1-7, 14, 26-48]. This is because fatigue and ultrasonic attenuation in a material are affected by a similar set of internal and external variables [46]. In general, greater fatigue damage in a material is accompanied by higher attenuation of ultrasonic waves. In order to obtain early detection of fatigue damage, the monitoring of ultrasonic attenuation has advantages over other potentially-useful ultrasonic techniques. For example, schemes involving the observation of a new ultrasonic reflection corresponding to a nascent crack require that the crack have both sufficient size and proper orientation to reflect enough ultrasonic energy to be detected. Since measurements of attenuation can effectively spatially average over the entire specimen, small and diffuse microstructural changes, such as those due to plastic deformation, can readily be detected. The inevitable precedence of gradual diffuse damage to the formation of such discrete defects as cracks provides the potential of attenuation measurements to give earlier warning than the aforementioned alternative methods.

The measurement of ultrasonic attenuation in specimens simultaneously subjected to cyclic loading is not hindered by the large amount of acoustical noise caused by the mechanical

loading apparatus. The effects of unwanted noise can be completely eliminated by appropriate electronic filtering. Such filtering is more readily implemented and more effective than that required, say, for acoustic emission work. The signal processing is made easier by the fact that ultrasonic attenuation is measured using, at predetermined instants of time, pulses of radio frequency(rf) energy whose frequency spectra are known and far different from the spectra of typical noise sources.

The greatest limitations to the use of ultrasonic attenuation for materials characterization result from the complex nature of ultrasonic wave propagation in solid media. The conversion of ultrasonic energy between the various possible modes of propagation must be avoided by the choice of an appropriate specimen geometry if unequivocal measurements are to be made; arbitrarily shaped specimens cannot be tested. Further, considerable a priori information is necessary since different mechanisms can similarly affect ultrasonic measurements. Results presented later in this report delineate the potential of ultrasonic attenuation used within these limitations.

Instrumentation

The ultrasonic attenuation system used in the present work is composed of a Matec Model 6600 pulser-receiver, with a Model 950B rf plug-in and a Model 2470A attenuation recorder. The attenuation recorder includes a time gate

permitting selection of any two echoes from the received wave train, automatic gain control to stabilize the amplitude of the echoes, and circuitry to obtain the logarithm of the ratio of the amplitudes of the two selected echoes. The application of rf pulses to the specimen was synchronized with the fatigue loading cycle by the use of an optical pick-up from the rotating shaft of the fatigue machine. This assured stability in the recorded data by avoiding beat frequency effects associated with random pulsing. A variable delay interposed between the optical trigger and the pulser-receiver allowed attenuation to be measured at any desired point in the load cycle.

ACOUSTIC EMISSION

Background

One of the consequences of the application of stress sufficient to activate the various deformation mechanisms in a material can be the generation of elastic waves. Critical to the future development of acoustic emission as a tool for materials characterization is the hypothesis that the acoustic emissions from distinct deformation mechanisms are uniquely distinguishable. Difficulties both theoretical and practical have precluded the unequivocal linking of causative mechanisms and associated elastic waves, with very few exceptions [49]. However, it has long been known that useful information, such as the stress history or the present condition of a specimen can sometimes be inferred from the time and frequency of occurrence of acoustic emission "events", rather than from any distinguishing features of the emitted waves themselves. Although it cannot be used to assess the state of damage, the occurrence of an acoustic emission event indicates that additional damage has ensued. Since propagation effects such as mode conversion can be ignored to the extent that knowledge of waveform details is unimportant, acoustic emission can in some cases be used with specimen geometries too complicated to allow the measurement of ultrasonic attenuation. In this research, propagational effects had to be taken into account in the choice of specimen geometry since the examination of acoustic emission waveform details was to be attempted.

Instrumentation

The acoustic emission systems used in this research were an Admiralty Materials Laboratory(AML) Type 3 Acoustic Emission Amplifier and a Trodyne Model 7500-4 Acoustic Emission Source Location System. Although both systems were equipped for event counting, independent proof of performance testing of the instruments was limited to the analog circuitry since the research did not involve event counting. Frequency response was measured both for the amplifier sections alone and for the complete systems including transducers. The amplifier section tests were made using a Hewlett Packard 310A Wave Analyzer to drive the amplifier input through a suitable termination. The frequency response of each complete system was measured by driving its transducer with an acoustical signal generated by a second transducer excited by the wave analyzer. The frequency response of the system transducer and the second transducer were independently measured electrically. The output broadband noise voltage with no input voltage applied, i.e. the noise floor, of each system was measured with the Fluke 8920A true rms voltmeters used to measure the acoustic emission levels during fatigue tests. The transducers were electrically coupled but acoustically isolated for the noise floor tests.

AML Acoustic Emission System

The AML unit was the less complicated of the two acoustic emission systems used. The transducers supplied with the unit

consisted of a small cube of PZT-8(lead zirconate titanate), with a primary resonance at 400 kHz, mounted in a brass housing containing an rf matching transformer. A Mu metal and copper screen cable was provided to carry the low level acoustic emission input signal to an 18 dB preamplifier contained in the main amplifier cabinet. The bandwidth is constant over the available gains of 60-100 dB since the gain is increased by switching in additional 10 dB stages. Electrical frequency response tests showed that the bandwidth is reduced and modulated by transducer resonances. The rms noise floor voltage, over a bandwidth of 20 MHz varied from 2.6 mV at 60 dB gain to 210 mV at 100 dB gain, which is consistant with the design of the unit. Since the maximum rms voltage swing at the analog output pack is 1 volt, the available dynamic range varies from 30 dB at 60 dB to 14 dB at 100 dB gain. The available dynamic range is completely adequate for event counting; since these evaluation experiments involved precision analog measurements care had to be taken to maintain sufficient gain while avoiding overload.

Trodyne Acoustic Emission System

The Trodyne Model 7500-4 AE source location system utilized a small 10 dB preamplifier module to minimize the effects of the coaxial cable connecting the transducer to the preamplifier input. The system has provisions for time discrimination and event counting procedures for source localization, although these features were not needed in the present

work. The electrical frequency response of the main amplifier at various gains, measured with none of the available bandpass filters in use is shown in Fig. 1. Figure 2 shows both the frequency response of the system, again with no filtering, connected to a Panametrics Type AE-01-2 transducer (solid line) and the response of the Panametrics transducer and test circuit (broken line). The gradual increase in transducer response with increasing frequency is largely an artifact of the test circuit used. The sharp excursions indicate characteristic transducer resonances. Thus, Fig. 2 shows that the receiving transducer causes considerable coloration of the frequency response. The available bandpass filters have excellent slope and rejection characteristics. The rms noise floor measured 40 mV regardless of system gain indicating that the system performance was not limited by the preamplifier, but by later stages of amplification.

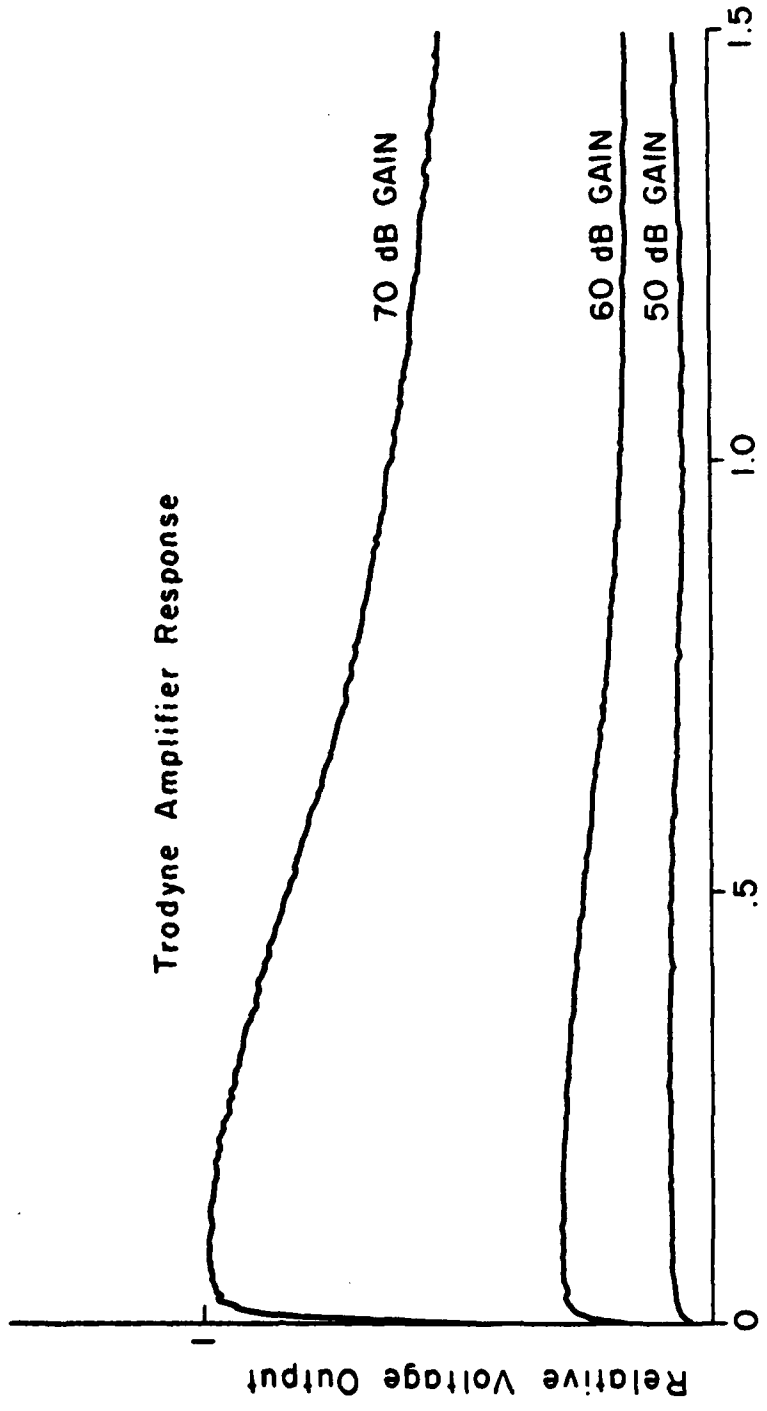

FIGURE 1. FREQUENCY RESPONSE OF TRODYNE AMPLIFIER

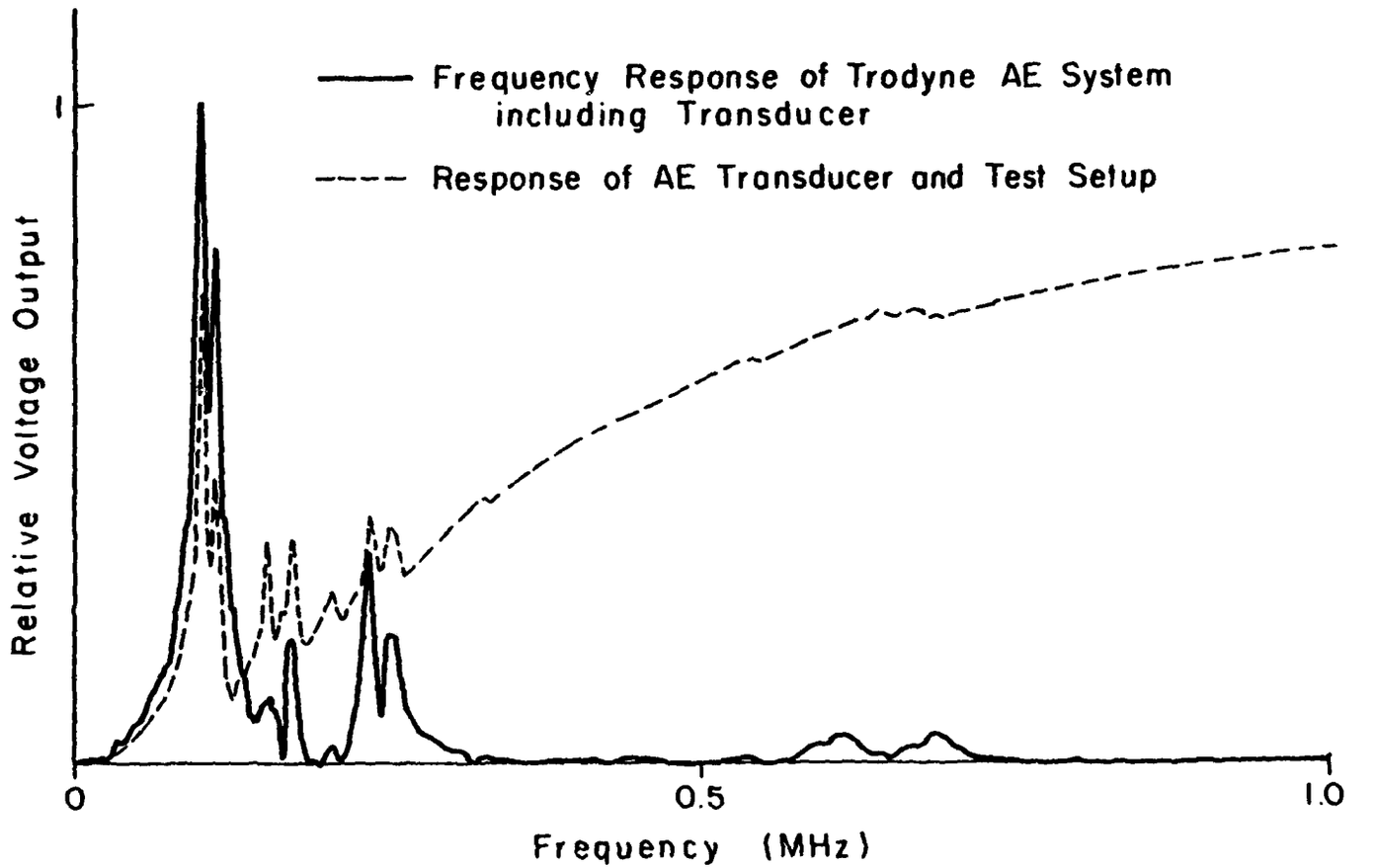

FIGURE 2. FREQUENCY RESPONSE OF TRODYNE SYSTEM

SPECIALIZED INSTRUMENTATION

The ultrasonic attenuation and acoustic emission systems were combined in several different ways during the course of this study. Most of the data was obtained with these systems time-shared between two fatigue machines operating simultaneously. The long duration of many of the fatigue tests provided ample motivation for the development of customized electronics to maximize the information gathered by the available ultrasonic equipment. In addition to multiplexing the ultrasonic equipment, the specially designed electronics served to stop either fatigue test when its data met pre-established criteria. This allowed such occurrences as crack initiation to be conveniently investigated by staff members. Where necessary other specialized circuitry was constructed to synchronize various tests with the operation of the fatigue machines.

A block diagram of the fatigue damage detection experiment showing electrical connections between components is shown in Fig. 3. A photograph showing the arrangement of the experimental apparatus is presented in Fig. 4. A multichannel strip chart recorder (Leeds and Northrup Speedomax 250 Series), used to record all analog data, provides a synchronizing signal to the controller and the cut-off circuitry. The controller generates the proper sequence of operations for the attenuation system; the cut-off circuitry removes the ac power to

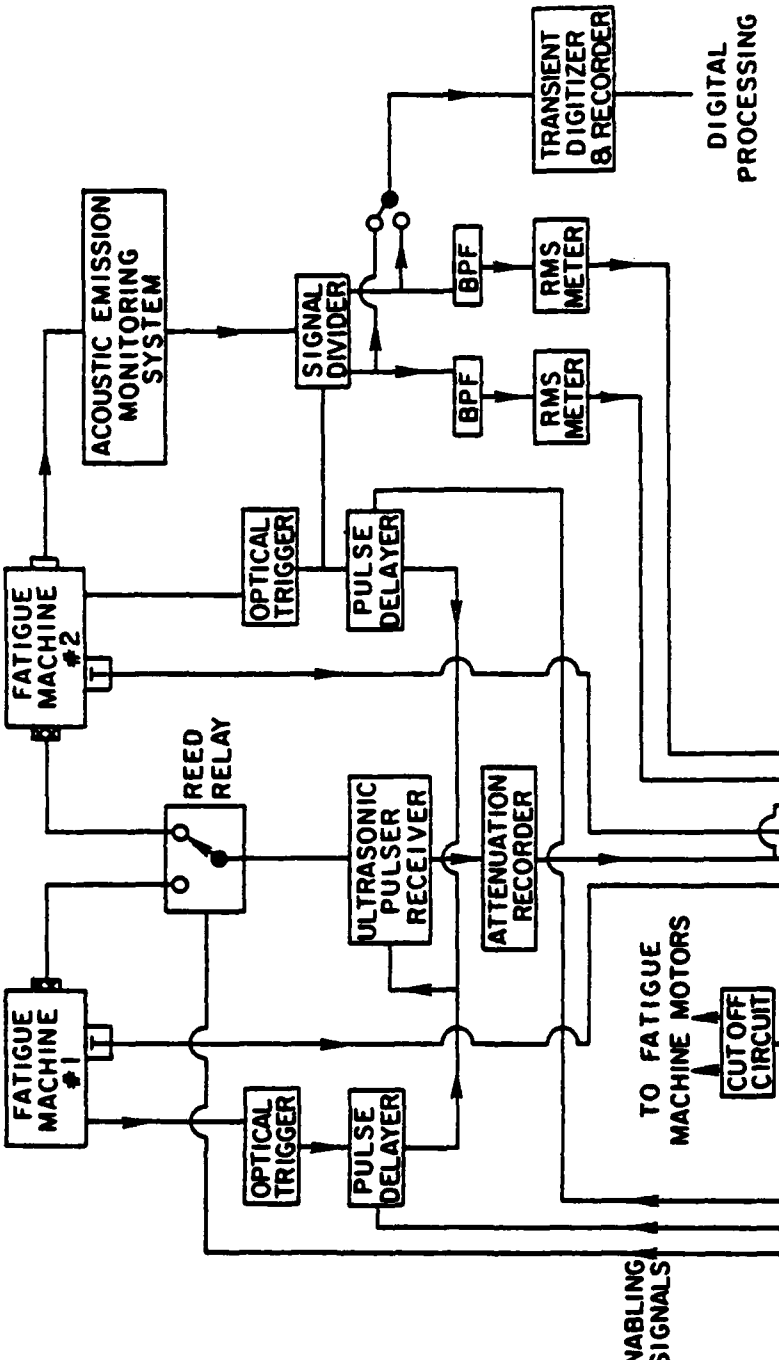

FIGURE 3. FATIGUE DAMAGE DETECTION EXPERIMENT

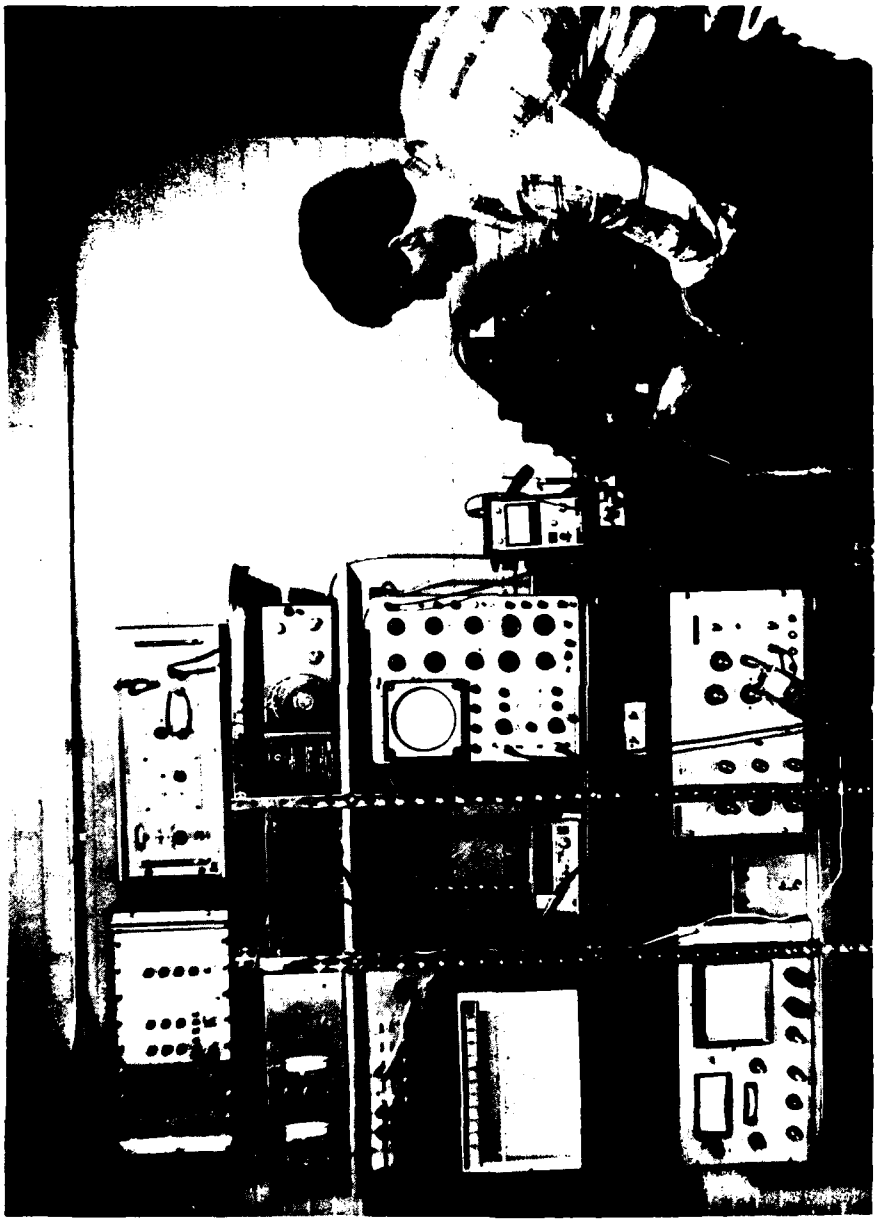

FIGURE 4. ARRANGEMENT OF EXPERIMENTAL APPARATUS

either fatigue machine when the attenuation for its specimen exhibits appropriate changes (of either rate-of-rise or absolute value). The attenuation system is turned on or off by the application or removal of synchronizing signals from the appropriate optical pick-up; the use of independent pulse delayers for each fatigue machine allows independent choice of the point in the load cycle at which the attenuation measurement is made. A reed relay switches the pulser-receiver between transducers on either specimen. The sequence of operations is arranged so that ultrasonic energy for attenuation measurements is never applied to a specimen while acoustic emission data are being recorded; this precludes any possible interference. For reasons described later, specimen temperature is recorded before each attenuation measurement.

For most experiments both acoustic emission systems were used on separate specimens except when comparative tests of the systems themselves were made. The block diagram (Fig. 3) shows an arrangement designed to examine a specific feature of the acoustic emission encountered in the fatigue tests of this study. The objective was to selectively examine acoustic emission occurring during various portions of the load cycle; the reasoning and results are presented later in this report. An electrical SPDT switch, called a signal divider in the figure, synchronized by a signal from the optical trigger, provided two signal outputs to separate bandpass filters, whose output was measured using true rms voltmeters. A Nicolet

Explorer III transient digitizer was used to obtain samples of acoustic emission waveforms from each part of the load cycle.

TENSILE TESTS

Acoustic emission and ultrasonic attenuation measurements were made simultaneously during tensile elongation tests of specimens of four different aluminum alloys. Tensile tests were performed initially because they are simpler and more easily controlled than fatigue tests. On all specimens tested the acoustic emission activity (large frequent bursts) was most extensive prior to yield. With the equipment used, no perceptible change in ultrasonic attenuation was observed prior to yield.

One inch diameter rod stock of various aluminum alloys (1100H, 6061-T6, 2024-T3, 7075-T651) was machined to have a reduced gauge section in a "dogbone" configuration. Gauge sections of 5.08 and 10.16 cm in length and diameters of 1.27 and 1.02 cm were used. The end faces were machined flat and parallel. In general, the specimens were given no further preparation since the examination of commercial products was the primary interest.

All of the specimens were subjected to uniaxial tensile loading using an Instron testing machine. In these studies, crosshead rates of 0.05 and 0.02 cm/min were used. The fixtures connecting the grips to the testing machine were specially designed to maintain the straightness of the specimen during deformation, since flexure would cause spurious ultrasonic measurements. The grips, which were specifically designed for this study, provided uniform uniaxial application

of the load, reasonable acoustical isolation from the loading machine, and easy access to either end of the specimen for transducer placement. No influence of the mechanical or electrical operation of the Instron testing machine on either the ultrasonic attenuation or acoustic emission monitoring was encountered.

Continuous ultrasonic attenuation measurements were made using the Matec equipment described earlier. By subtracting the initial attenuation value and dividing by the instantaneous specimen length, the change in attenuation per unit length (dB/cm) was obtained. In conjunction with this monitoring system a 0.5 in.(1.27 cm) diameter Aerotech 10 MHz Gamma transducer was operated in the pulse-echo mode at a repetition rate of 200 per second. The transducer was directly coupled to the upper specimen face with nonaqueous stopcock grease. A 3 kg weight was used to apply a constant load to the transducer, while a specially designed spacing ring was used to assure central positioning, avoiding excessive reflections of the pulse from the lateral surfaces. Care was taken to avoid interaction between the attenuation and acoustic emission systems.

Acoustic emission was detected by a one inch diameter 100 kHz Panametrics Model 5070 resonant sensor coupled directly to the lower end face of the specimen with nonaqueous stopcock grease and held in place by a spring. The signal from the transducer was amplified and bandpass filtered from 10 kHz

to 300 kHz by a Tektronix 1A7A High Gain Amplifier. Further filtering by a Kronhite Model 3202 Filter from 80 kHz to 120 kHz conditioned the signal which was counted by a Monsanto Model 112A counter.

Load, ultrasonic attenuation, and acoustic emission were monitored as a function of extension for the four aluminum alloys. For all alloys tested, it was found that the acoustic emissions detected before the yield point was reached had much greater amplitude and frequency of occurrence than those detected after yield; in most cases, nearly no acoustic emission was detected after yield. The ultrasonic attenuation, however, was found to exhibit a different behavior, in that the change in attenuation per unit length prior to yield was essentially imperceptible.

Two additional series of tensile tests were performed on specimens of 7075 aluminum monitoring acoustic emission only. Part of the motivation for selection of this particular alloy was the availability of previously published opinions of other investigators on the origin of the observed acoustic emission signals. In the first series, an examination was made of the burst type of emission observed prior to macroscopic yield of 7075 aluminum in the T6 heat-treated condition. In these experiments, no acoustic emission activity was observed upon immediate reloading of the test specimen to load levels not in excess of those applied on the first loading. However, when the test specimen was

allowed to sit at room temperature for three days between first loading and reloading, the burst type emissions were once again observed prior to macroscopic yield. This result appears to contradict the theory which attributes all burst type emissions to particle cracking, because the fractured intermetallic particles would not heal themselves. In the second series of tests, low level acoustic emission activity was monitored by recording the true rms voltage output from the detection system during tensile deformation. As-received material was found to behave in such a manner that this low level activity peaked in the range of 3 - 5% strain. A typical set of test results is shown in Fig. 5. Burst type emission was evident prior to and during yield while low level emission activity gradually increased beyond yield and reached a maximum at 4.5% strain. Overall examination of the acoustic emission detected during the deformation of 7075-T651 aluminum suggests the possible utilization of this type monitoring for detecting the onset of plastic deformation. This may be successfully accomplished by noting the sharp decrease in burst type emission and the gradual increase of low level activity.

In order to determine the role played by the precipitate particles in the acoustic emission activity, similar tests were performed on solution treated specimens. Marked differences were observed as shown by the results of a typical

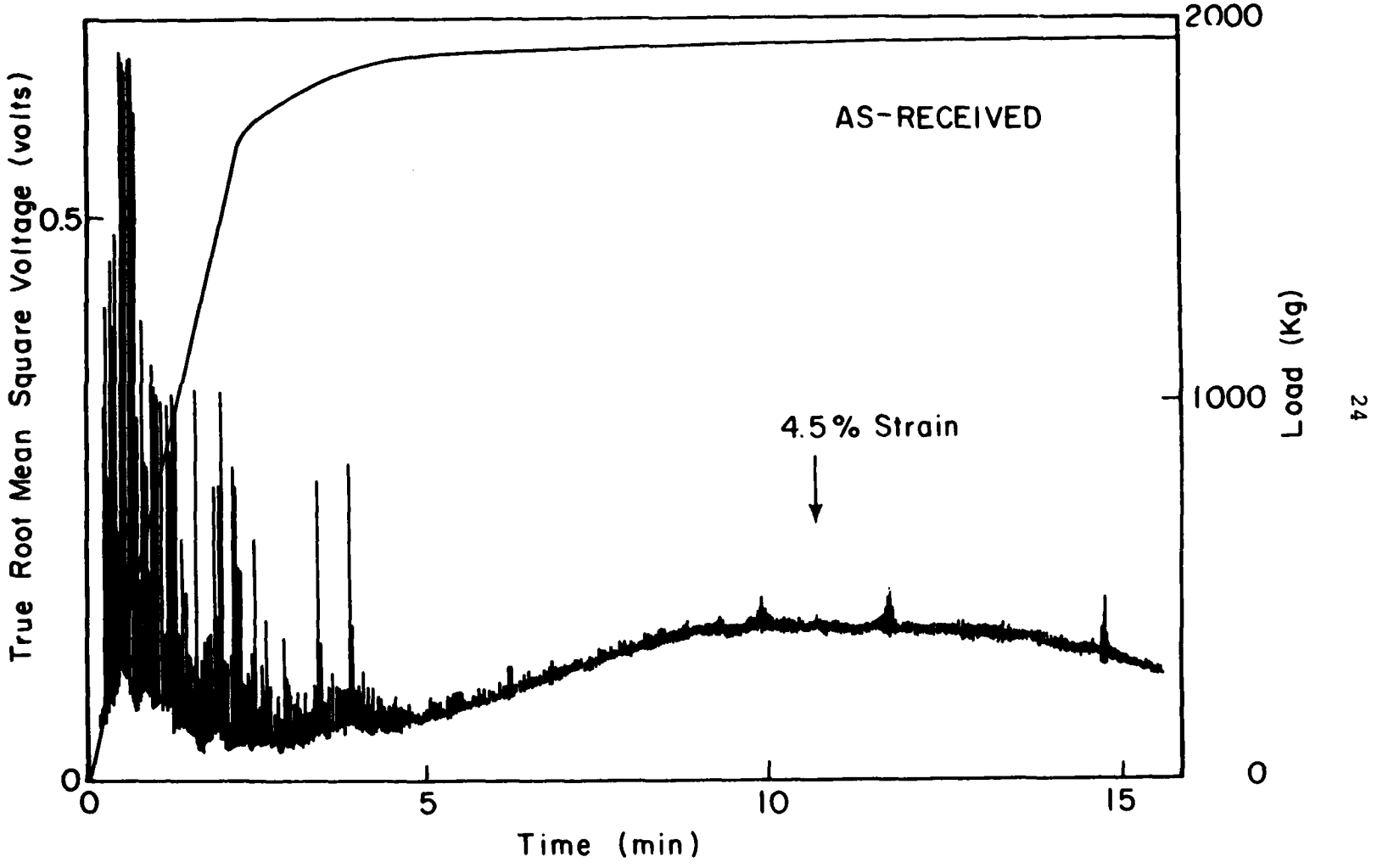

FIGURE 5. TYPICAL TENSILE TEST ACOUSTIC EMISSION DATA
(7075-T651 Al, as-received. Elongation rate: 0.05 cm/min.)

test depicted in Fig. 6. Whereas a small almost imperceptible peak in the low-level emission occurred near yield in the as-received material (Fig. 5), an extremely large sharp peak is observed at yield in the solution-treated samples (Fig. 6). In these latter specimens, little burst type emission was observed. A peak in the low-level emission is again observed at approximately 5 or 6% strain, but the maximum is not well defined. Additional elongation of the solution-treated samples led to a region of discontinous yielding with corresponding fluctuations in the acoustic emission behavior.

Analysis of the tensile tests indicates that the source of burst type acoustic emissions occurring both before and after the yield are the same in 7075-T651, 7075-T6 and 7075 solution-treated aluminum alloys, and result from the breakaway of pinned and piled up dislocations. Intermetallic particle fracture was discounted as a primary source of emissions because the solution-treated specimens, which do not contain intermetallic particles, exhibited a great deal of acoustic emission activity. The large number of low level acoustic emissions occurring at yield in the 7075 solution-treated specimens are thought to be the result of elastic strain energy released from newly generated dislocations which activate other sources causing avalanching. Subsequent interaction of the glissile dislocations with strong pinning points (e.g.

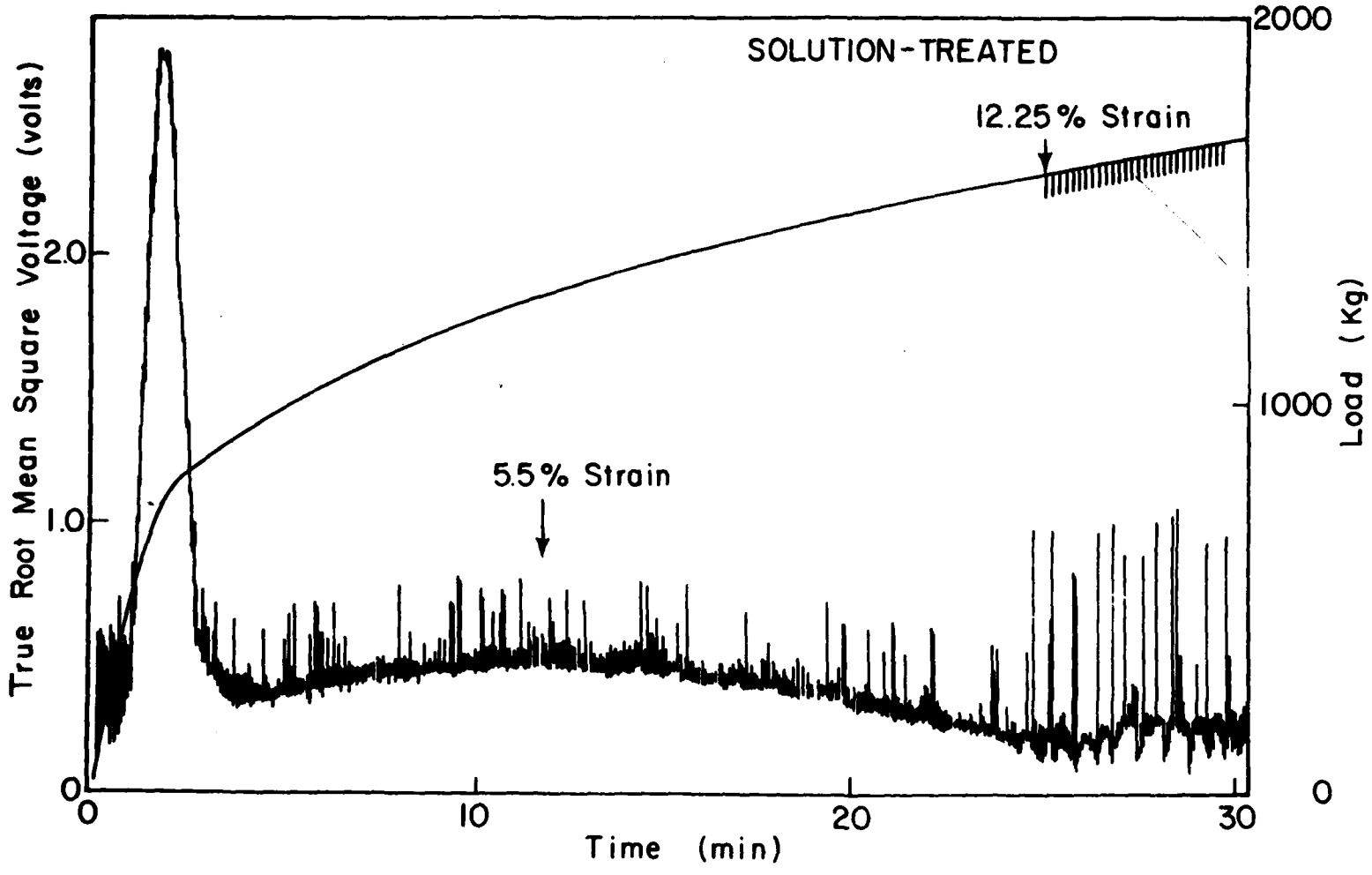

FIGURE 6. TYPICAL TENSILE TEST ACOUSTIC EMISSION DATA
(7075 Al, solution-treated. Elongation rate: 0.05 cm/min.)

sessile dislocations) and weak pinning points (e.g. vacancies, impurity atoms, precipitates, and inclusions) causes the rate of dislocation generation and the associated acoustic emission to decrease. Since no such low level acoustic emissions were observed at yield in the 7075-T651 or 7075-T6 specimens, it is apparent that the precipitate particles prevented glissile dislocation motion.

FATIGUE TESTS ON SHEET SPECIMENS

Sheet specimens made from 7075-T6 aluminum of thickness typical of the outer skin of an aircraft were fatigue tested, while ultrasonic measurements were made throughout the tests. This study indicated that attenuation monitoring gave early warning of fatigue damage at approximately 90% of the elapsed fatigue life of these specimens. To minimize differences in alloy composition, cold work and heat treatment, specimens were cut from the same sheet of 7075-T6 aluminum stock. Care was taken to assure the similarity of the surface condition and to note the rolling direction of each specimen. The sheet specimens were fatigue tested in a Krouse Fatigue Machine which subjected the specimens to cyclic loading in reverse bending as a cantilever beam at a rate of 1725 cycles per minute. Stepless adjustment of an eccentric cam permitted variation of the beam deflection over a wide range of values.

Figure 7 is a schematic diagram of the experimental apparatus. The Matec equipment described earlier was used to continuously monitor ultrasonic attenuation, while the pulse-echo waveform itself was monitored periodically by visual and photographic means.

Three specimen configurations, typifying those which might be encountered in an aircraft, were tested. Shown in Fig. 8(b) and 8(c) are two specimen configurations including fastener hole patterns; one with screws located near the end of the

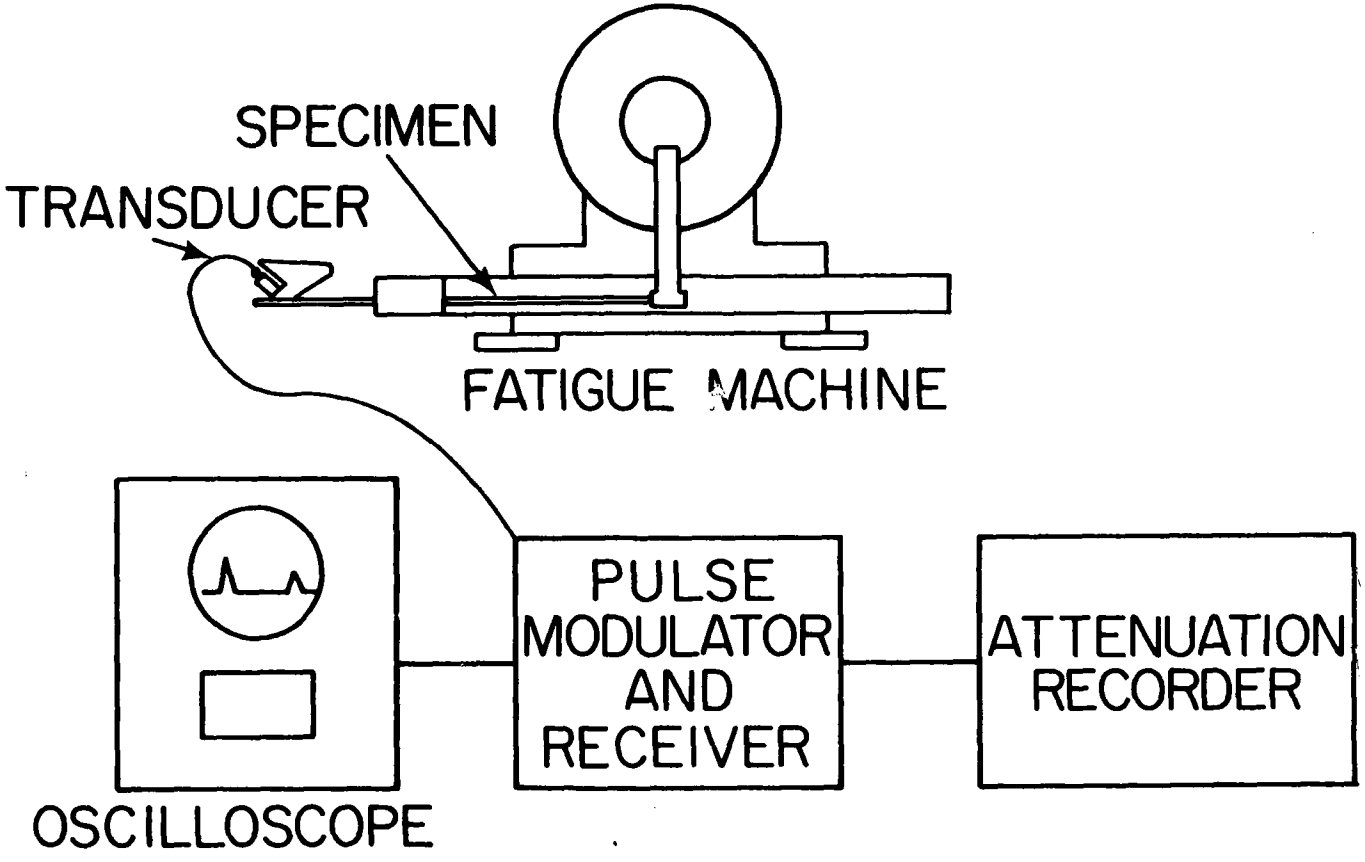

FIGURE 7. EXPERIMENTAL APPARATUS FOR SHEET SPECIMENS

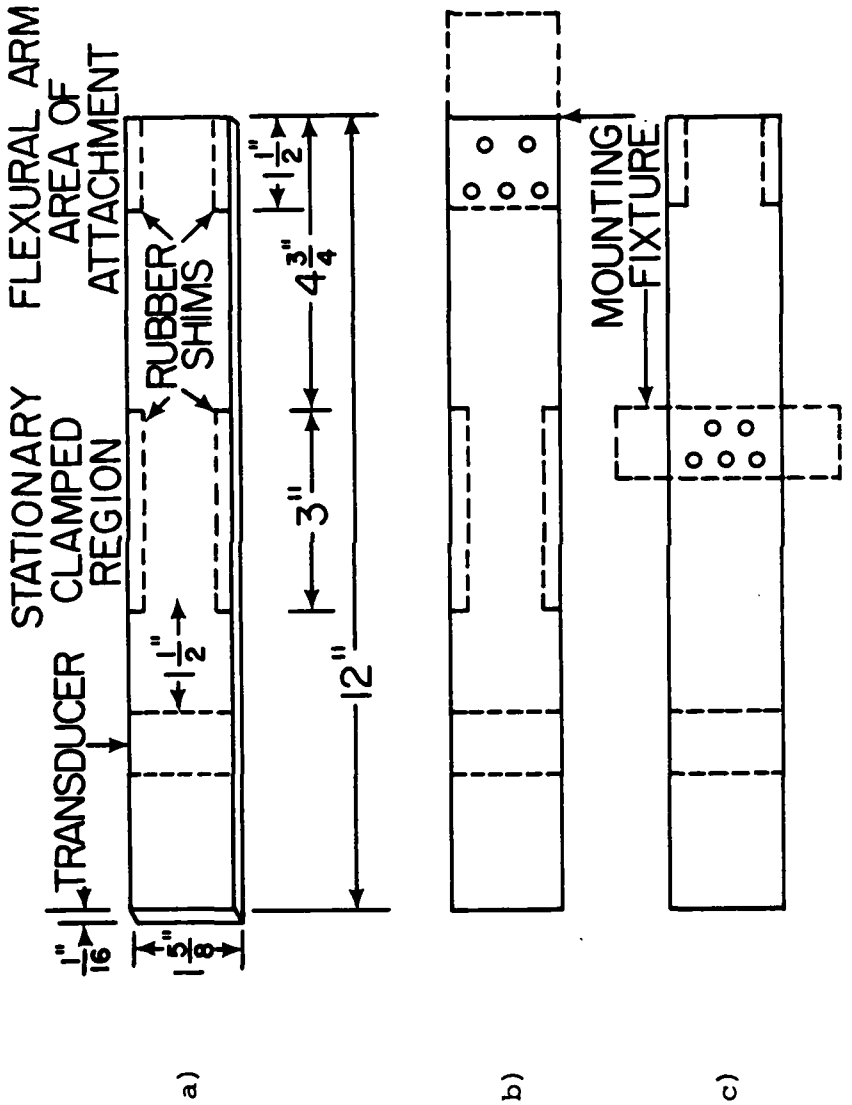

FIGURE 8. SHEET SPECIMEN GEOMETRIES
a) Plain
b) End-rivet simulated
c) Center-rivet simulated

specimen and the other with screws located near the middle of the specimen. Screw fasteners were used rather than rivets to facilitate examination of these regions after fatigue failure. The remaining specimens were tested plain (Fig. 8(a)) with no fasteners or fixtures. The dimensions, the area of clamping, and the transducer position are also shown in Fig. 8.

A 0.5 in. x 1 in. 2.25 MHz longitudinal transducer was used in conjunction with a modified mode conversion block (made of Lucite) designed to launch shear waves at an angle of 45° to the surface normal. The mode conversion block or "wedge" was coupled to the specimen with an ethylene glycol-based couplant. This method of introducing the ultrasound into the specimen was required because the thin cross section precluded mounting of the transducer on the end of the specimen. Modification of the mode conversion block was necessary to obtain adequate signal levels. The modification served to limit the area of contact between the wedge and the specimen to the projected area of the active element of the transducer onto the base of the wedge. In thick specimens, no difference was observed in the amplitude of the return echoes using either the commercially available wedge or the modified wedge. However, in the thin specimens, a large difference in amplitude was observed between the return echoes detected using the two wedges. The difference in the observed amplitude

was caused by energy losses in the excess material of the commercial mode conversion wedge. With thin specimens, energy was lost before the generated pulse propagated out from under the wedge and again energy was lost before the return pulse reached the transducer. In the case of thick specimens no energy was lost because the pulse had propagated out from under the wedge before it returned to the upper surface. Schematic diagrams illustrating the wedge-specimen configurations for the four possible cases are shown in Fig. 9. Because of the high attenuation caused by the multiplicity of surface-to-surface reflections in thin specimens, attenuation could not be measured conventionally by the use of two successive reflections from a specimen surface. Instead, the amplitude of a particular reflection was compared with a stable electronic reference signal.

During the actual tests with the plain specimens, the attenuation was continously recorded using a strip-chart recorder, and the pulse-echo pattern displayed on an oscilloscope was monitored visually and photographed. The echo from the end of the specimen was amplified to 6 V and observed at 2 V/cm on the oscilloscope. The oscilloscope gain was then increased to 0.05 V/cm and the pattern photographed. Once this was done, the fatigue test was started. At 0.05 V/cm any new or additional pulse could

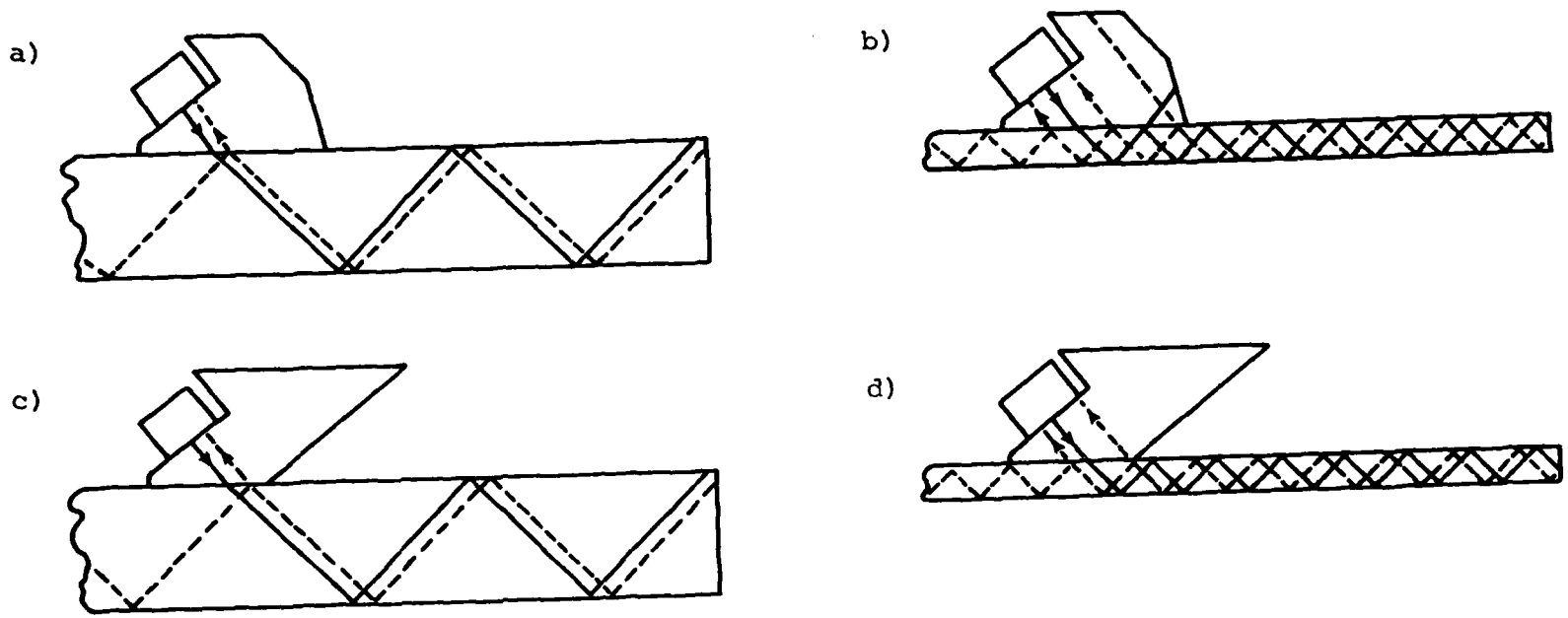

FIGURE 9. MODE CONVERSION WEDGES ON THICK AND THIN SPECIMENS

a) Normal situation.
b) Excessive absorption due to close surface reflections in thin specimens.
c) Normal situation unaffected by wedge modification.
d) Excessive absorption avoided by modification of wedge shape.

be positively identified as such when it reached an amplitude of 0.03 V by comparison with the initial photograph. For the rivet-simulated specimens only the attenuation was monitored due to the more complex pattern.

Figure 10 depicts two typical plots of ultrasonic attenuation versus percent fatigue life. The data for a plain specimen with its length parallel to the rolling direction are shown in Fig. 10(a). Although the attenuation increased slowly during the early stages of fatigue, no significant change in attenuation nor any significant additional pulses were observed during the first 85% of the fatigue life of the specimen. An additional echo having an amplitude of 0.03 V was first observed at 5.75×10^5 cycles or 86% of the fatigue life. At the same time the attenuation began to increase significantly. The total fatigue life of the specimen (100%) was 6.69×10^5 cycles. Similar data are shown in Fig. 10(b) for a specimen having its length perpendicular to the rolling direction. The attenuation changed very little in the first 83% of the fatigue life. It began to increase at 83% of the fatigue life and an additional pulse was observed at approximately 84% or 2.95×10^5 cycles. The total fatigue life (100%) was 3.48×10^5 cycles. As would be expected due to the differences in texture, the fatigue life of the plain specimens whose length were perpendicular to the rolling direction were less than those with the length parallel to the rolling direction.

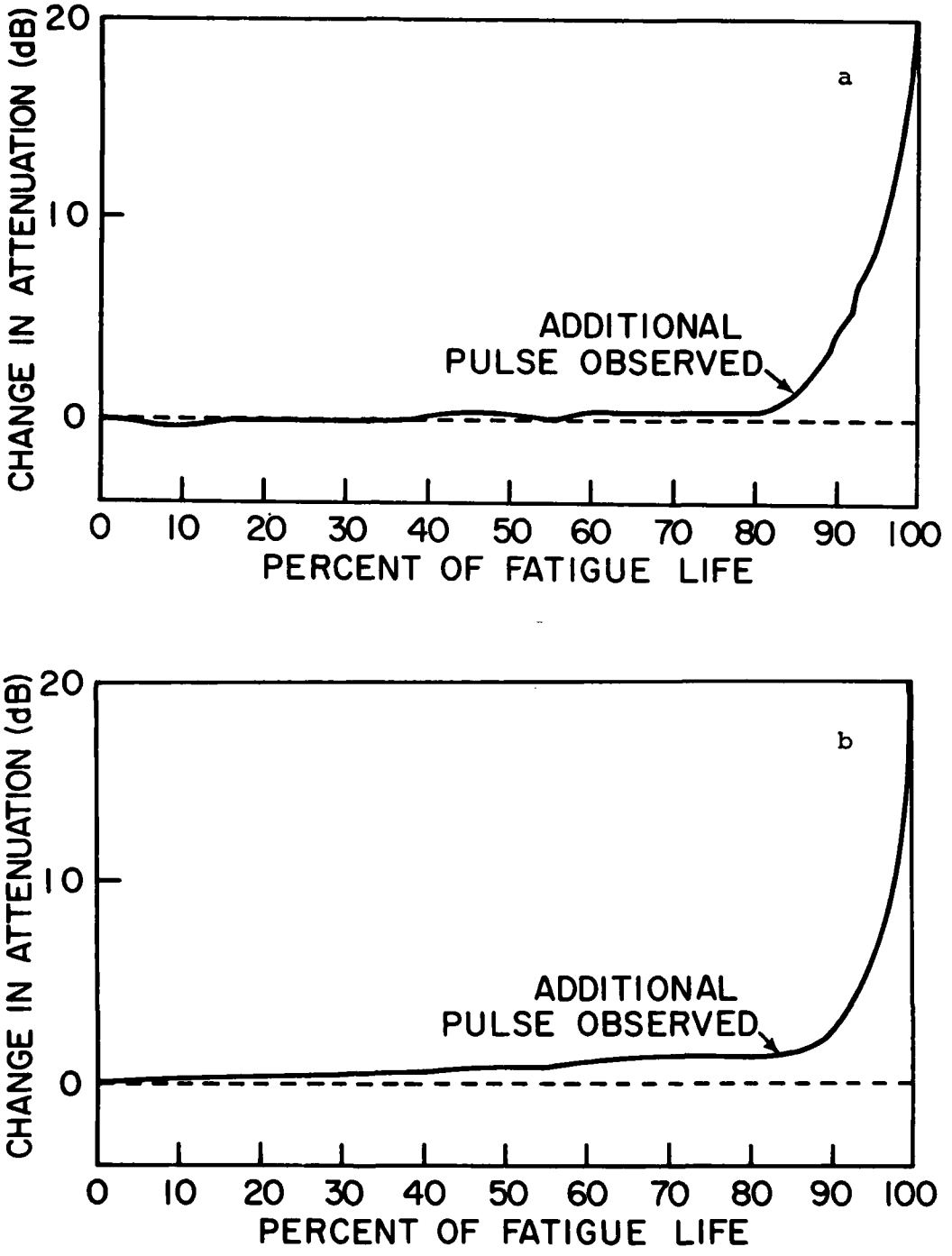

FIGURE 10. SHEET SPECIMEN FATIGUE TEST ATTENUATION DATA
a) Plain geometry, rolling direction || length
b) Plain geometry, rolling direction ⊥ length

These experiments indicated that by continously monitoring the change in the ultrasonic attenuation, an early warning of approximately ten percent of the fatigue life is possible before failure occurs in 7075-T6 aluminum sheet. It was also found that there was more change in the attenuation in the early portion of the fatigue life for the rivet-simulated specimens than for the plain specimens. As a result, more difficulty was encountered in relating the magnitude of the change in attenuation to the remaining fatigue life for these type specimens.

FATIGUE TESTS ON RECTANGULAR BAR SPECIMENS

A large body of previous work (referenced earlier in this paper) has shown that ultrasonic attenuation measurements provide a reliable indication of fatigue damage in aluminum bar specimens with as much as 40% of the specimen fatigue life remaining. The extent of early warning is highly dependent on specimen composition and heat treatment. For this study, continuous acoustic emission monitoring was combined with ultrasonic attenuation monitoring on rectangular bars of 7075-T651 and 7075 solution-treated aluminum. The fatigue test results on these two heat treatments of 7075 aluminum in general appear very similar, with the ultrasonic attenuation exhibiting little variation until a rapid increase occurred between 90% and 95% of the elapsed fatigue life. Similar behavior was observed in the records of rms acoustic emission voltage vs. percent fatigue life. After some initial fluctuations, the rms voltage was smooth until the period between 85% and 95% of the elapsed fatigue life where the rms voltage began increasing rapidly.

The bar specimens were 1 in. wide, 12 ins. long and 1/2 in. thick and were fatigued at a maximum bending displacement of 9.0 mm peak-to-peak. The fatigue machine and ultrasonic attenuation monitoring system were the same as those used for the sheet specimens, except for the transducer. A 10 MHz, 1/2 in. diameter, end-mounted, longitudinal transducer

was used on the bar specimens. The Admiralty Materials Laboratory acoustic emission system was used in conjunction with a true rms voltmeter with logarithmic output and a multichannel strip-chart recorder.

Figures 11 and 12 display the results of typical fatigue tests on 7075-T651, as-received, and 7075 solution treated specimens, respectively. In Fig. 11 the change in ultrasonic attenuation exhibits no appreciable alteration until 80% (1.5×10^6 cycles = 100%) of the fatigue life at which point it changes rapidly, going off scale at approximately 97% of the fatigue life. Examination of raw experimental data showed that the attenuation continued to increase for the remainder of the fatigue life. The true rms voltage output of the acoustic emission signal, which was amplified by 70 dB, was seen to fluctuate at the start of the test, level off and begin to steadily increase at 80% of the fatigue life, with a more rapid increase occurring after 95% of the fatigue life. Unlike the smooth, nearly monotonic behavior of the ultrasonic attenuation curve the rms curve is seen to have local maxima and minima. The peaks, in actuality, consist of many individual burst indications compressed together because of the time scale of the recording. Very similar behavior is seen in Fig. 12 which is typical of the solution-treated specimens. The change in ultrasonic attenuation shows a small but

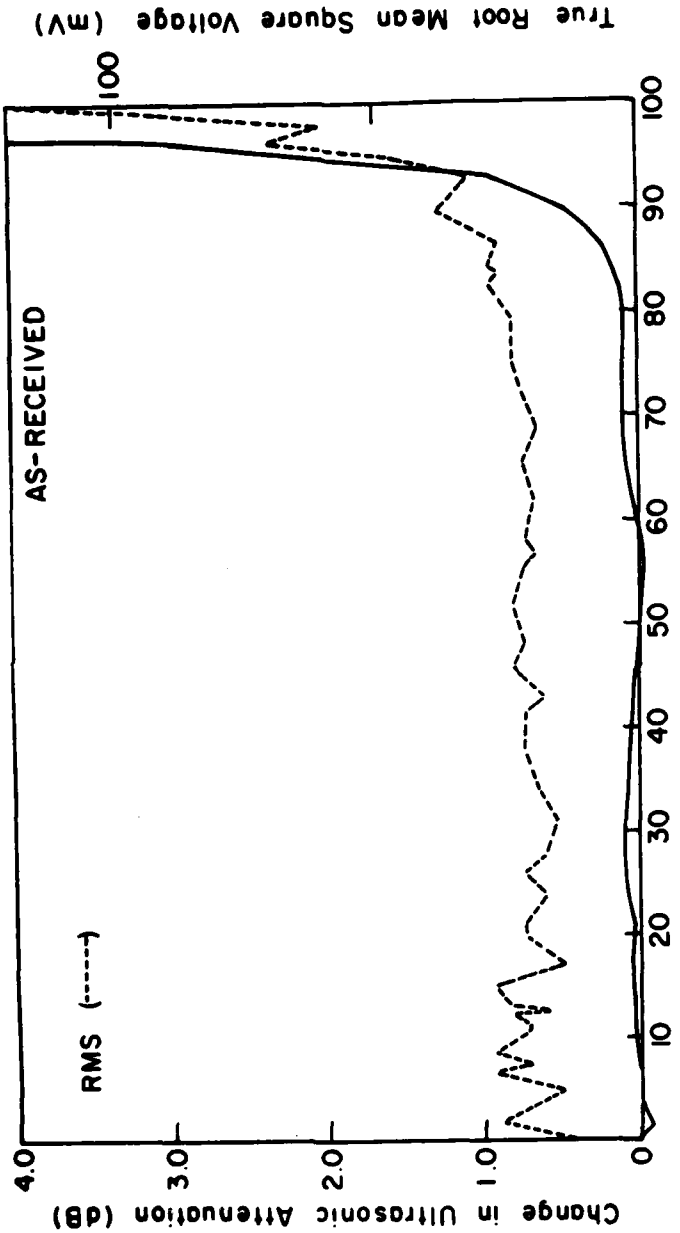

FIGURE 11. COMBINED ULTRASONIC ATTENUATION AND ACOUSTIC EMISSION DATA FROM FATIGUE TEST OF 7075-T651 BAR SPECIMEN
Solid curve: Ultrasonic attenuation
Dashed curve: Acoustic emission

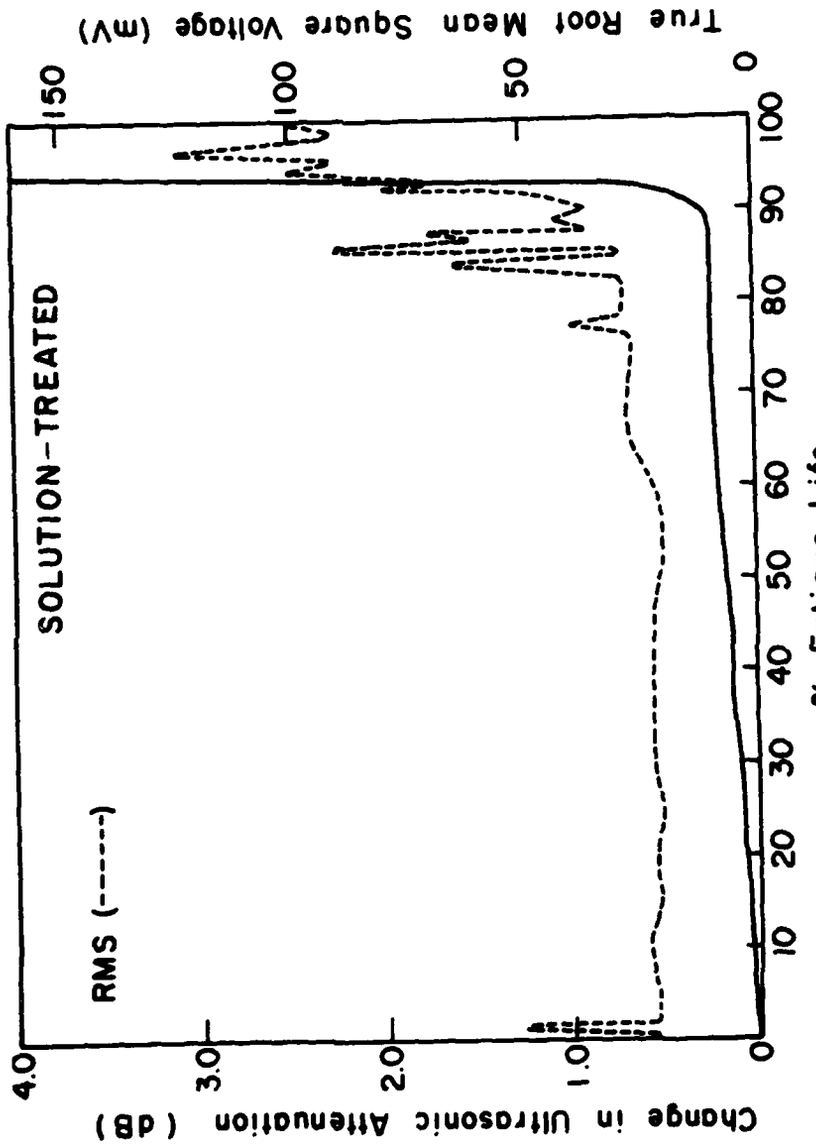

FIGURE 12. COMBINED DATA FROM FATIGUE TEST OF 7075 SOLUTION-TREATED SPECIMEN
Solid curve: Ultrasonic attenuation
Dashed curve: Acoustic emission

steady increase until 90% of the fatigue life (7.4×10^6 cycles = 100%), when it begins to increase rapidly, going off scale at 94% of the fatigue life. Similarly, the rms curve, after a peak at the beginning of the deformation, levels off until approximately 78% of the fatigue life, when the overall rms curve begins to increase slowly, with several large peaks superimposed on the overall increasing trend. A rapid, overall increase began at 87% of the fatigue life, and leveled off at an elevated value, at 95% of the fatigue life. It is important to note that the ultrasonic measurement was performed synchronously with the cyclic deformation such that the specimen was undeflected at the time of the actual measurement. Both ultrasonic attenuation and acoustic emission measurements consistently provided some degree of early warning of fatigue damage in the 7075 aluminum bar specimens tested.

FATIGUE TESTS ON T-BAR SPECIMENS

Background

The rectangular bar shape used previously was modified to permit simultaneous ultrasonic attenuation and dual (i.e. with two separate instruments) acoustic emission measurements to be made in combination with in situ eddy current and visual inspection. The fatigue machine; acoustic emission, ultrasonic attenuation, and eddy current instrumentation; and the specimen mounted in the fatigue machine are illustrated schematically in Fig. 13. The new T-bar specimen geometry and its mounting arrangement are shown in Fig. 14. A sharp reduction in cross-sectional area was included in the specimen design to provide a region of stress concentration and thus localize the region of probably failure. This localization simplified the visual and eddy current examination for surface breaking cracks during fatigue cycling.

As will be detailed later, the modified specimen shape also allowed the use of a novel scheme for attenuation measurement that provided enhanced sensitivity to crack formation. The shoulder of the reduced cross-section was located sufficiently far from the steel grips of the fatigue machine to eliminate any possible deleterious effects on eddy current testing caused by close proximity. The constriction in area also ensured that the radiated sound field of the transducer overfilled the region where fatigue damage occurred.

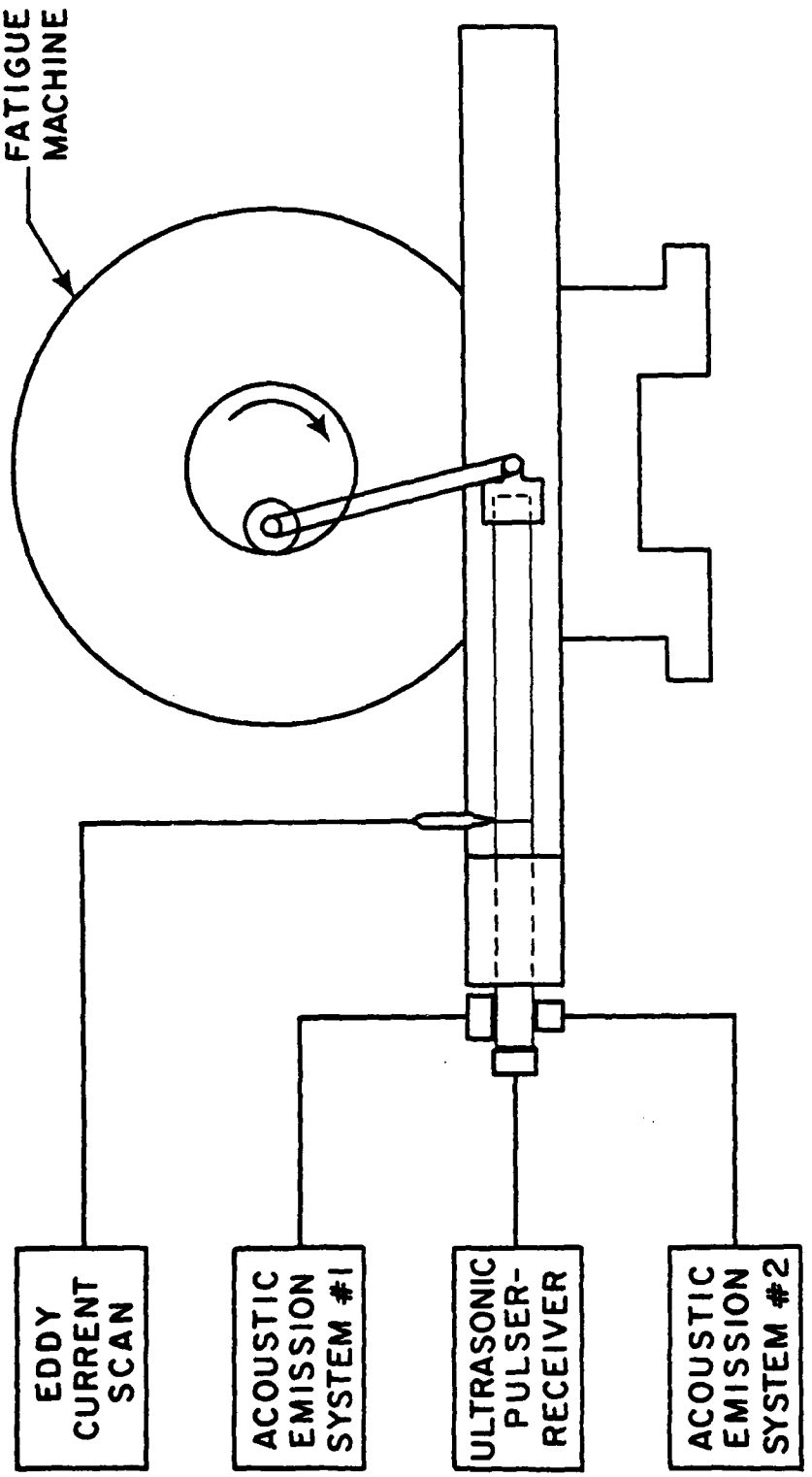

FIGURE 13. TESTING ARRANGEMENT FOR T-BAR SPECIMEN

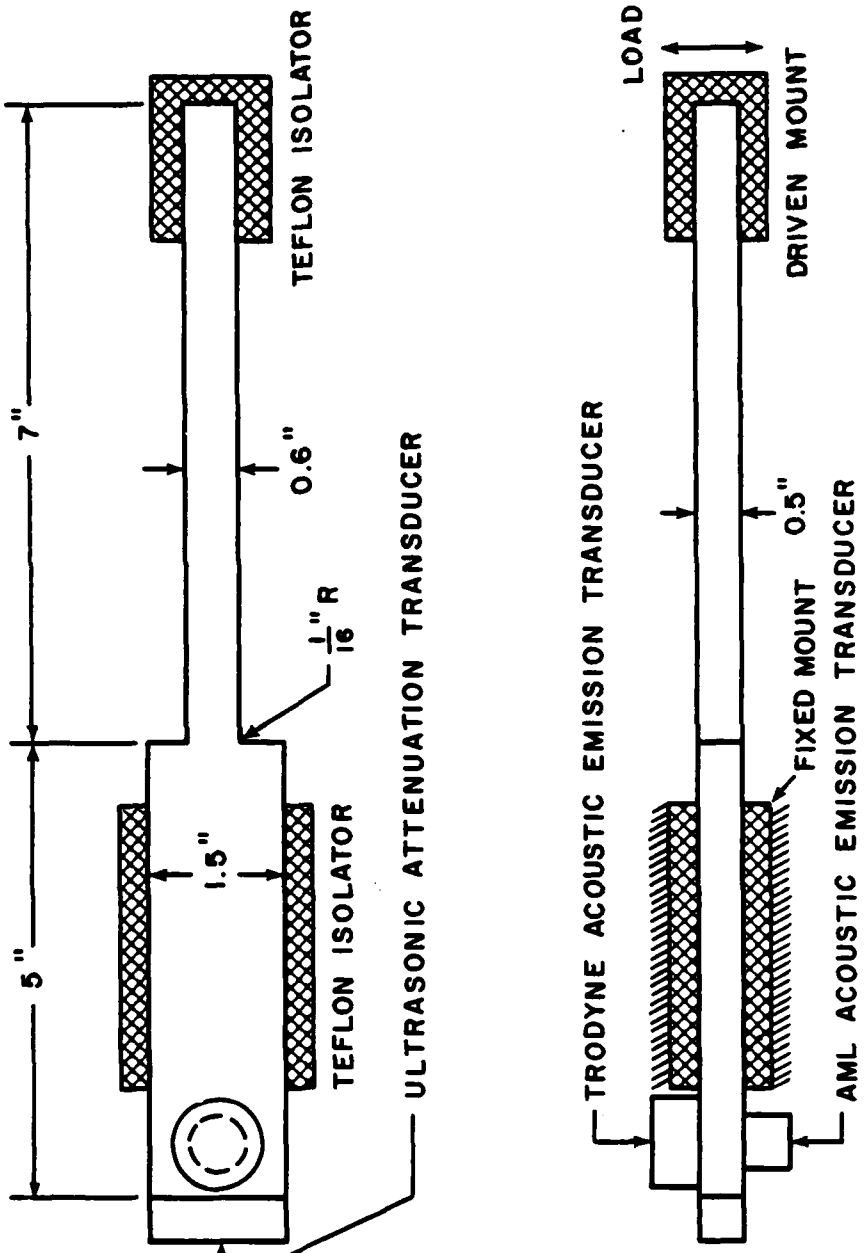

FIGURE 14. TRANSDUCER PLACEMENT ON T-BAR SPECIMEN

The initial ultrasonic attenuation and acoustic emission measurements conducted in the most recent research were made on specimens which possessed sharp, square corners at the reduced cross-section shoulder. It was found that the notch effect at the sharp corners caused a severe stress concentration which often led to premature crack formation and fracture. This problem was solved by incorporating a 1/16" radius into all corners formed at the reduction in cross-section of the specimens. Various alloy compositions, heat treatments, and surface finishes were used in order to study their effect on fatigue damage and early warning of fatigue damage.

Fatigue Test Results

To provide a data base and to verify expectations involving the effects of fatigue test amplitude, heat treatment, and specimen surface preparation on fatigue life, a variety of tests were conducted. Figure 15 shows a plot of bending stress versus number of fatigue cycles for 45 fatigue tests run on 7075 aluminum specimens. The use of a logarithmic scale to plot the number of fatigue cycles facilitated the compact display of the wide range of test durations. The different symbols in Fig. 15 represent different specimen conditions: triangles indicate fine or rough surface polished 7075-T651 aluminum, circles correspond to as-received surface condition of 7075-T651, and squares denote as-received

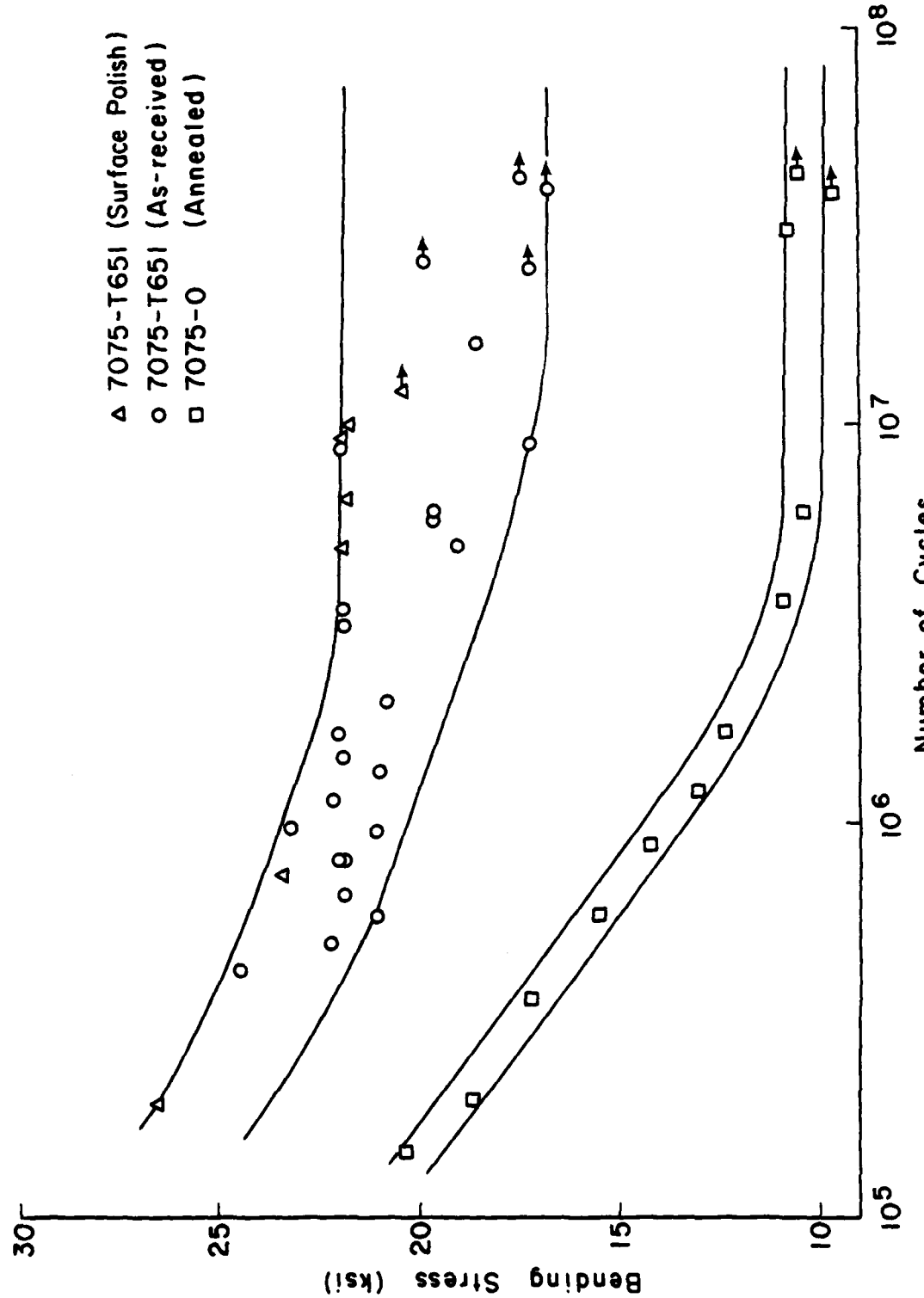

FIGURE 15. S-N DATA FROM 45 TESTS OF 7075 ALUMINUM

surface condition annealed 7075 aluminum. The curves shown in Fig. 15 were drawn to enclose all data points and do not represent any theoretical prediction of fatigue life. However, the upper curve passing through the highest stress for a given number of cycles indicates an endurance limit (the value of stress for which the specimen will not break at any number of cycles) of 22 ksi which may be considered in close agreement with the American Society for Metals Handbook value of 23 ksi for 7075-T6 aluminum using a different fatigue testing apparatus and polished "dogbone" shaped specimens. The arrows beside several of the data points indicated that these specimens showed no sign of imminent failure after more than twelve million cycles.

Ultrasonic Attenuation Measurements and Results

The ultrasonic attenuation measurements made on these specimens were not conventional because the attenuation values recorded were not obtained from the amplitude ratio of two successive reflections from the same part of the test specimen. Instead, the amplitude of the first reflection from the specimen shoulder was compared with the amplitude of the first reflection from the specimen end. This was done for two reasons. First, these two reflections had larger amplitudes than any of the other detectable reflections. Secondly, this procedure offered enhanced system sensitivity to crack formation. Since crack initiation occurs near or in

the plane of the shoulder, and since there is reflection of ultrasound from the crack, the first reflection from the shoulder is increased by crack formation. Conversely, a crack at the shoulder will disperse ultrasound traveling the full length of the specimen and thus reduce the amplitude of the first reflection from the specimen end. Hence, the relative change of the ratio of the amplitudes of the reflections from the shoulder and specimen end will be greater than that of two successive reflections from the specimen end. A typical pulse-echo pattern, photographed from the monitoring oscilloscope of a fatigue specimen before testing and a schematic drawing showing corresponding wave paths is shown in Fig. 16. As shown, peak A is due to the reflection of ultrasonic energy from the reduced cross-section shoulder of the specimen. The next large echo, peak B, is due to reflection from the end of the specimen.

A pulse-echo pattern as photographed from the monitoring oscilloscope after a test specimen had exhibited crack initiation is shown in Fig. 17. Comparison of this pattern with the pattern photographed prior to fatigue crack initiation, Fig. 16, reveals several significant differences. The amplitude of the first reflection from the specimen end, peak B, is much smaller in Fig. 17 than in Fig. 16. This decrease in amplitude of peak B is caused both by the enhanced reflection from the diminished transmission through the crack, and by the action of the automatic gain control circuitry in the attenuation recorder. Any increase in the amplitude of the first

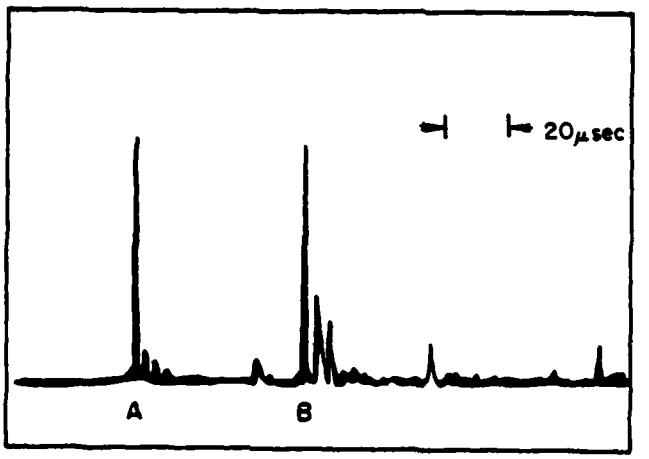

TYPICAL PULSE-ECHO PATTERN

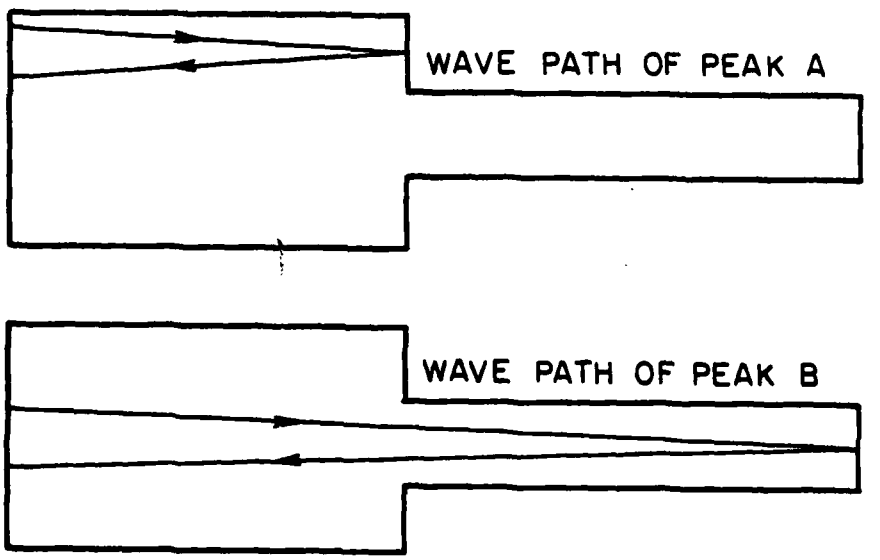

FIGURE 16. PULSE-ECHO WAVEFORM AND PROPAGATION PATHS IN T-BAR SPECIMEN BEFORE CRACK INITIATION

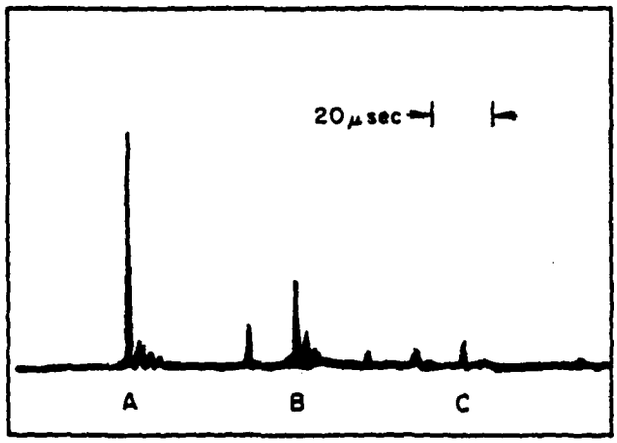

TYPICAL PULSE-ECHO PATTERN
AFTER CRACK INITIATION

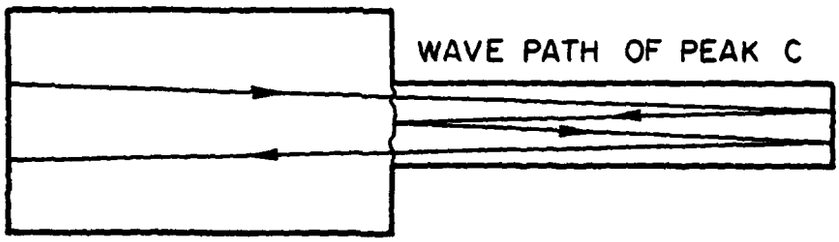

FIGURE 17. PULSE-ECHO PATTERN AND WAVE PATH AFTER CRACK INITIATION

reflection from the shoulder, peak A, is cancelled by the automatic gain control, which by decreasing the overall system gain effectively decreases the amplitudes of all other echoes.

Crack detection can also be accomplished by inspection of the pulse-echo waveform. Although the use of a reduction in cross-section to localize crack formation causes a large reflection of ultrasound from the shoulder thus created, the appearance of new echoes signalling crack initiation is not precluded. For example, peak C in Fig. 17 has no counterpart in Fig. 16. The time of arrival for echo C corresponds to a reflection from the specimen end, followed by a reflection from the crack, a second reflection from end, and finally transmission of the pulse past the crack to the transducer. It follows from the specimen geometry that the decrease in cross-sectional area at the shoulder causes partial reflection of a pulse traveling away from the transducer, but has an insignificant effect on a pulse traveling from the specimen end to the transducer. The second and third reflections from the shoulder-crack plane, show increased amplitudes relative to their counterparts in Fig. 16. This illustrates the increased reflectivity caused by the presence of the crack. Also, the echo due to the second reflection from the specimen end, has traversed the shoulder plane four times and is therefore greatly attenuated when a crack is present.

Ambient temperature was discovered to influence the value of the ultrasonic attenuation; a fluctuation of 6°F changed the indicated attenuation by as much as 0.4 dB. For this reason, specimen temperature was monitored concommitant with the attenuation measurements. A small inexpensive germanium signal diode, strapped to the specimen, served as the temperature sensor. A Wheatstone bridge circuit provided electrical interface to the strip-chart recorder. A calibration curve for a typical diode over the temperature range of interest is given in Fig. 18. By monitoring the temperature continously real attenuation changes could be separated from those due to changes in specimen temperature.

In over 90% of the tests on specimens fatigued until crack formation occurred, the presence of a crack easily detectable by eddy current scanning was indicated by at least a 0.5 dB change in ultrasonic attenuation. In some cases the 0.5 dB change in attenuation observed was a decrease rather than an increase. All attenuation changes beyond 1.0 dB were increases and portended imminent failure.

Early warning of fatigue attainable with ultrasonic attenuation was found to be strongly dependent on specimen surface condition. Figures 19 and 20 show typical changes in ultrasonic attenuation versus percent fatigue life curves for highly polished and as-received surface condition 7075-T651 specimens fatigued to fracture. Ultrasonic attenuation gave earlier warning of fatigue damage for specimens in the as-received

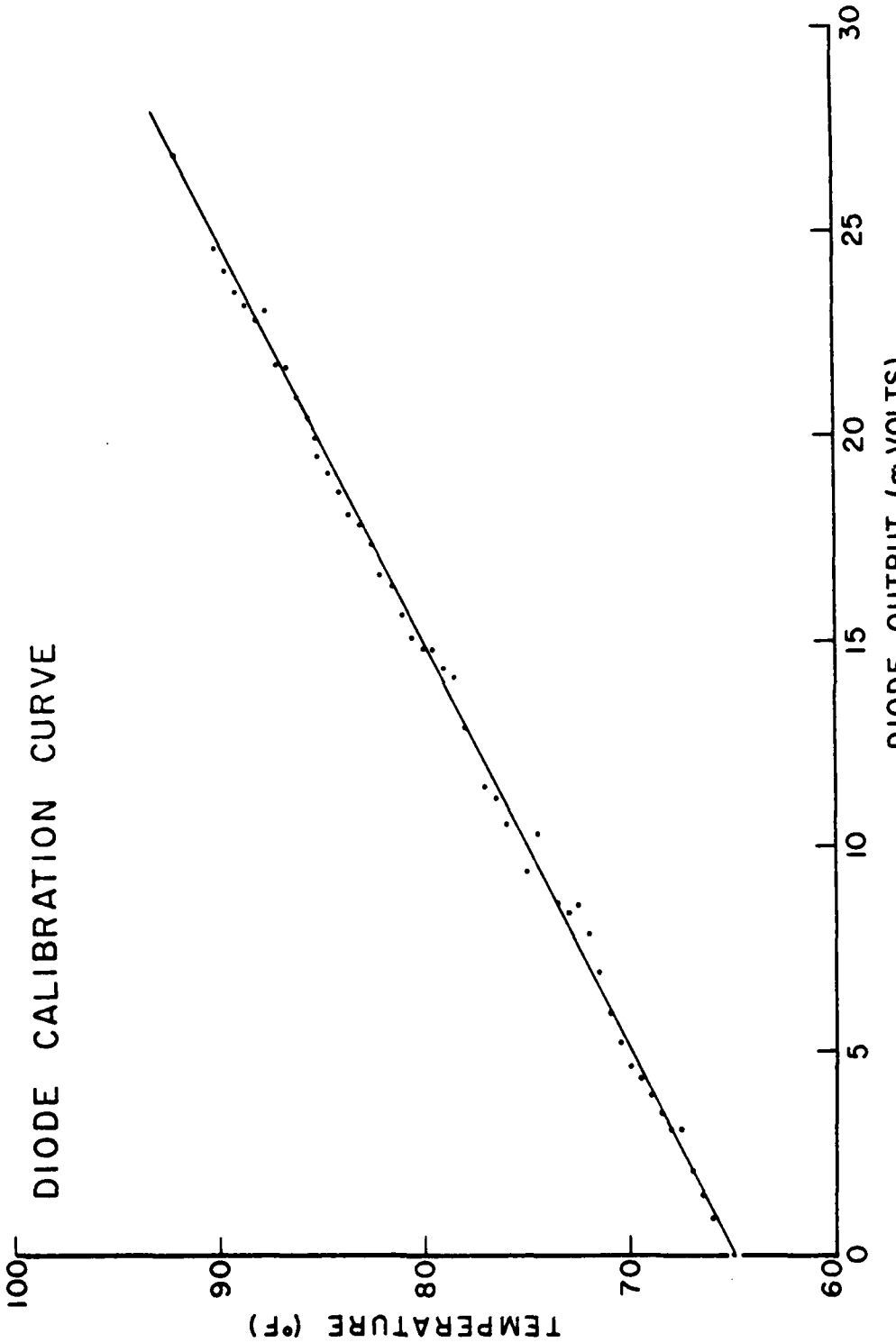

FIGURE 18. SPECIMEN TEMPERATURE SENSOR CALIBRATION CURVE

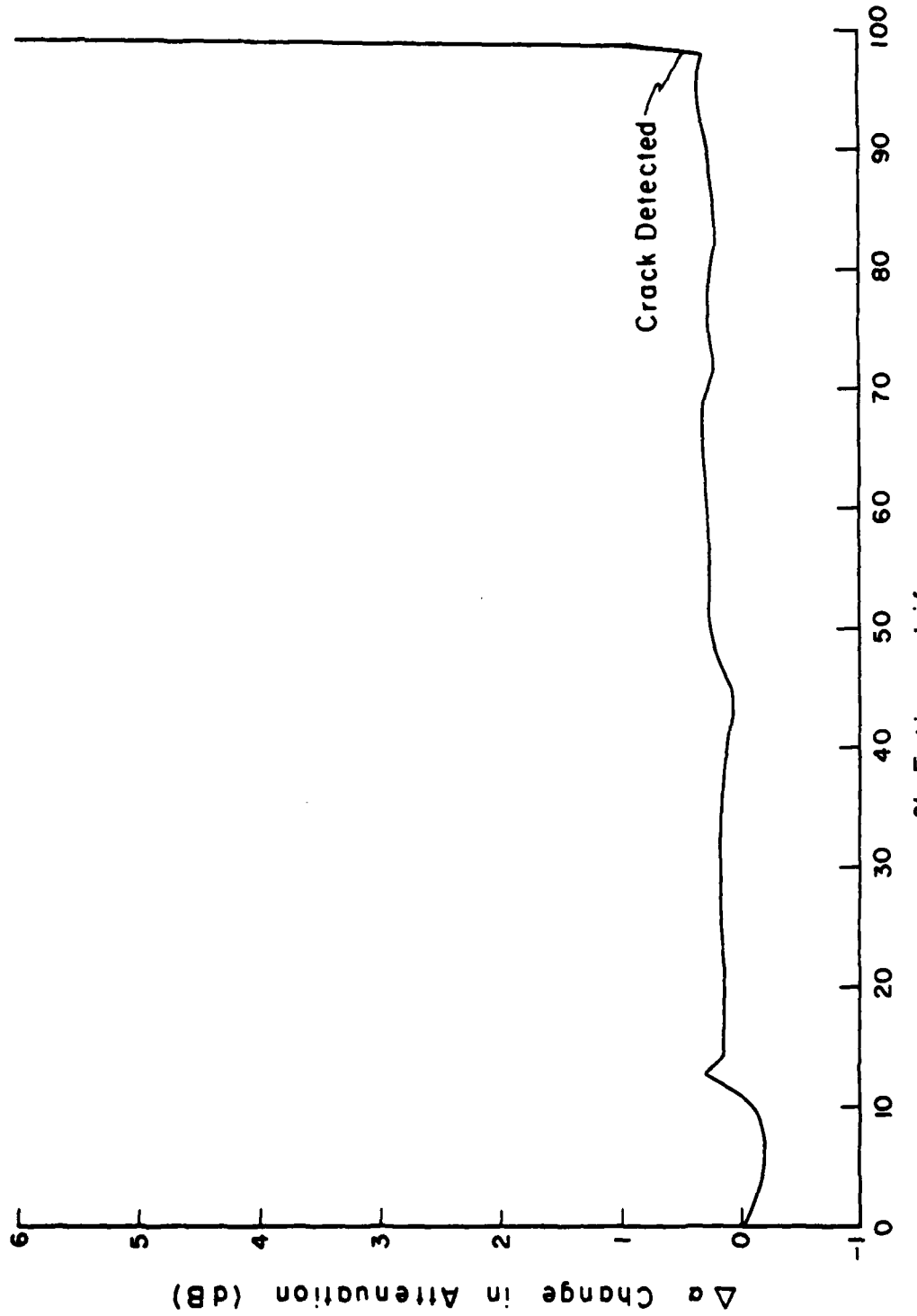

FIGURE 19. ATTENUATION DATA FROM FATIGUE TEST OF HIGHLY-POLISHED 7075-T651 SPECIMEN

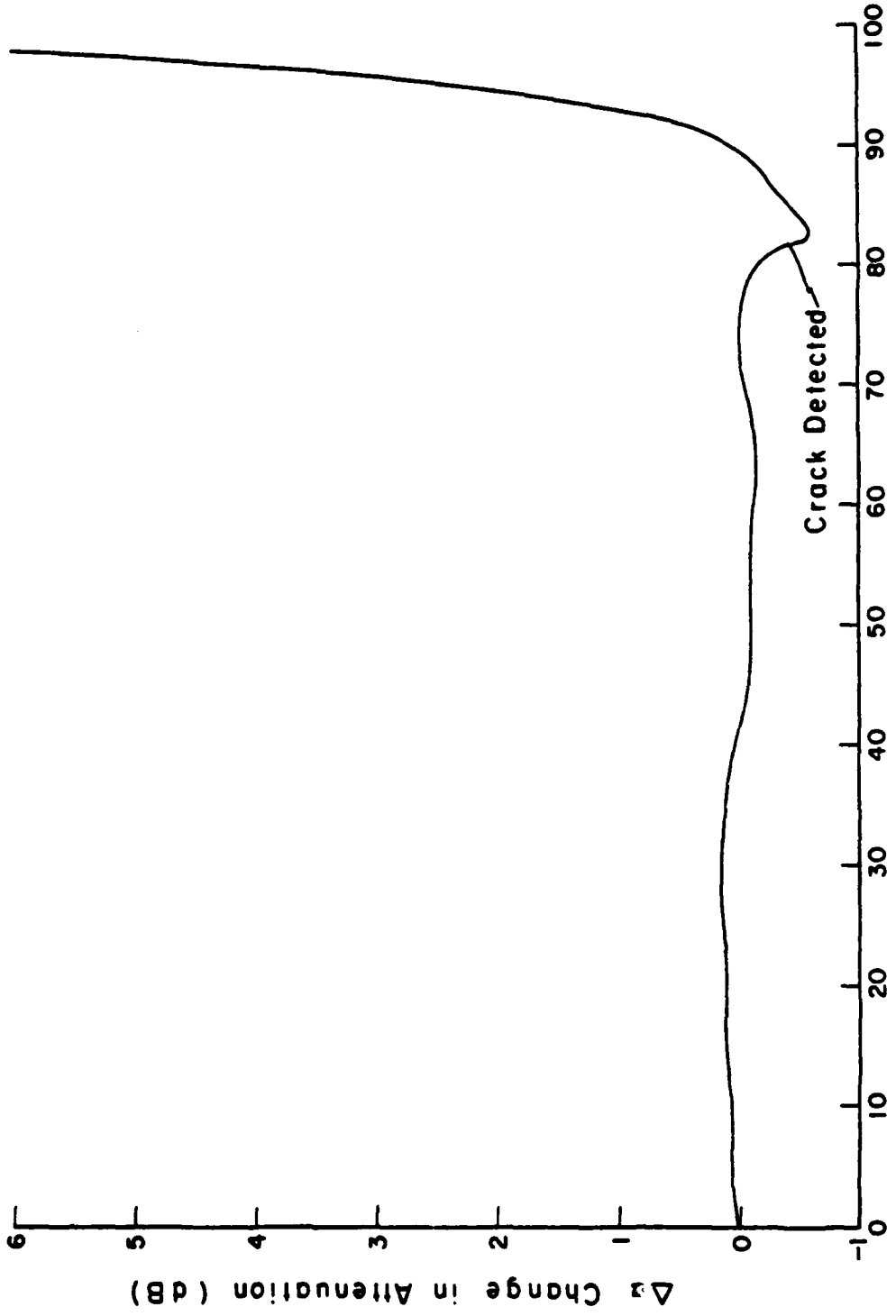

FIGURE 20. ATTENUATION DATA FROM FATIGUE TEST OF 7075-T651 SPECIMEN IN AS-RECEIVED CONDITION (Bending amplitude 6.25 mm, test duration 6.0 x 106 cycles)

surface condition than for specimens with highly polished surfaces. Comparison of the experimental results obtained for two specimens showed that, for fatigue tests of similar length, the number of fatigue cycles from crack initiation to specimen fracture was 2.97×10^5 for the as-received specimen and only 1.08×10^5 for the highly polished specimen. In both cases, when surface crack initiation occurred, the ultrasonic attenuation changed significantly. Several explanations for this behavior are possible. Consider the well-established fact that polishing increases the fatigue strength, i.e., the stress at which, for a given number of cycles, a specimen will fail. Thus, for tests of comparable length run during the present research, the more highly polished specimens were fatigued at higher stress amplitudes than the as-received and less polished specimens. In spite of the higher stress amplitudes, crack initiation occurred later in the fatigue life of the polished specimens. This delay in crack initiation can be attributed to the reduction in number and severity of potential crack initiation sites as a result of surface polishing. Since crack initiation is invariably accompanied by substantial changes in ultrasonic attenuation, this explanation is consistent with the experimental results. The relative lack of early warning obtained with the highly polished specimens is also consistent with two other factors. First, a highly polished specimen will fracture faster, once a

crack has been initiated, because of the higher stress amplitude being applied during the fatigue test. Second, because of the higher stress amplitude and longer test duration prior to crack initiation, the highly polished specimens will have sustained more extensive bulk damage than the unpolished specimens. Once initiated, the crack propagates easily and rapidly through the highly polished specimen until fracture. This severely limits the amount of early warning attainable with highly polished specimens by ultrasonic attenuation monitoring. In the case of the as-received specimens, earlier warning was possible because at the time of crack initiation the surrounding material was still relatively unchanged except for a small plastically deformed region around the crack tip and sides.

The experimental results also showed the effect of heat treatment on the sensitivity of ultrasonic attenuation as a predictor of fatigue failure. To study this effect, tests on 7075 aluminum in the T651 and annealed(O) conditions were performed. Data for 7075-T651 aluminum has been presented earlier in this section. Annealed 7075 aluminum specimens fatigued at high amplitudes of bending behaved in a manner similar to the solution treated 7075 aluminum rectangular bar specimens discussed previously. The ultrasonic attenuation, as presented in Fig. 21 for an annealed specimen, showed a small but steady increase until about 70% of the fatigue life where it reached a plateau and a crack was detected using eddy current scanning. The slow but steady increase in the attenuation

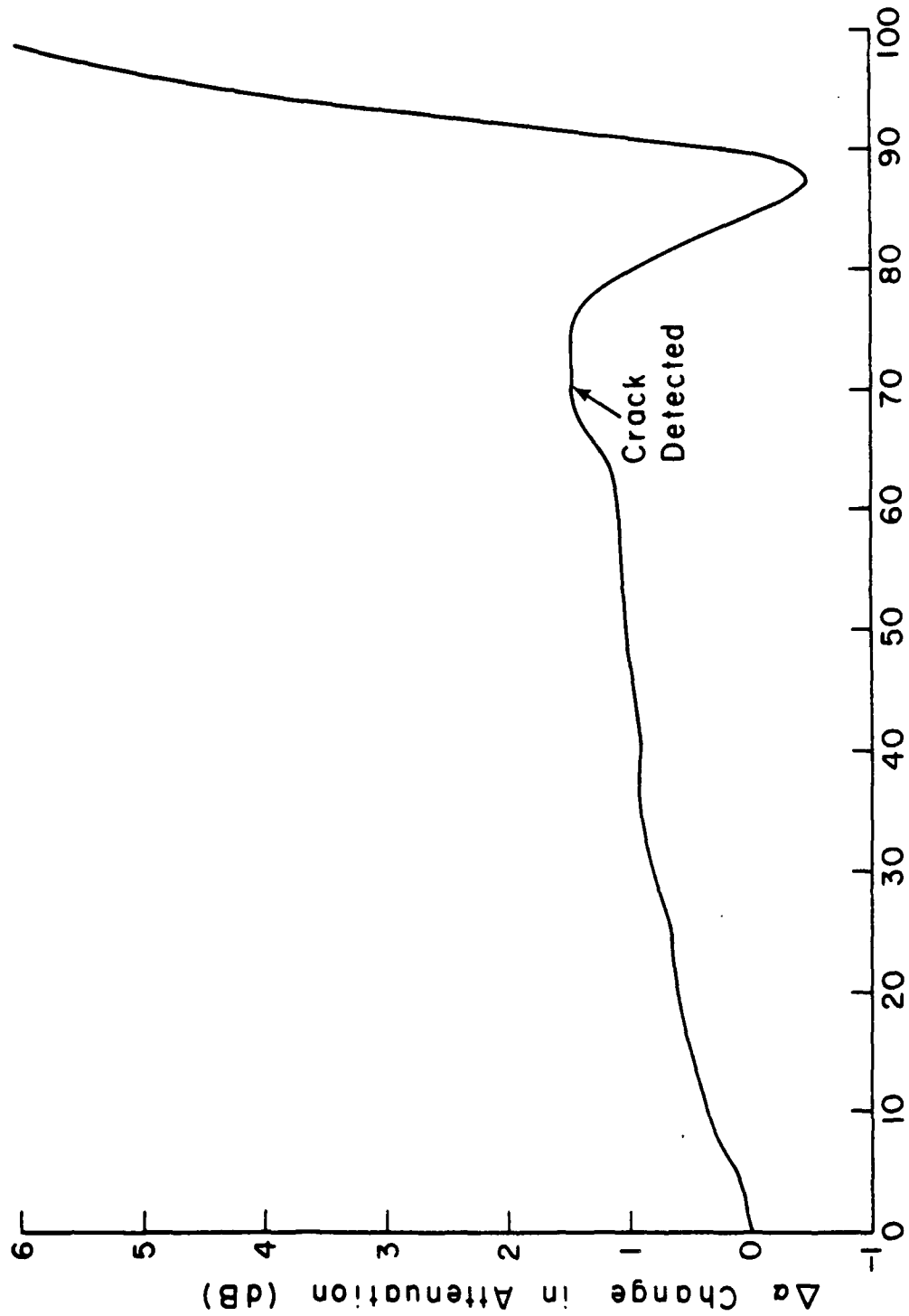

FIGURE 21. ATTENUATION DATA FROM FATIGUE TEST OF ANNEALED 7075 SPECIMEN

is believed to be due to work hardening caused by an increase in dislocation density, especially on the surface, with increasing fatigue cycles. This behavior is not expected or observed with the already high dislocation density 7075-T651 aluminum. It is also not observed in annealed specimens fatigued at low amplitudes of bending. Perhaps work hardening is less severe and more recoverable at lower amplitudes of bending. Immediately after crack formation the attenuation often decreased in specimens fatigued at high amplitudes. Two possible explanations for this are that the dislocation density was still low in the remaining uncracked material or that the orientation of the crack tip caused an unusual reflection or wave cancellation to occur. Eventually the energy reflected from the propagating crack dominated and caused the attenuation to increase rapidly till failure.

In addition to 7075 aluminum, T-bar specimens of 2024-T4 were tested. The change in attenuation with fatigue life exhibited by these specimens was similar to that of the 7075-T651 aluminum specimens. A plot of the change in attenuation versus percent fatigue life for a typical 2024-T4 aluminum specimen is displayed in Fig. 22.

In general, the time, place, and extent of crack initiation are determined by the surface condition of the specimen whereas crack propagation is governed by bulk properties. The number of fatigue cycles required to initiate a crack and thus the total fatigue life, will vary greatly from specimen to specimen if the surfaces are not uniform, as is the case for specimens

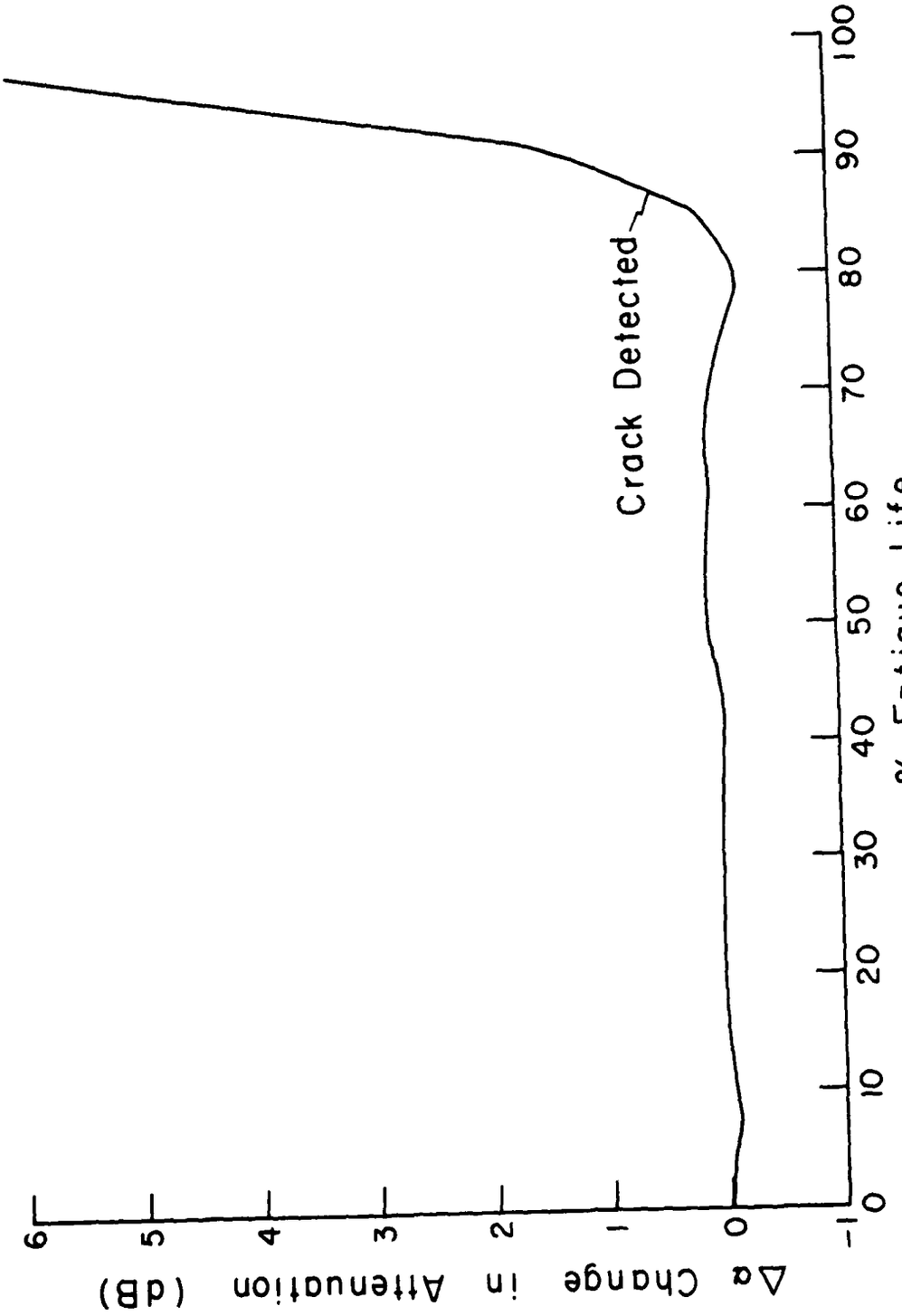

FIGURE 22. ATTENUATION DATA FROM FATIGUE TEST OF 2024-T4 SPECIMEN IN AS-RECEIVED CONDITION

tested in the as-received condition. However, the number of cycles from crack initiation to fracture will be relatively constant from test to test if the material through which the crack propagates is reasonably stress-free, as in the case with annealed specimens. For these reasons, the number of cycles between crack initiation and specimen fracture can be correlated with applied bending amplitude while the number of cycles to crack initiation cannot. If early warning of fatigue failure is measured by the number of cycles between crack initiation and failure, greater early warning is expected with specimens tested at lower applied bending amplitudes.

Experimentally, an 0.5 dB change in ultrasonic attenuation or a 2.5 dB change in acoustic emission output was always found to have occurred just before or at the time of crack initiation. Crack initiation was verified by eddy current testing. Data showing the correspondence between bending amplitude and early warning are included in Table I, a compilation of results from 9 fatigue tests. Percentage (of the total test duration) early warning is included in the table to illustrate the fact that, because of large variability in the number of cycles to crack initiation, percentage early warning is not correlated with either applied bending amplitude or total test duration. This can also be seen by comparing Figs. 20 and 23, which depict results of tests wherein the same degree of early warning (approximately 80%) could be calculated despite large differences in applied bending amplitude (6.25 mm vs. 7.05 mm) and total test duration (6.0×10^6 cycles vs. 1.7×10^6 cycles).

Specimen Number	Bending Amplitude (mm)	Bending Stress (Units of 10^3 psi)	Cycles to Fracture or Termination (Thousands)	Cycles to Fracture After 0.5 dB Change in Acoustic Emission (Thousands)	Cycles to Fracture After 2.5 dB Change in Acoustic Emission (Thousands)	Percentage Fatigue Life Remaining After 0.5 dB Change in Attenuation	Percentage Fatigue Life Remaining After 2.5 dB Change in Acoustic Emission
725-0	6.49	20.3	149	-	75	-	50
726-0	5.99	18.7	200	-	97	-	49
727-0	5.50	17.2	359	301	-	84	-
728-0	4.95	15.5	591	323	-	55	-
739-0	4.15	13.0	1195	355	161	30	14
730-0	3.97	12.4	1680	538	323	32	19
731-0	3.48	10.9	3671	538	538	15	15
735-0	3.48	10.9	31154	570	-	2	-
733-0	3.33	10.4	5973	1130	1011	19	17

TABLE I. EXPERIMENTAL RESULTS-ANNEALED 7075 ALUMINUM

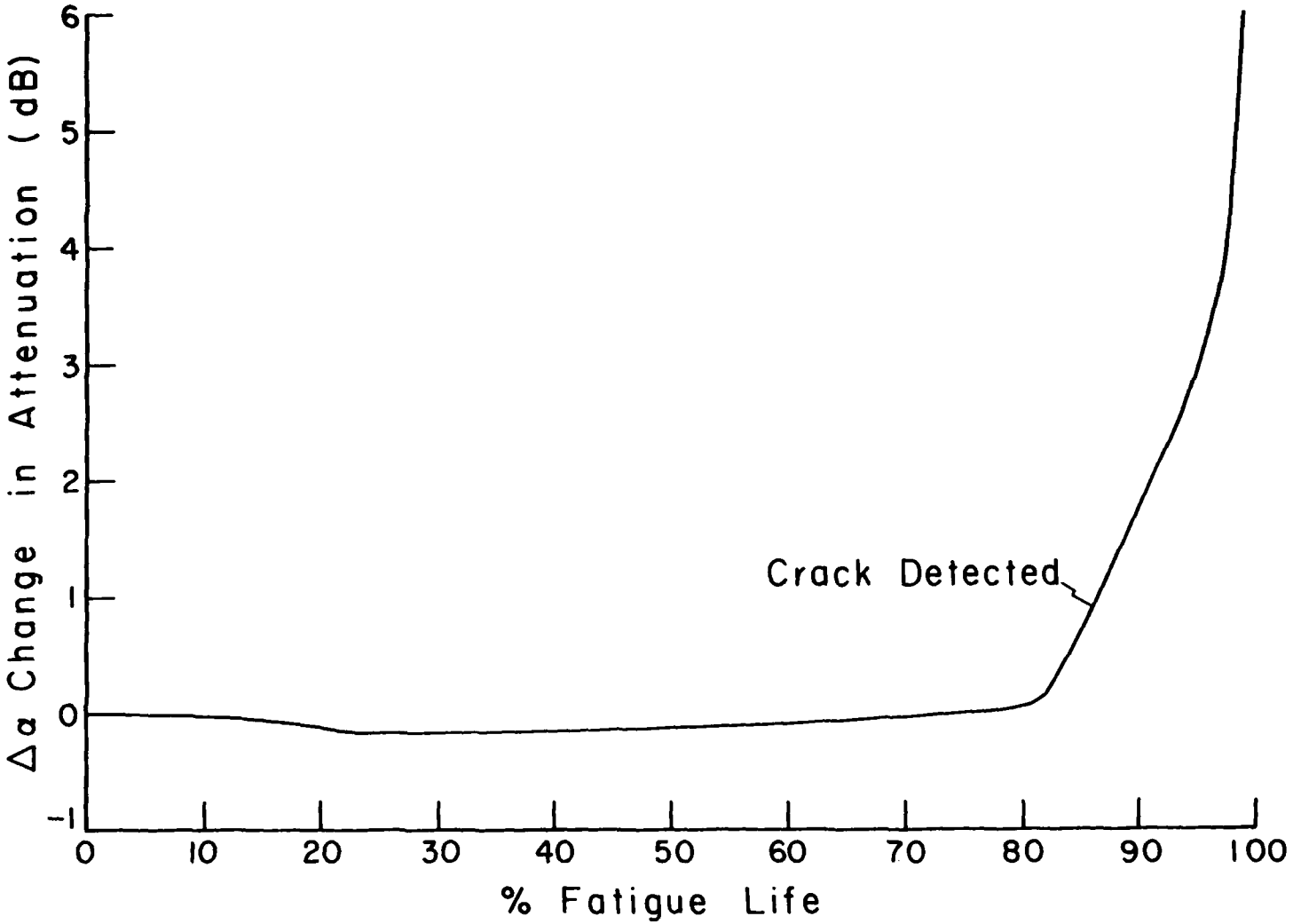

FIGURE 23. ATTENUATION DATA FROM FATIGUE TEST OF 7075-T651 SPECIMEN IN AS-RECEIVED CONDITION (Bending amplitude 7.05 mm, test duration 1.7×10^6 cycles)

Acoustic Emission Measurements and Results

Acoustic emission data was gathered using the two systems described earlier. In the absence of any a priori information suggesting a different approach, the frequency responses of the two systems were selected to be approximately equal. As expected, the observed differences in system performance and in the data itself from the two systems is negligible. In contrast to the situation with ultrasonic attenuation monitoring, considerable acoustic emission activity in the form of burst emission transpired early in the fatigue tests. A typical set of burst waveforms, one from each system, is shown in Fig. 24. The relatively long, 1.5 m sec., duration of the bursts is attributable to multiple reverberations inside the specimens. The one way travel time along the specimen length is 50 μsec. The different transducer resonances of the two acoustic emission systems can be clearly seen in Figs. 25 and 26. The burst captured through the Trodyne system has a maximum amplitude in the frequency spectra at 100 kHz whereas the burst captured through the Admiralty system has a maximum amplitude at 400 kHz. The presence of many sharp peaks in both spectra, rather than a smooth, more continuous curve, supports the hypothesis that high order vibrational modes are present.

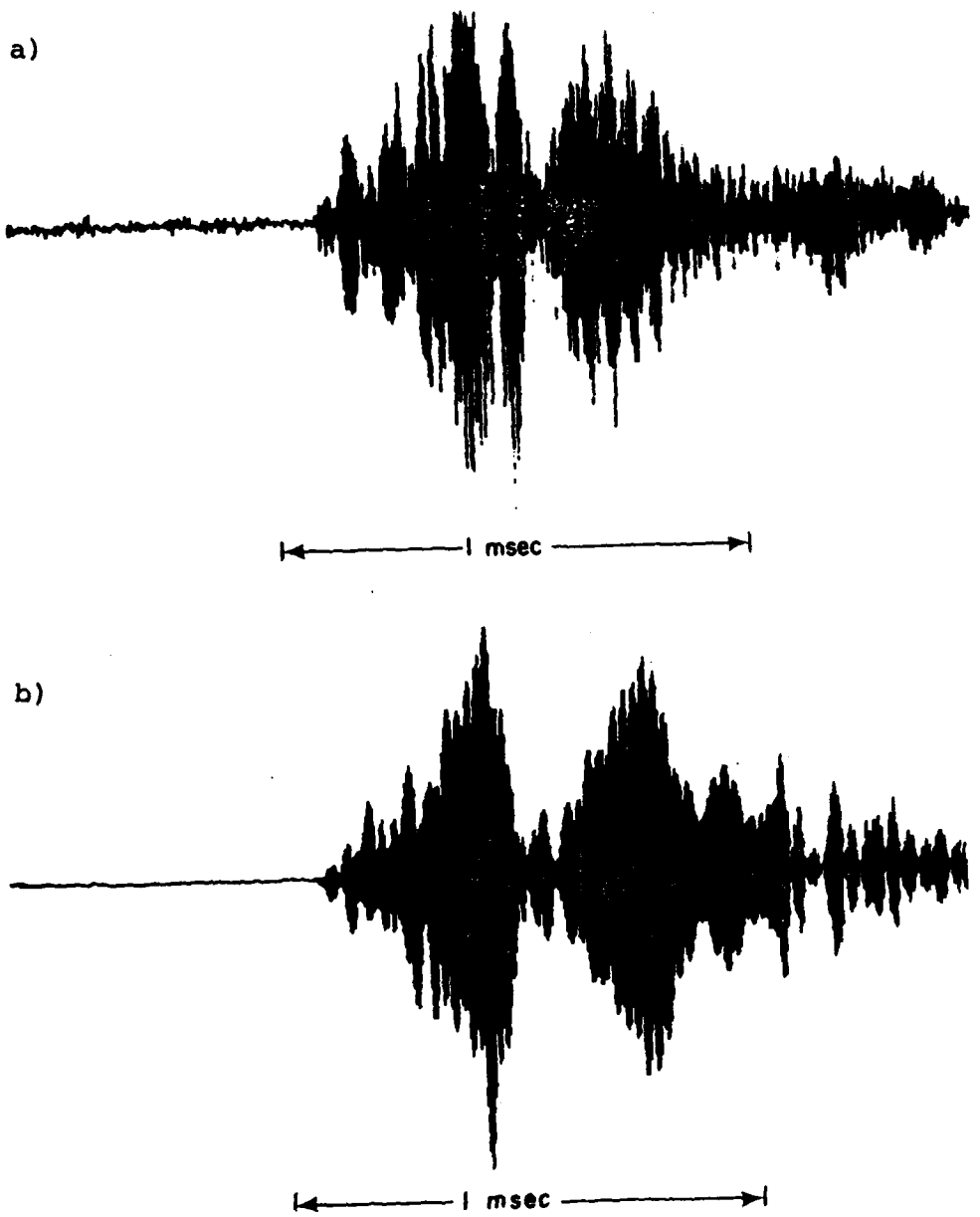

FIGURE 24. TYPICAL MULTIPLE ACOUSTIC EMISSION BURST
a) Admiralty System
b) Trodyne System

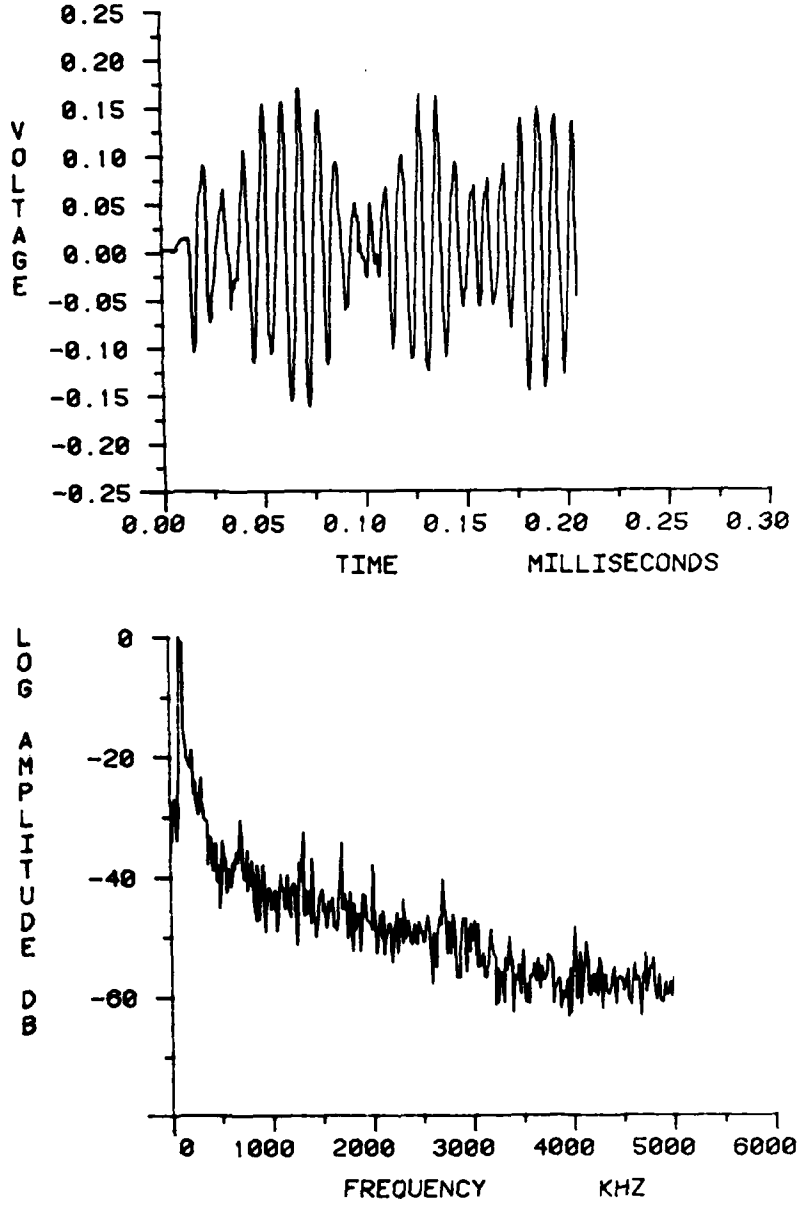

FIGURE 25. TIME AND FREQUENCY DOMAIN ACOUSTIC EMISSION(AE) DATA BEFORE CRACK INITIATION 7075-T651 ALUMINUM (TRODYNE SYSTEM)

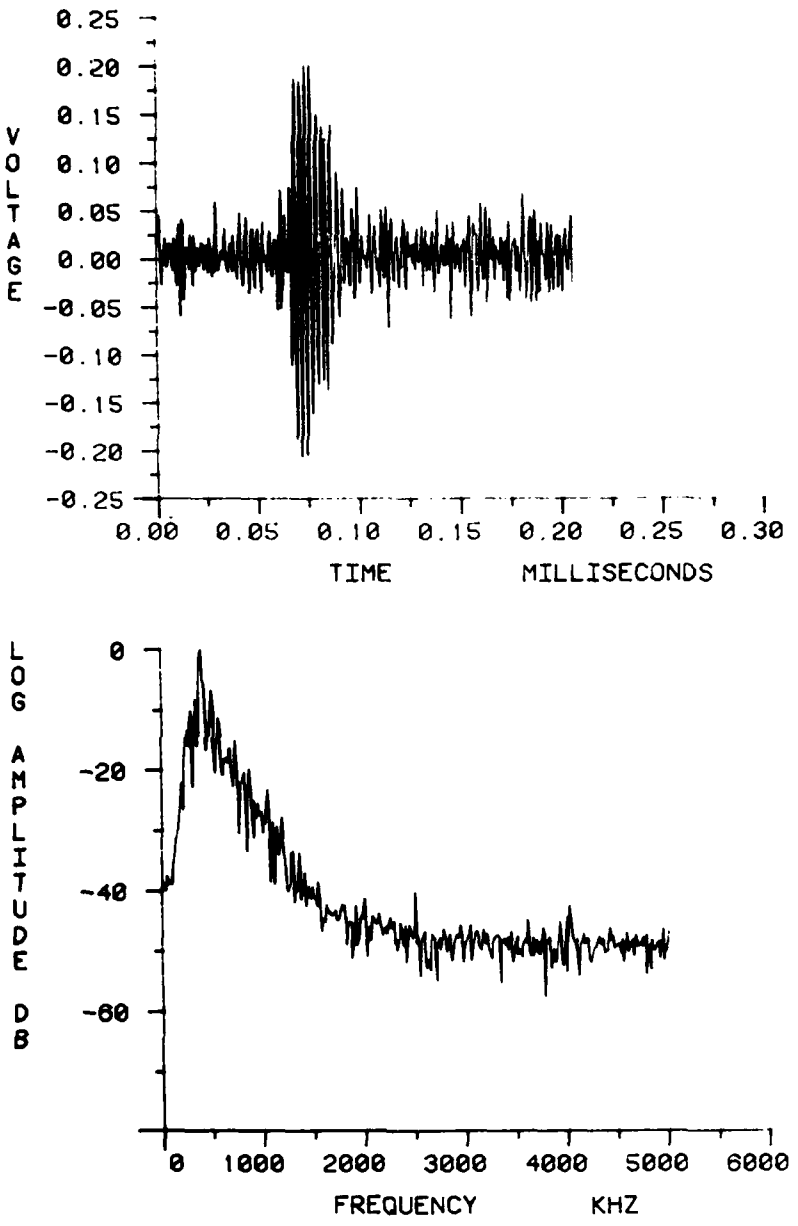

FIGURE 26. TIME AND FREQUENCY DOMAIN AE DATA BEFORE CRACK INITIATION (ADMIRALTY SYSTEM)

Acoustic emission waveforms were obtained at intermittent stages of the aluminum alloy T-bar specimen fatigue tests. To allow evaluation of the effects of machine induced noise, waveforms were also obtained for acoustic emission specimens loaded statically (gripping the specimen by hand) rather than dynamically (i.e., loaded by the fatigue machine). Fast Fourier Transform (FFT) computations were used to generate frequency spectra from the time domain waveforms. Interpretation of the frequency spectra requires consideration of the instrumentation frequency response measured as described earlier. The Trodyne system was used for the frequency spectra work about to be presented here.

Figures 27, 28, 29 and 30 show typical frequency spectra for acoustic emission bursts recorded during fatigue testing. In Fig. 27, both bursts occurred when the surface of the specimen where the crack initiated was in dynamic tension. The upper half of Fig. 27 shows the spectrum of a burst that occurred prior to crack initiation and the lower half shows the spectrum of a burst that occurred after crack initiation. The burst resulting from the crack being pulled in tension (Fig. 27(b)) has relatively more energy in the higher frequencies than does the burst captured prior to crack initiation (Fig. 27(a)). Although it is not apparent in the frequency spectra, because all spectra were normalized to the amplitude of the largest spectral component, the

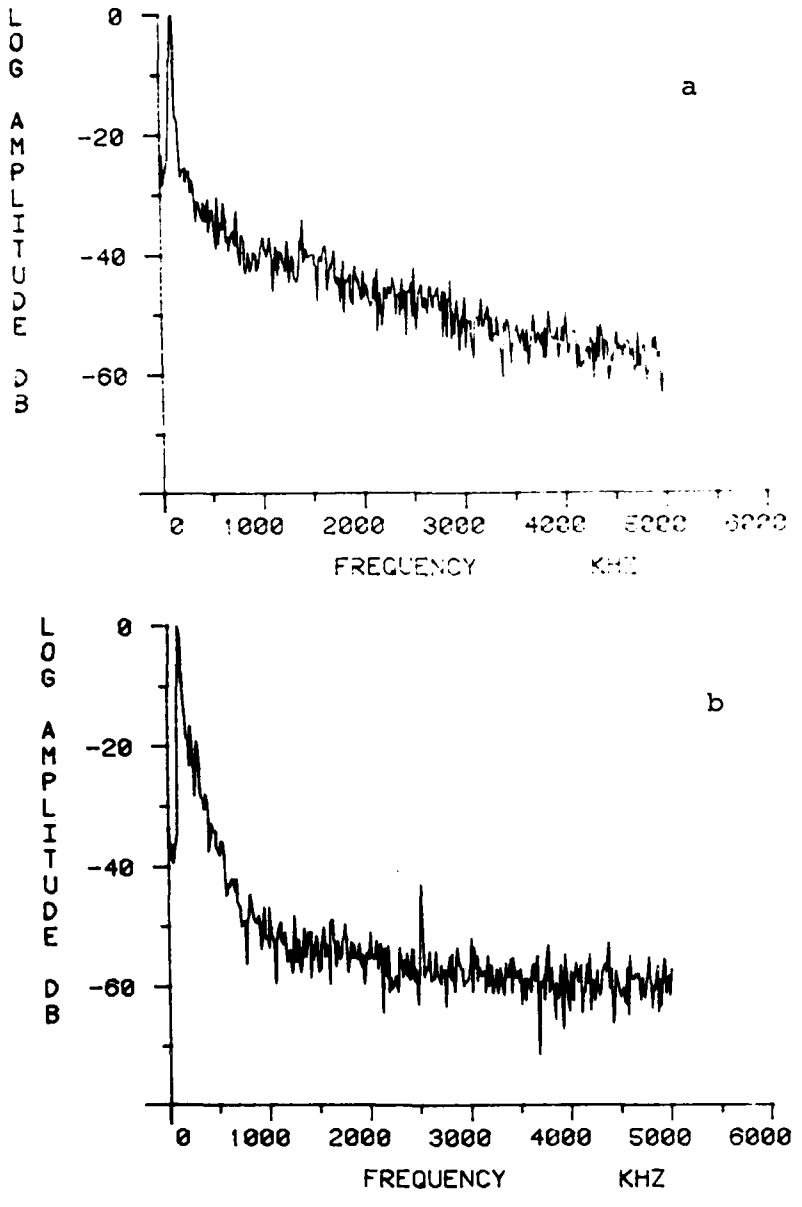

FIGURE 27. FREQUENCY DOMAIN AE DATA BEFORE AND AFTER CRACK INITIATION (TRODYNE SYSTEM)
a) before, b) after

after-crack burst was of larger amplitude than the precrack burst.

Figure 28 shows typical frequency spectra of acoustic emission bursts due to dynamic loading of the crack in compression (Fig. 28(a)) and tension (Fig. 28(b)). The bursts are of similar amplitude and have several frequency component peaks in common. At various times during the fatigue test, the fatigue machine was stopped and the specimen was hand loaded statically. Figures 29(a) and 29(b) compare the frequency spectra of two acoustic emission bursts resulting from static and dynamic loading, respectively at approximately the same number of cycles into the fatigue test. Because the specimen was loaded by hand, machine noise was largely removed; therefore the higher frequency spectral components appear relatively larger in the normalized frequency spectrum. Additionally, a large amount of energy in the low frequencies is primarily attributable to the frequency response of the Trodyne acoustic emission system and transducer (see Fig.2) which greatly colors the true signal.

Figures 30(a) and 30(b) compare the frequency spectra of two acoustic emission bursts occurring when the fatigue crack was statically loaded in tension at two different times when the fatigue test was interrupted. Both spectra have several peaks in common: 1300, 1700, 2000, 2700, and

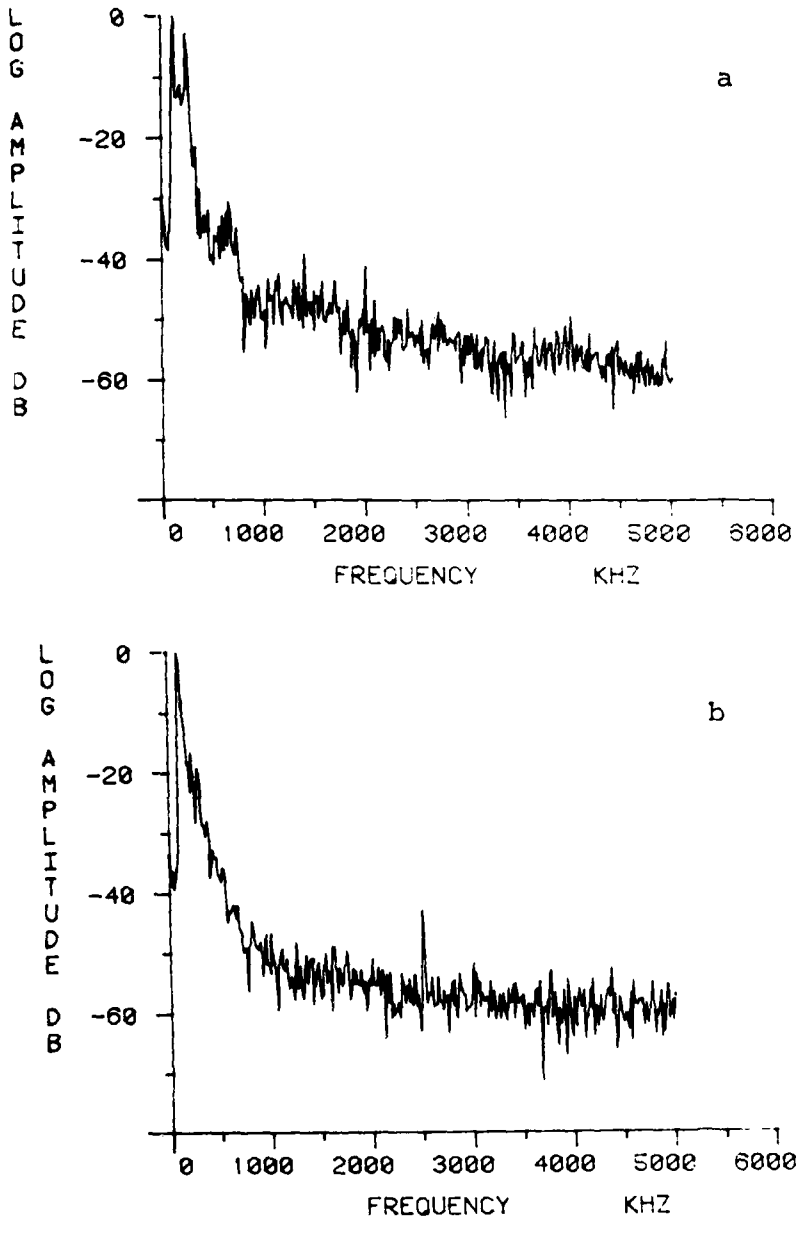

FIGURE 28. FREQUENCY DOMAIN AE DATA FROM COMPRESSION AND TENSION OF A FATIGUE CRACK(TRODYNE SYSTEM)
a) compression, b) tension

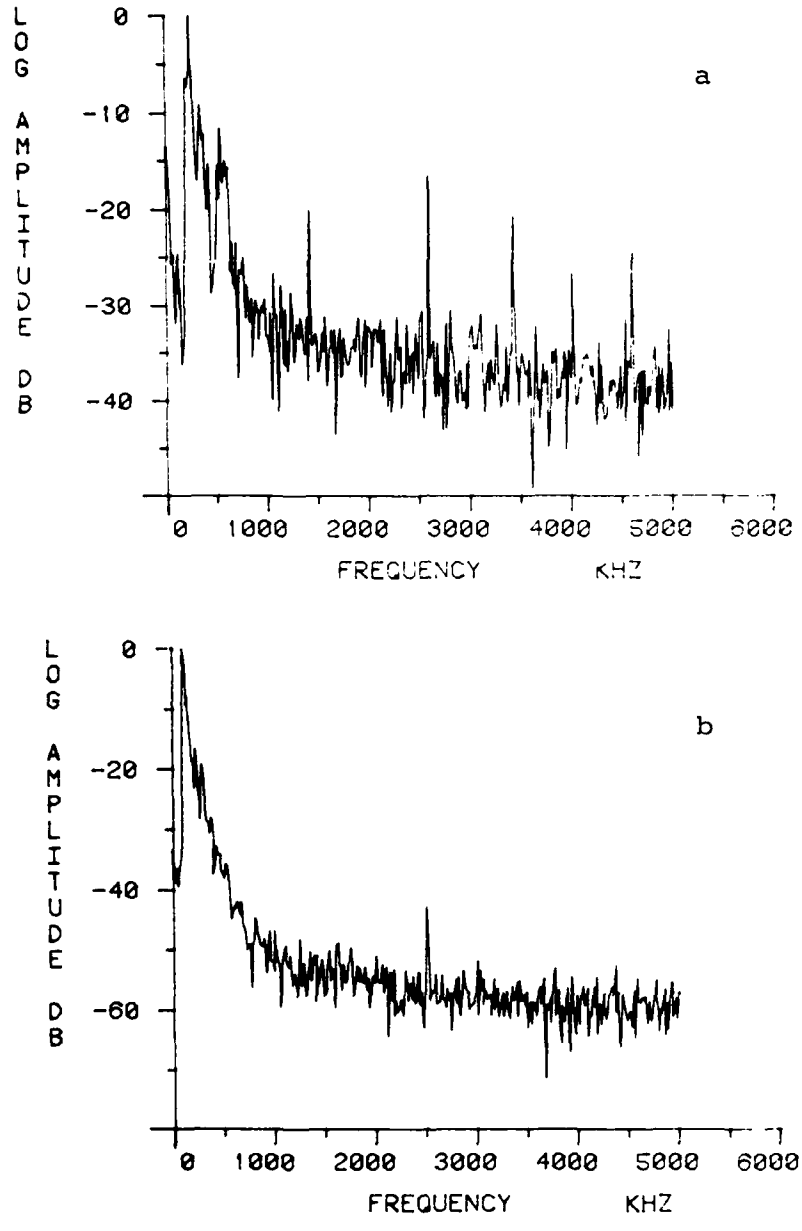

FIG. 39. FREQUENCY DOMAIN AE DATA FROM STATIC AND DYNAMIC LOADING OF A FATIGUE CRACK (TROPYNE SYSTEM)
a) static, b) dynamic

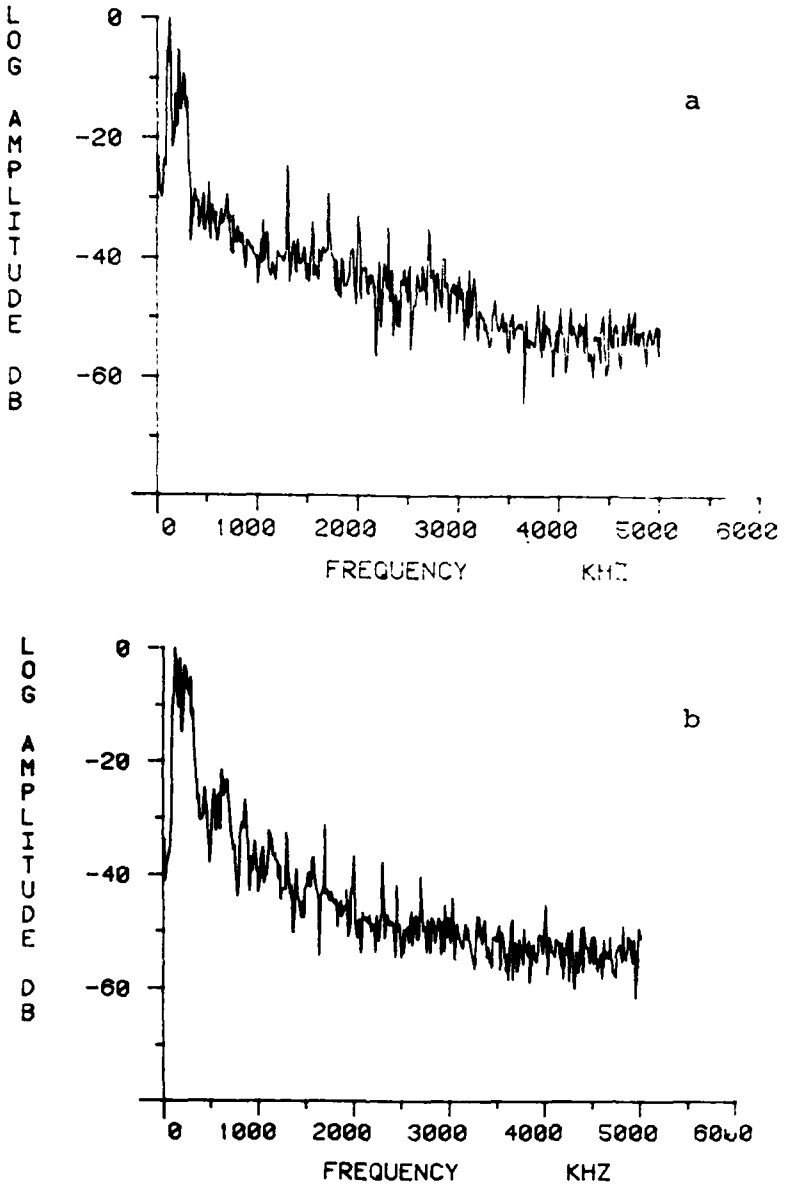

FIGURE 30. FREQUENCY DOMAIN AE DATA FROM STATIC LOADING OF CRACK AFTER INITIATION AND BEFORE FAILURE
a) after initiation
b) before failure

2800 kHz. The spectrum in Fig. 30(b) has a higher amplitude than the spectrum in Fig. 30(a). The burst whose FFT is shown in Fig. 30(b) occurred later in the fatigue test than the burst whose FFT is shown in Fig. 30(a). Thus the crack was larger and advancing more rapidly so a higher amplitude emission would be expected.

Figure 31 shows the time domain waveform (a) and the frequency spectrum(b) of the noise in the Trodyne acoustic emission system. The noise energy is fairly evenly distributed over the spectrum and the effect of the 3 mHz filter cut-off is clearly evident.

The trends revealed by continuous monitoring of acoustic emission also provided insight into the fundamental nature of fatigue damage. In Fig. 32 the relative changes in the averaged rms voltage output of both the Admiralty and Trodyne systems are displayed. As can be seen, the overall acoustic emission level increased when a crack formed and propagated. It was conjectured that the bulk of high amplitude acoustic emissions after crack initiation were due to the newly created crack walls abrading against each other during subsequent fatigue cycles. To test this hypothesis, an electronic switch was used to allow the acoustic emission output signals originating at different parts of the load cycle to be separately metered. The switch was synchronized

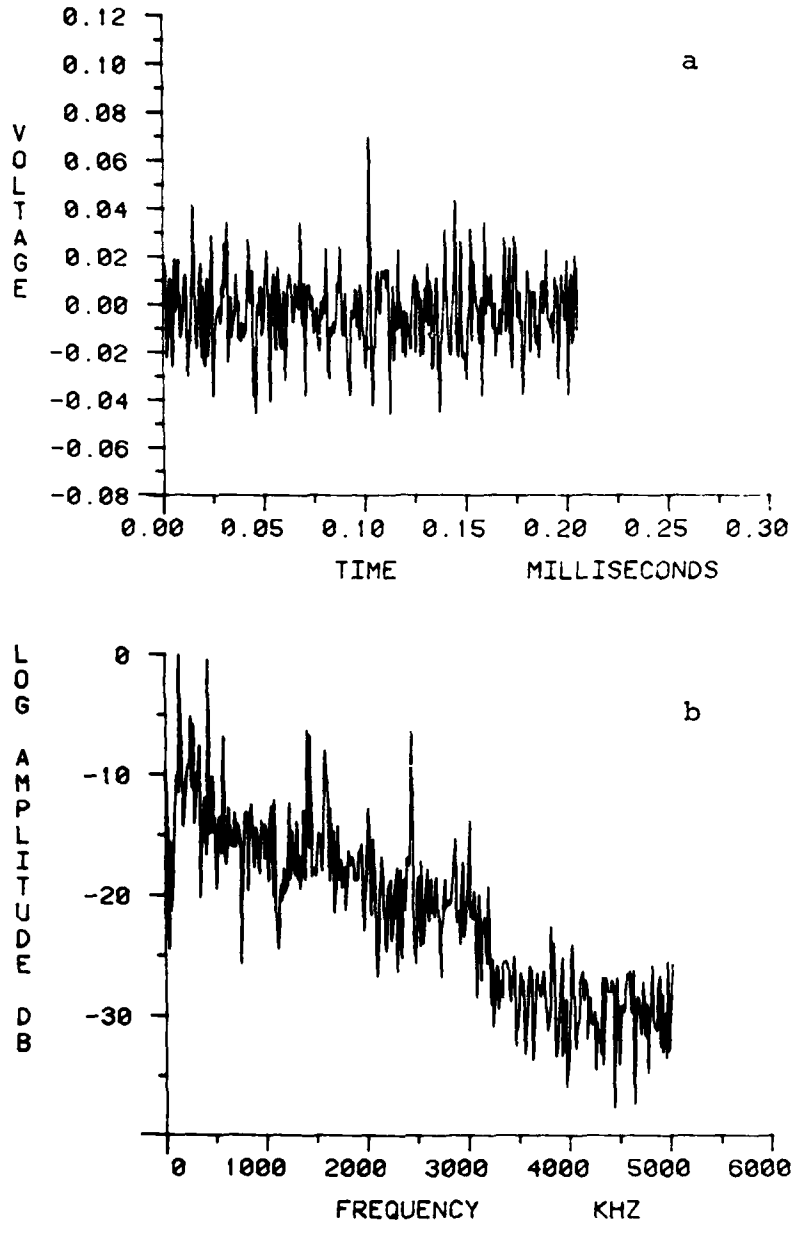

FIGURE 31. TIME AND FREQUENCY DOMAIN DATA FROM TRODYNE SYSTEM NOISE TESTS

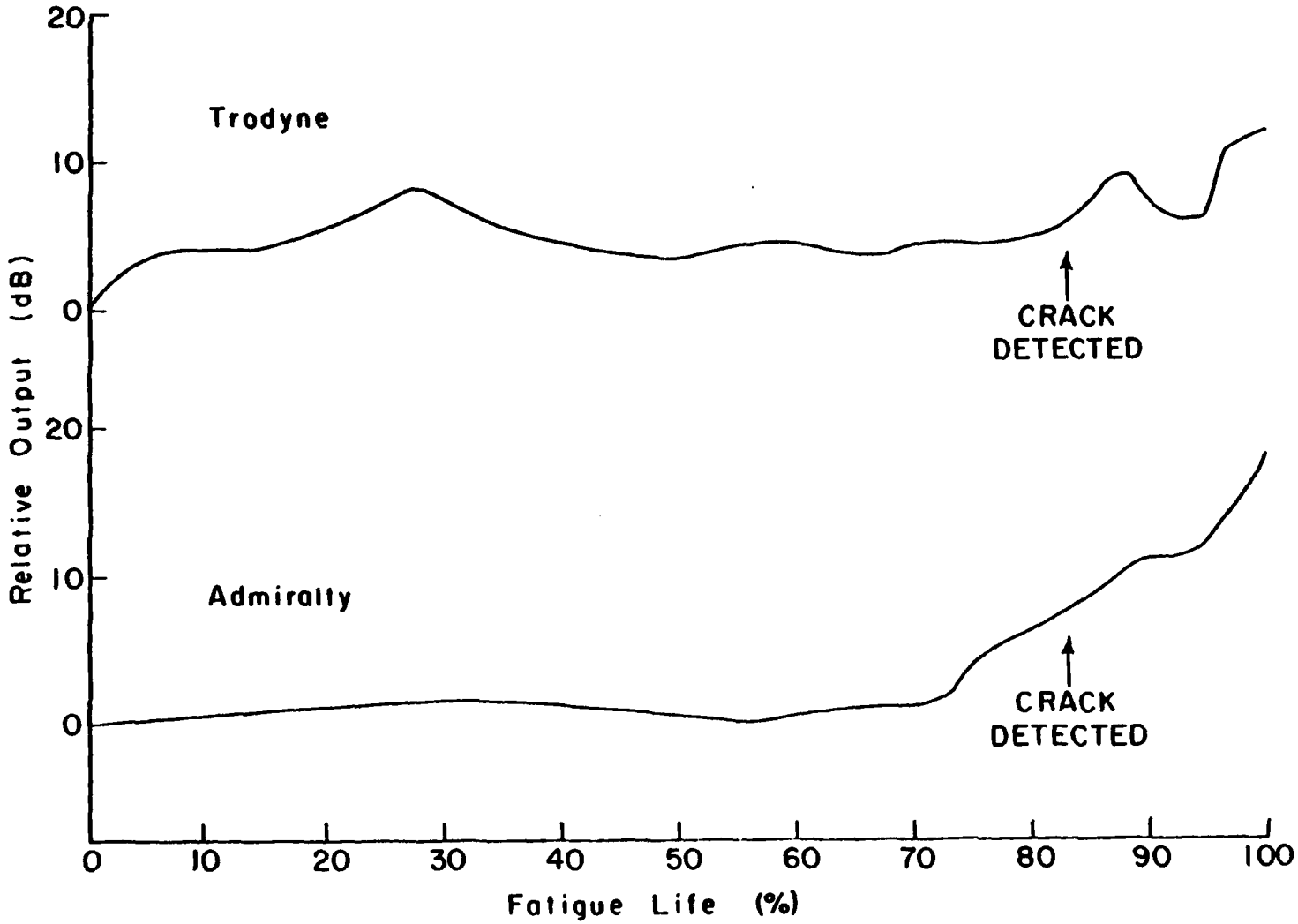

FIGURE 32. TYPICAL RMS AE DATA FROM FATIGUE TEST OF 7075-T651 SPECIMEN IN AS-RECEIVED CONDITION

with the fatigue machine so that two equal parts of the load cycle were separated, one half corresponding to the upper surface of the specimen in compression and the other half corresponding to the same surface of the specimen in tension. This enabled separate recording of acoustic emissions due to crack wall abrasion and acoustic emissions due to crack propagation. The specimen position for each of these two cases is illustrated in Fig. 33. These results showed the largest contribution to the rms acoustic emission level after crack initiation was the acoustic emission caused by the crack propagating and not the acoustic emission caused by the crack wall rubbing. This behavior is clearly shown in Fig. 34 where the rms output from both halves of the fatigue cycle are plotted versus percent fatigue life for a 7075-T651 aluminum specimen.

Eddy Current Examination

A Halec eddy current-crack detector unit, shown in Fig. 35, was used to locate surface-breaking fatigue cracks after the occurrence of a significant change in either ultrasonic attenuation or acoustic emission levels. This instrument operated at a frequency of 3 MHz and was therefore only sensitive to surface-breaking cracks. A pencil-shaped eddy current probe with a rounded tip enabled detection of surface cracks down to 1/16" long. An advantage of the rounded probe

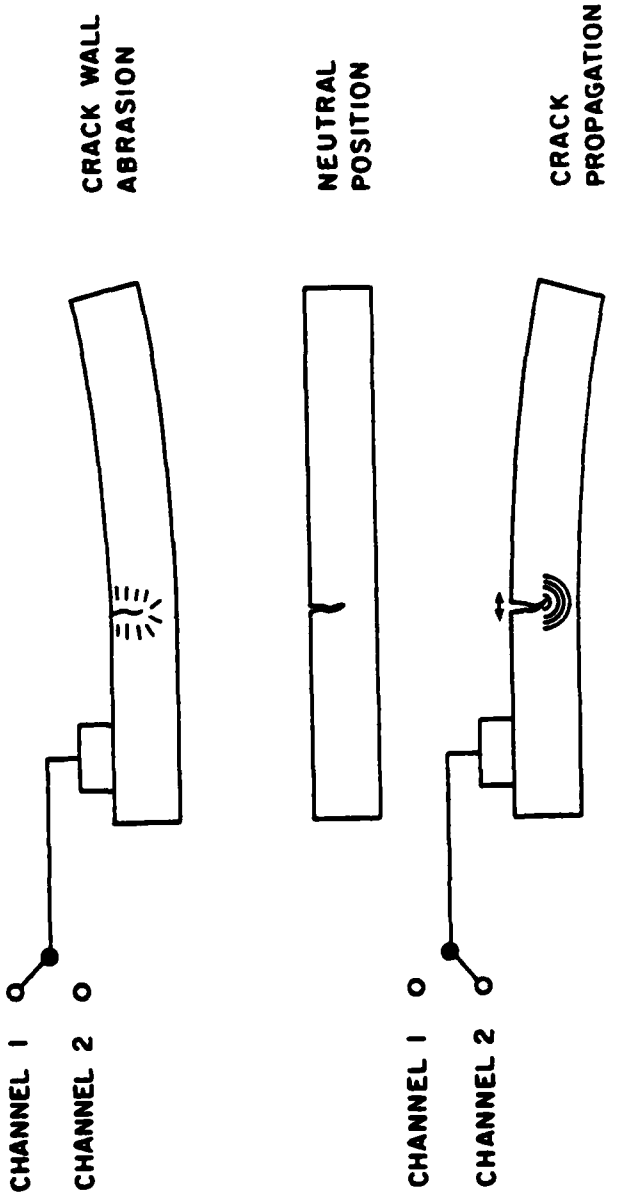

FIGURE 33. SPECIMEN POSITIONS DURING CRACK WALL ABRASION AND CRACK PROPAGATION

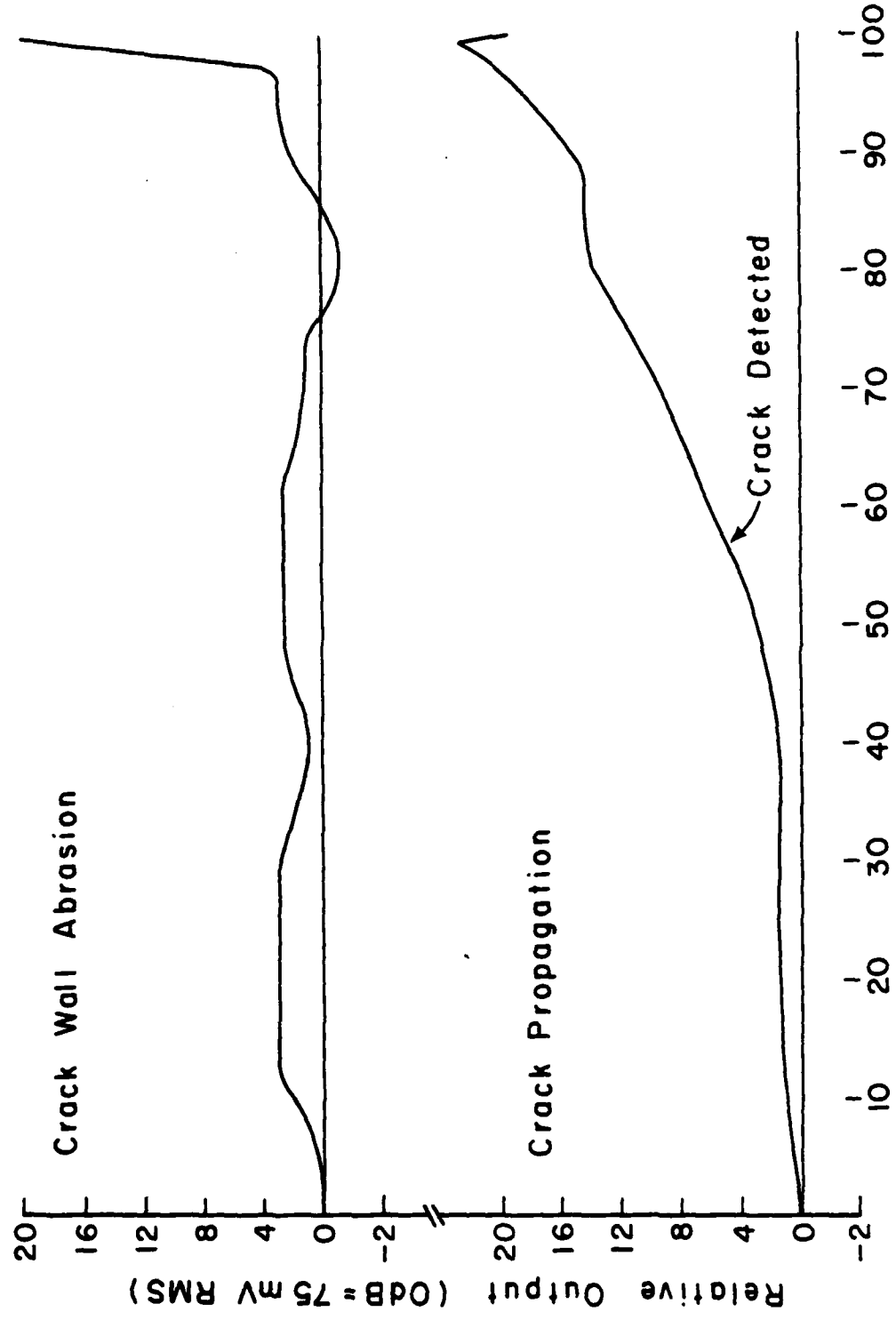

FIGURE 34. TYPICAL RMS DATA FROM CRACK WALL ABRASION AND CRACK PROPAGATION DURING FATIGUE TEST (TRODYNE SYSTEM)

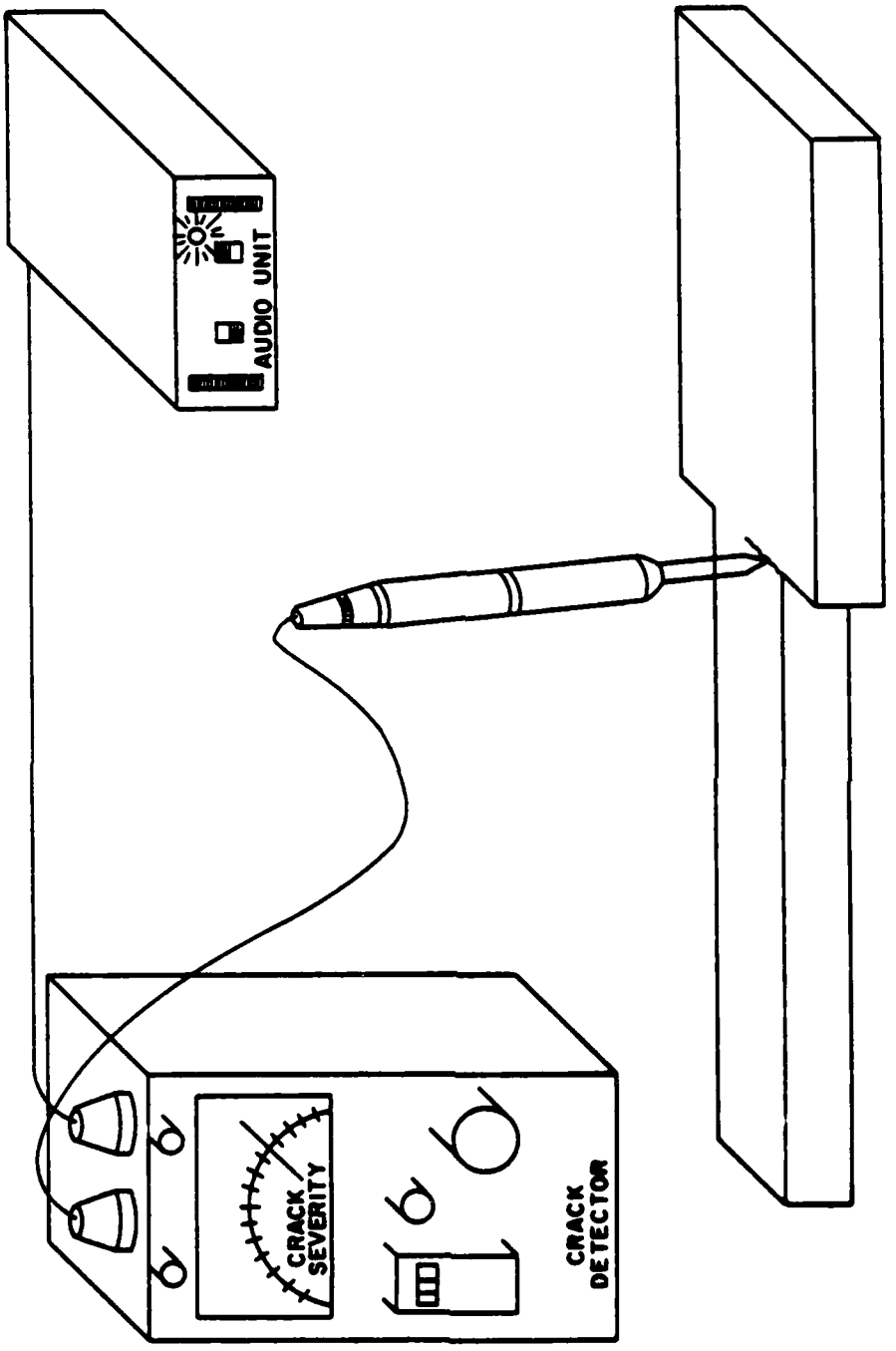

FIGURE 35. EDDY CURRENT SCANNING OF A FATIGUE CRACK

tip was its insensitivity to departures of as much as 15 degrees from the ideal angular orientation normal to the specimen surface

Eddy current response is affected not only by specimen dimensions, geometry, and surface discontinuities, but also by the electrical conductivity and magnetic permeability of the specimen material. However, for fatigue cycled aluminum any such changes are concentrated near the crack and thus contribute to the eddy current indication from the crack itself. Since changes in the total volume of metal beneath the probe affect the eddy current signal, the probe was typically maintained at least 1/8 in. from all specimen edges during scanning (scans nearer to a specimen edge could be made only with the use of special procedures). At this distance the induced eddy currents due to edge effects are too small to affect instrument response. The utility of eddy current scanning of fatigue specimens is enhanced by the fact that the geometry of a typical fatigue crack (tight and deep) is optimal for eddy current detection. A previously used rectangular bar specimen design had to be changed to a T-shaped specimen design to permit eddy current probe access to the fatigue damaged region. The eddy current examination was performed at stated intervals and when appropriate indications were obtained from the ultrasonic attenuation and acoustic emission monitoring. As described

previously, a cut-off circuit was used to stop the fatigue test when a specified change in attenuation occurred. Then eddy current scanning was used to test for the presence of a surface crack. It is interesting to note that every positive eddy current crack indication could be verified using optical microscopy. Due to the symmetric loading, there were four highly probable sites for crack initiation on each specimen. These sites were located at the four corners of the reduced cross-section shoulder. The presence of multiple potential crack initiation sites precluded any simple continuous eddy current monitoring.

After the existence of a crack was confirmed, further eddy current scanning was employed in order to determine the length and relative severity of the crack. A series of scans for a typical fatigue specimen is shown in Fig. 36. The eddy current pencil probe was used to scan along the specimen length at 0.01 in. intervals starting 0.1 in. from the specimen edge. The amplitudes of the peaks represent the relative crack depth at different locations along its length. The positions of the peaks represent the position of the crack along the scanned specimen length. The scans shown in Fig. 36 indicate that the crack scanned was perpendicular to the specimen length and originated at the top edge of the scanned width. This scanning procedure gave a very accurate and fast method of crack location and relative

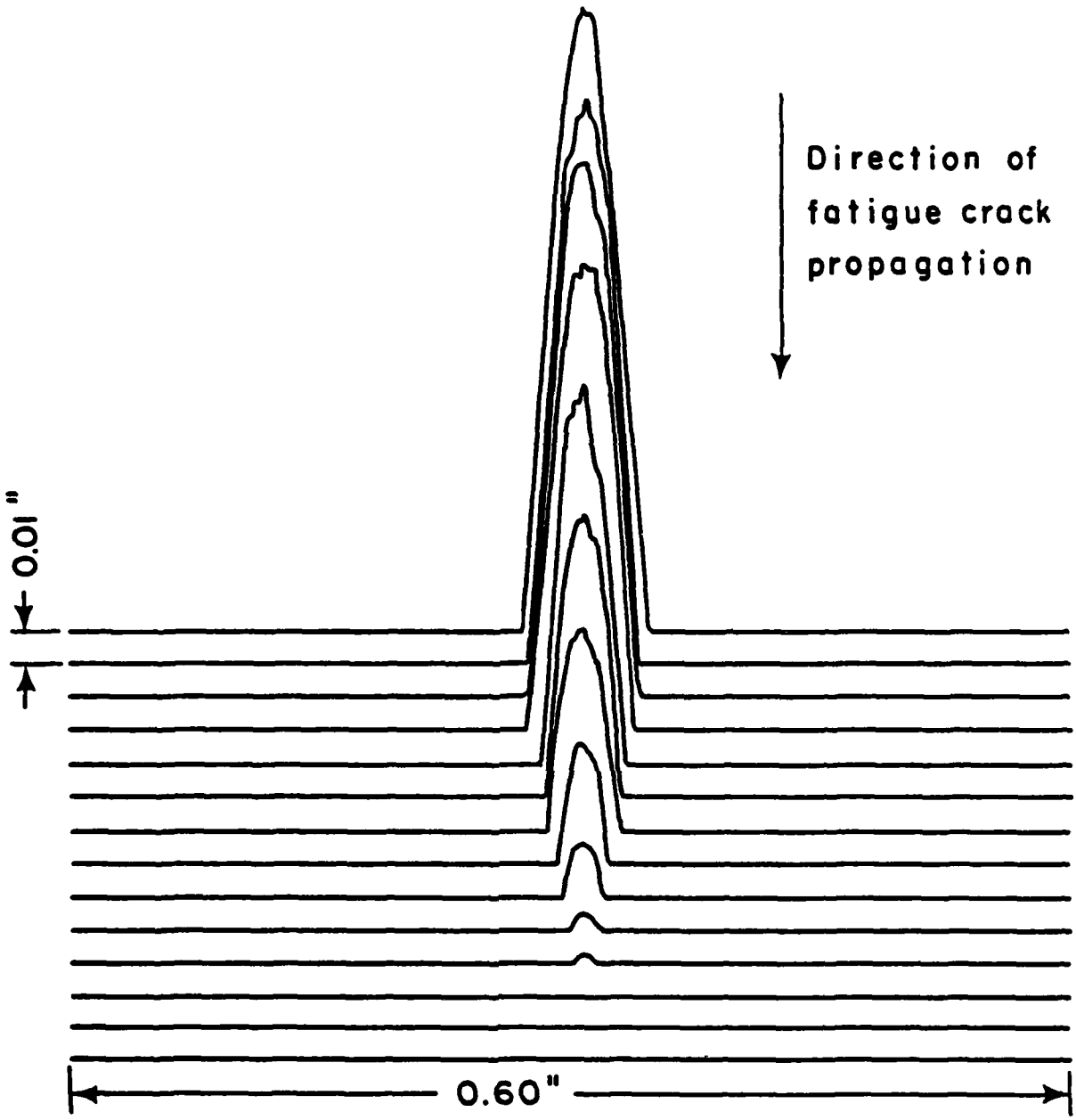

FIGURE 36. MULTIPLE EDDY CURRENT SCANS OF A SURFACE FATIGUE CRACK

size. When the fatigue test was continued to specimen fracture, the propagation of the crack across the specimen surface could be easily monitored using eddy current scanning. This was of particular importance when testing specimens with as-received surfaces, because the crack was undetectable visually in its early stages.

Metallographic Examination

After the presence of a crack was detected by a change in ultrasonic attenuation or acoustic emission and verified by eddy current probing, the fatigue test was either continued until specimen fracture or terminated to allow metallographic examination. In cases where the specimen fractured, the fracture surfaces were examined under low magnification to determine the site of crack initiation. A representative set of fracture surfaces was examined using an ISI Model 60A scanning electron microscope (SEM) at magnifications up to 3800X. The exceptional depth of field afforded by the scanning electron microscope aided the identification of voids and intermetallic particles on the specimen fracture surface. In the cases where the fatigue test was terminated prior to fracture, the region of the specimen surface close to the crack was carefully examined with a Bausch and Lomb metallographic microscope. Subsequent to this surface examination, the specimen was sectioned, mounted in a metallographic mount and etched to delineate the microstructure.

The specimen microstructure was examined for the presence of regions of high plastic deformation such as deformation bands, and for the effects of grain boundaries, inclusions, and precipitates on crack propagation.

Metallographic analysis performed on the fatigue specimens showed several interesting features. Figure 37 indicates the location of the fracture surfaces shown in the scanning electron micrographs of Figs. 38 through 42. Examination of the fracture surface of 7075-T651 aluminum specimens with high surface polish revealed many voids, and voids containing intermetallic particles. Figure 38 shows a void with an intermetallic particle at its base and a void with a microcrack running through it. In Fig. 39 a void containing a fractured intermetallic particle is shown. Fractured intermetallic particles are not uncommon since they are, in general, more brittle than the matrix material. The propagation of microcracks and fracture of intermetallic particles are two likely sources of the acoustic emission observed before and during macrocrack propagation leading to failure. Fatigue striations indicating extensive localized plastic deformation, like those in Fig. 40, are easily observed at 800X on the fracture surfaces of the 7075-T651 aluminum specimens. As mentioned previously, the high surface polish specimens sustain more bulk damage prior to surface macrocrack formation than their as-received surface counterparts. Comparison of

AD-A090 799 JOHNS HOPKINS UNIV BALTIMORE MD DEPT OF MATERIALS SC--ETC F/G 14/2
ULTRASONIC AND ACOUSTIC EMISSION DETECTION OF FATIGUE DAMAGE.(U)
JUL 80 S R BUXBAUM, C L FRIANT, S E FICK F44620-76-C-0081
UNCLASSIFIED AFOSR-TR-80-1069 NL

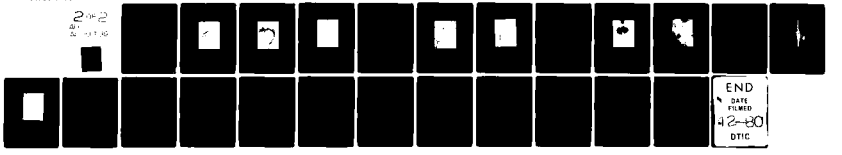

END
DATE FILMED
12-80
DTIC

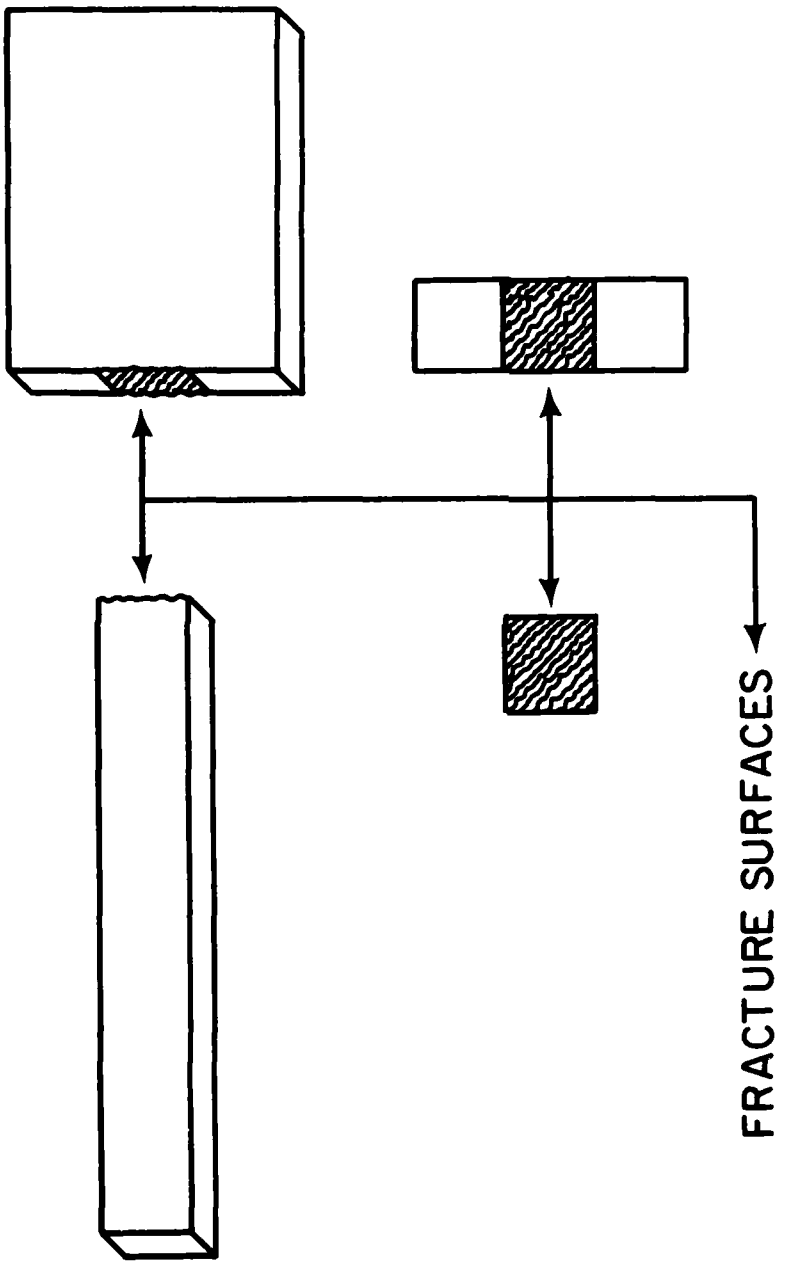

FIGURE 37. SCHEMATIC REPRESENTATION OF FRACTURE SURFACES

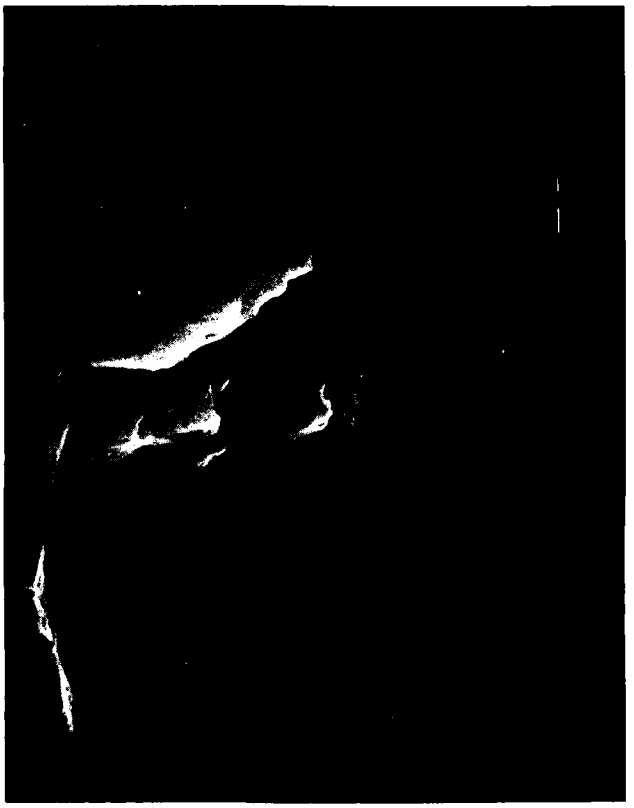

FIGURE 38. SCANNING ELECTRON MICROGRAPH(3700X)
High surface polish 7075-T651 aluminum
Void containing intermetallic particle,
microcrack running through void

FIGURE 39. SCANNING ELECTRON MICROGRAPH(3800X)
Void containing fractured inter-
metallic particle

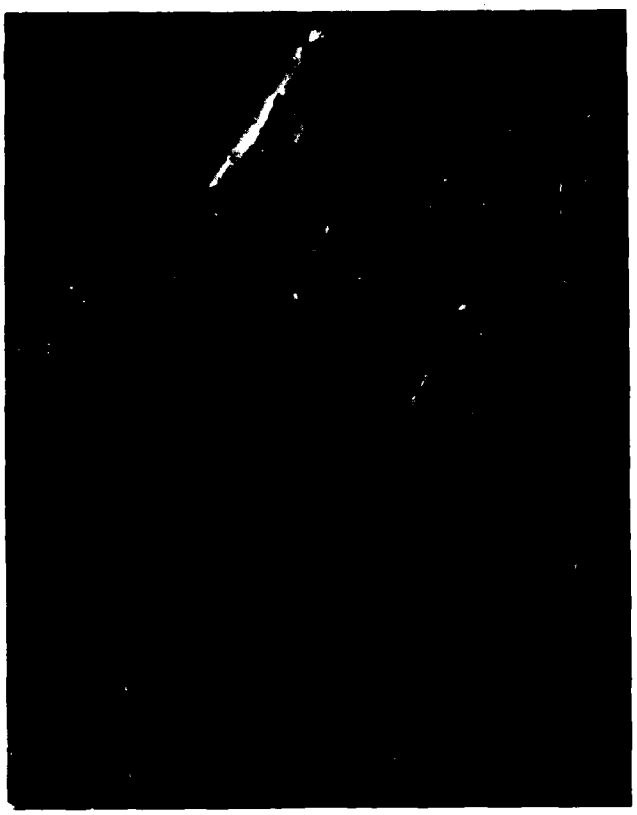

FIGURE 40. SCANNING ELECTRON MICROGRAPH(800X)
Fatigue striations on fracture surface

the fracture surfaces of each type specimen verified this fact because the high surface polish specimen's fracture surface revealed more voids and fractured intermetallic particles. Figure 41 shows a portion of the fatigue fracture surface of a 7075-T651 aluminum specimen that was tested in the as-received surface condition. The fracture surface at 650X reveals numerous voids in the matrix, aligned with two grain boundaries that run parallel to each other. The fracture surface of an annealed 7075 aluminum fatigue specimen at 100X is shown in Fig. 42. Large striations can be seen in the ductile matrix where cracks progressed toward the center from all four corners of the cross-section.

Some specimens with surface breaking cracks were removed from the fatigue machine prior to failure, and a metallurgical microscope was used to examine the cracked surfaces. Figure 43 is a schematic representation of the fatigue crack region on the specimen. Figure 44 shows the transgranular propagation of a fatigue crack in a typical as-received 7075-T651 aluminum specimen. The elongation of the grains indicates the rolling direction of the bar stock from which the specimen was fabricated. It can also be seen that the crack initiated and propagated perpendicular to the rolling direction. The path of a fatigue crack on the top surface of the specimen at high magnification is shown in Fig. 45.

FIGURE 41. SCANNING ELECTRON MICROGRAPH(650X)
As-received 7075-T651 aluminum
Void coalescence at grain boundaries

FIGURE 42. SCANNING ELECTRON MICROGRAPH(100X)
Annealed 7075 aluminum
Large fatigue striations

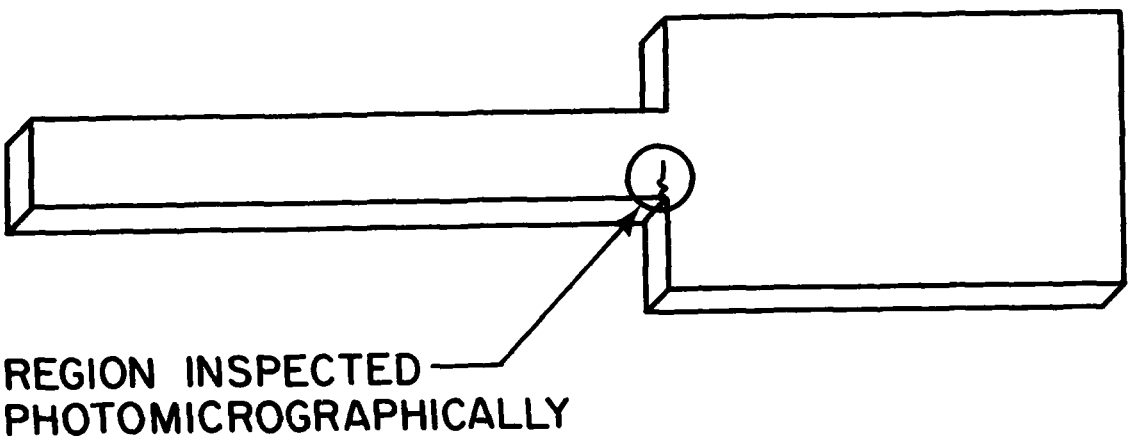

FIGURE 43. SCHEMATIC REPRESENTATION OF FATIGUE CRACK REGION

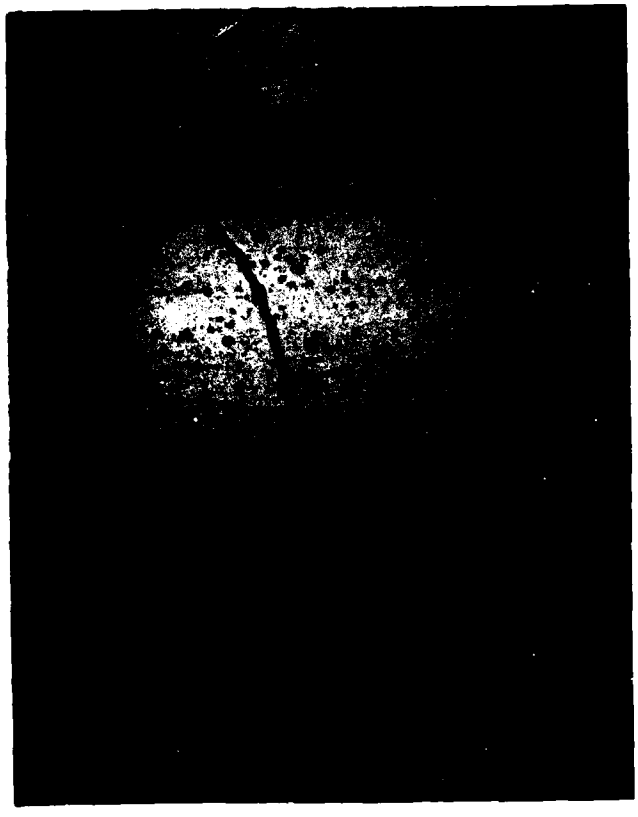

FIGURE 44. OPTICAL MICROGRAPH(70X)
As-received 7075-T651 aluminum
Fatigue crack propagating
transgranularly

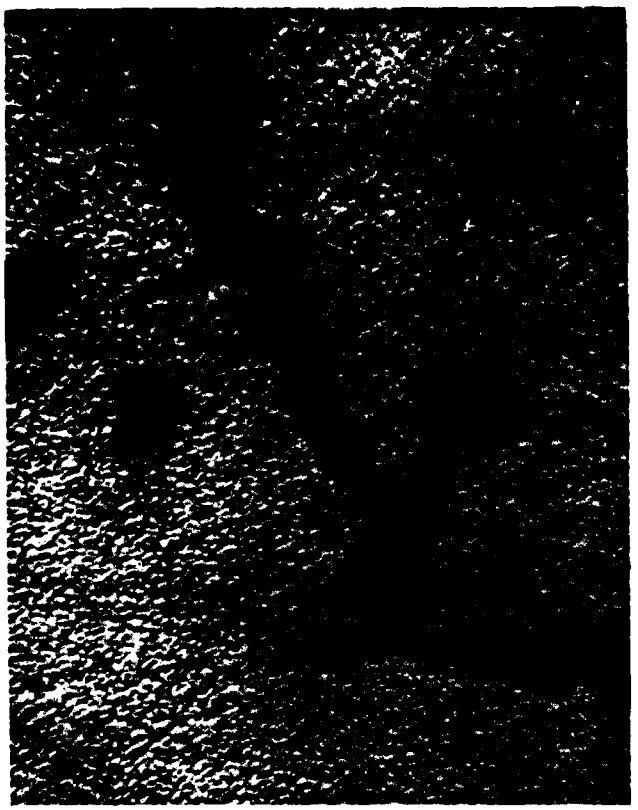

FIGURE 45. OPTICAL MICROGRAPH(2000X)
Fatigue crack propagating
through void

This is similar to the microcrack on the fracture surface shown previously in Fig. 38 since both cracks propagate through a void. Figure 46 is an example of secondary cracking branching off and running parallel to the main fatigue crack before rejoining it. Figure 47 shows under high magnification (1500X) a stepped portion of the same fatigue crack displayed in Fig. 44. The stepped nature of the crack suggests that the crack tip followed localized deformation bands during propagation similar to those on the fracture surface shown previously in Fig. 40.

FIGURE 46. OPTICAL MICROGRAPH(75X)
Secondary fatigue cracking

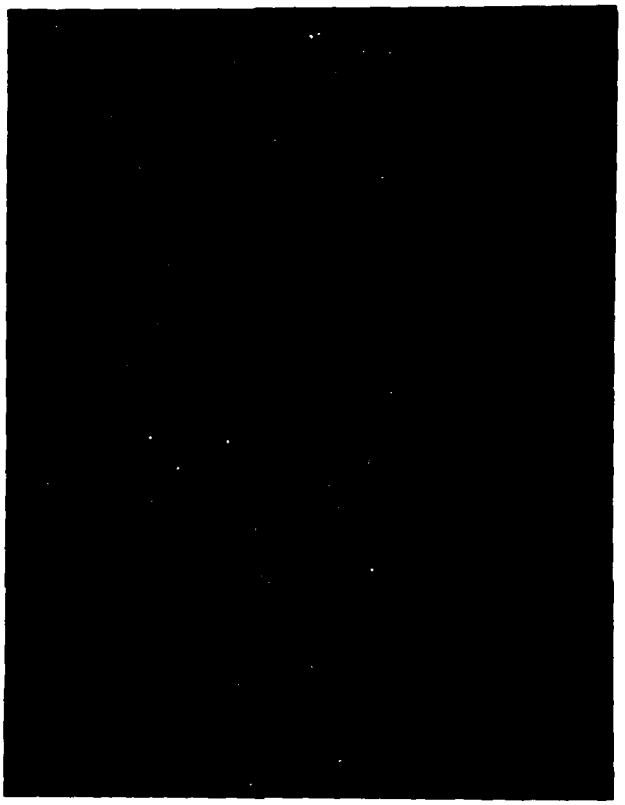

FIGURE 47. OPTICAL MICROGRAPH(1500X)
Fatigue crack propagating
in step-like path

CONCLUSIONS

Overall results indicate that significant features of fatigue damage (e.g. crack propagation) can be correlated with extractable characteristics of ultrasonic data (e.g. acoustic emission spectral signature and rms level). Further, ultrasonic attenuation and acoustic emission techniques can be used to reliably detect the presence of fatigue damage. Since there is some uncertainty in the degree of early warning obtainable with either method, combined monitoring increases the likelihood of successful early warning. However, no synergistic effects are apparent. Conventional body wave and surface wave ultrasonic methods have been shown to be inferior to ultrasonic attenuation and acoustic emission techniques for early detection of fatigue damage.

For attenuation measurements, the problem associated with complex geometries can successfully be overcome by interrogating the specimen using guided modes of propagation. Attenuation measurements can be made reliably even in the presence of high levels of background noise. Comparatively poor in noise immunity, acoustic emission measurements are useful even when propagation modes are unknown since the occurrence of microstructural changes can still be inferred from the data, provided the acoustic emission signals are larger than the background noise. Characterization of such changes awaits substantial improvements in data acquisition and reduction methodology. Data generated by both acoustic emission and ultrasonic

attenuation testing can be strongly influenced by the alloy composition, microstructure, degree of deformation, and prior thermal and mechanical history of the specimens. Specialized instrumentation can be used to significantly reduce the time and effort that would otherwise be needed to generate the large volume of data required for an exhaustive study of the methods of ultrasonic evaluation of fatigue damage. Optimization of an acoustic emission technique to permit reliable measurements in the presence of background noise is a prerequisite for fatigue test monitoring. Acoustic emission monitoring will not be optimally suited for in-service fatigue damage detection until much more work is done to elucidate the basic causes and physical characteristics of the emission directly attributable to structural defects.

REFERENCES

1. Green, Robert E., Jr., and Duke, John C., Jr.,"Ultrasonic and Acoustic Emission Detection of Fatigue Damage," International Advances in Nondestructive Testing 6, 125-177, Cordon and Break, New York (1979)

2. Green, Robert E., Jr., and Pond, Robert B., Sr., "An Ultrasonic Technique for Detection of the Onset of Fatigue Damage," Annual Report (1971-72), Air Force Office of Scientific Research AFOSR-TR-72-1199 (1972).

3. Green, Robert E., Jr., and Pond, Robert B., Sr., "An Ultrasonic Technique for Detection of the Onset of Fatigue Damage," Annual Report (1972-73) Air Force Office of Scientific Research AFOSR-TR-73-0901 (1973).

4. Green, Robert E., Jr., and Pond, Robert B., Sr., "An Ultrasonic Technique for Detection of the Onset of Fatigue Damage," Final Report (1971-76) Air Force Office of Scientific Research AFOSR-TR-76-0811 (1976).

5. Green, Robert E., Jr., and Pond, Robert B., Sr., "Ultrasonic Detection of Fatigue Damage in Aircraft Components," Annual Report (1976-77), Air Force Office of Scientific Research AFOSR-TR-77-0658 (1977).

6. Green, Robert E., Jr., and Pond, Robert B., Sr., "Ultrasonic and Acoustic Emission Detection of Fatigue Damage," Annual Report (1977-78), Air Force Office of Scientific Research AFOSR-TR-78-1284.

7. Buxbaum, S. R., Friant, C. L., Fick, S. E., Green, R. E., Jr., "Ultrasonic and Acoustic Emission Detection of Fatigue Damage," Annual Report (1978-79), Air Force Office of Scientific Research AFOSR-TR-79-1287.

8. Gerberich, W. W. and Hartbower, C. E., "Some Observations on Stress Wave Emission as a Measure of Crack Growth," International J. of Fract. Mech. 3, 185-192 (1967).

9. Hartbower, C. E., Gerberich, W. W., and Liebowitz, H., "Investigation of Crack-Growth Stress-Wave Relationships," J. of Eng. Fract. Mech. 1, 291-308 (1968).

10. Hartbower, C. E., Gerberich, W. W., and Crimmins, P. P., "Monitoring Subcritical Crack Growth by Detection of Elastic Stress Waves," The Welding Journal WEJUA 47, 1-18s, (1968).

11. Dunegan, H. L., Harris, D. O., and Tetelman, A. S., "Detection of Fatigue Crack Growth by Acoustic Emission Techniques," Proc. Seventh Symposium on Nondestructive Evaluation of Components and Materials in Aerospace Weapons Systems and Nuclear Applications, San Antonio, Texas (April 1969), 20-31, Materials Evaluation 28, 221-227 (1970)

12. Harris, D. O., Dunegan, H. L., Tetelman, A. S., "Prediction of Fatigue Lifetime by Combined Fracture Mechanics and Acoustic Emission Techniques," Lawrence Radiation Laboratory Report, UCRL 71760,(October 1969).

13. Harris, D. O., Dunegan, H. L.,"Verification of Structural Integrity of Pressure Vessels by Acoustic Emission and Periodic Proof Testing," Dunegan Research Corporation, Livermore, California, Technical Report DRC-71-2 (May 1971).

14. Moore, J. F., Tsand, S., and Martin, G., "The Early Detection of Fatigue Damage," Technical Report AFML-TR-71-185, AD 730 348 (1971).

15. Kusenberger, F. N., Lankford, J., Jr., Francis, P. H., Barton, J. R., "Nondestructive Evaluation of Metal Fatigue," AFOSR-TR-72-1167 (1972).

16. Egle, D. M., Mitchell, J. R., Bergey, K. H., and Appl, F. J., "Acoustic Emission for Monitoring Fatigue Crack Growth," Instrument Soc. Amer. Trans. 12, 368-374 (1973).

17. Egle, D. M., "Detecting High Cycle Fatigue Crack Growth Using Acoustic Emission," Presented at the Fracture and Flaws Symposium, Albuquerque, New Mexico, (March 1973).

18. Mitchell, J. R., Egle, D. M., and Appl, F. J., "Detecting Fatigue Cracks with Acoustic Emission," Proc. Okla. Acad. Sci. 53, 121-126 (1973).

19. Harris, D. O., Dunegan, H. L., "Continuous Monitoring of Fatigue Crack Growth by Acoustic Emission Techniques," Dunegan-Endevco Technical Report DE-73-2 (Feb. 1973), Exp. Mech. 14, 71-81 (1974).

20. Morton, T. M., Harrington, R. M., and Bjeletich, J. G., "Acoustic Emissions of Fatigue Crack Growth," Eng. Fract. Mech. 5, 691-697 (1973).

21. Bailey, C. D., Pless, W. M., "Acoustic Emissions Used to Nondestructively Determine Crack Locations in Aircraft Structural Fatigue Specimen," Proc. Ninth Symposium on NDE, San Antonio, Texas (April 1973), 224-232.

22. Vary, A., and Klima, S. J., "A Potential Means of Using Acoustic Emission for Crack Detection under Cyclic-Load Conditions," Proc. Ninth Symposium on NDE, San Antonio, Texas (April 1973), 258-266.

23. Pless, W. M., and Bailey, C. D., "Detection of Large Crack Extensions in Aircraft Wing Structure by Acoustic Peak Detectors," Proc. Tenth Symposium on NDE, San Antonio, Texas, (April 1975), 30-43.

24. Hatano, H., "Acoustic Emission During High Cycle Fatigue Testing," J. Soc. of Materials Science Japan 24, 48-53 (1975).

25. Kishi, T., Obata, Y., Tanaka, H., Sakakibara, Y., Horiuchi, R., and Aoki, K., "Acoustic Emission Peak Under Cyclic Deformation," J. Japanese Inst. of Metals 40, 492-498 (1976).

26. Duke, John C., Jr., and Green, Robert E., Jr., "Simultaneous Monitoring of Acoustic Emission and Ultrasonic Attenuation During Fatigue of 7075 Aluminum," Talk presented at National Spring Meeting of ASNT, New Orleans (April 1977); International J. Fatigue 1, 125-132 (1979).

27. Duke, John C., Jr., "Nondestructive Investigation of the Mechanical Deformation of 7075 Aluminum," Ph.D. Dissertation, Department of Mechanics and Materials Science, The Johns Hopkins University, Baltimore, Maryland (1978).

28. Duke, John C., Jr., and Green, Robert E., Jr., "Capability of Determining Fatigue Mechanisms in 7075 Aluminum by Combining Ultrasonic Attenuation and Acoustic Emission Monitoring," Proceedings of ARPA/AFML Review of Progress in Quantitative NDE Meeting, La Jolla, California (July 1978), AFML-TR,78-205 (January 1979).

29. Green, Robert E., Jr., "Non-Destructive Methods for the Early Detection of Fatigue Damage in Aircraft Components," Proceedings of AGARD/NATO Lecture Series No. 103 Non-Destructive Inspection Methods for Propulsion Systems and Components, London, England and Milan, Italy, (April 1979), AGARD-LS-103, Paper No. 6 (1979).

30. Hutton, P. H., "Acoustic Emission - A New Tool for Evaluating Structural Soundness," Proc. Seventh Symposium on Nondestructive Evaluation of Components and Materials in Aerospace Weapons Systems and Nuclear Applications, San Antonio, Texas (April 1969), pp. 165-171.

31. Fick, Steven E., and Green, Robert E., Jr., "Specialized Instrumentation and Procedures for Improved Acoustic Emission and Ultrasonic Attenuation Monitoring of Fatigue Damage," Talk presented at National Spring Meeting of ASNT, Philadelphia (April 1980).

32. Friant, C. L., Buxbaum, S. R., Fick, S. E., and Green, R. E., Jr., "Fatigue Damage Evaluation by Combination of Acoustic Emission, Ultrasonic and Eddy Current Monitoring," Talk presented at National Spring Meeting of ASNT, Philadelphia (April 1980).

33. Buxbaum, S. R., Friant, C. L., Fick, S.E., Green, R. E., Jr., "Acquisition and Reduction of Acoustic Emission Data from Fatigue Tests," Talk presented at National Spring Meeting of ASNT, Philadelphia (April 1980).

34. Truell, R., and Hikata, A., "Fatigue in 2S Aluminum as Observed by Ultrasonic Attenuation Methods," Watertown Arsenal Technical Report No. WAL 143/14-47 (1956).

35. Truell, R., and Hikata, A., "Fatigue and Ultrasonic Attenuation," American Society for Testing and Materials, Special Technical Publication No. 213 (1957).

36. Truell, R., Chick, B., Picker, A., Anderson, G., "The Use of Ultrasonic Methods to Determine Fatigue Effects in Metals," WADC Technical Report 59-389 (1959).

37. Truell, R., Chick, B., Anderson, G., Elbaum, C., and Findley, W., "Ultrasonic Methods for the Study of Stress Cycling Effects in Metals," WADD Technical Report 60-920 (1961).

38. Chick,B., Hikata, A., Anderson, G., Findley, W., Elbaum, C., and Truell, R., "Ultrasonic Methods in the Study of Fatigue and Deformation in Single Crystals," WPAFB Report No. ASD-TDR-62-186 Pt. II, AD No. 408704 (1963).

39. Ponomarev, P. V., "Ultrasonic Control of Fatigue Damage to Materials," Zavodskaya Laboratoriya 28, 1345-1346, (1962), English Translation in Ind.Lab. 28, 1429-1431 (1963).

40. Pawlowski, Z., "Internal Friction of Metals and the Problem of Damage Cumulation with Static and Variable Loadings," Proc. of Vibration Problems (Warsaw) 4, 43-64 (1963).

41. Pawlowski, Z., "Ultrasonic Attenuation During Cyclic Straining," Proc. Fourth International Conference on Nondestructive Testing (1963), Butterworths, London (1964), 192-195.

42. Green, R. E., Jr., "Development of an Ultrasonic Attenuation In-Service Inspection Technique for Heavy-Walled Nuclear Reactor Pressure Vessels," Final Technical Report, Middle Atlantic Power Research Committee (1972).

43. Joshi, N. R., and Green, R. E., Jr., "Ultrasonic Detection of Fatigue Damage," Engr. Fract. Mech. 4, 577-583, (1972).

44. Green, R. E., Jr., "Ultrasonic Attenuation Detection of Fatigue Damage," Proc. Ultrasonic Internation 1973 Conference, London, England (March 1973), IPC Science and Technology Press Ltd., Guildford, England (1973) 187-193.

45. Panowicz, W. V., "Ultrasonic Detection of Fatigue Damage in Aluminum Specimens Containing Induced Latent Defects," Master's Thesis, Dept. of Mechanics and Materials Science, The Johns Hopkins University, Baltimore, Maryland (1975).

46. MacDonald, D.E., "Investigation of the State of Fatigue in Metals Using Ultrasonics," Proc. Ultrasonics International 1977 Conference, Brighton, England (June 1977), IPC Science and Technology Press Ltd., Guildford, England (1977), 346-363.

47. Joshi, N. R., "Precrack Damage and Crack Propagation Study with Ultrasonic Attenuation," Materials Evaluation 37, No. 10, 57-61 (September 1979).

48. Mignogna, Richard B., Duke, John C., Jr., and Green, Robert E., Jr., "Early Detection of Fatigue Cracks in Aircraft Aluminum Alloy Sheets," Materials Evaluation 38, No. 3, 37-42 (March 1980).

49. Bruchey, William J., "Optical Probing of Acoustic Emission During Deformation of Micro-Tensile Specimens," Ph.D. Dissertation, Department of Materials Science and Engineering, The Johns Hopkins University, Baltimore, Maryland (1980).

REPORTS, PUBLICATIONS, PAPERS DELIVERED

1. Duke, John C.,Jr., "Simultaneous Acoustic Emission and Ultrasonic Attenuation Monitoring of the Mechanical Deformation of Aluminum," Master's Essay, Department of Mechanics and Materials Science, The Johns Hopkins University, Baltimore, Maryland (1976).

2. Duke, John C.,Jr., and Green, Robert E.,Jr., "Simultaneous Acoustic Emission and Ultrasonic Attenuation Monitoring of the Mechanical Deformation of Aluminum," Talk presented and paper published in the Proceedings of the Second International Conference on Mechanical Behavior of Materials, Boston, Mass., pp.1646-1650 (August 1976).

3. Duke, John C.,Jr., "Acoustic Emission in 7075 Aluminum," Talk presented at Acoustic Emission Working Group Meeting, Williamsburg, Virginia (October 1976)

4. Kline, Ronald A., "The Acoustic Emission Behavior of Lead-Tin Alloy," Talk presented at Acoustic Emission Working Group Meeting, Williamsburg, Virginia (October 1976).

5. Green, Robert E.,Jr., and Pond, Robert B.,Sr., "Ultrasonic Detection of Fatigue Damage in Aircraft Components," Annual Report (1976-77), Air Force Office of Scientific Research AFOSR-TR-77-0658 (1977).

6. Green, Robert E.,Jr., "Acoustic Emission" A Critical Comparison Between Theory and Experiment," Talk presented and paper published in Proceedings of the Ultrasonic International 1977 Conference, Brighton, England, (June 1977) pp.235-244, IPC Science and Technology Press Ltd., Guildford, England (1977).

7. Mignogna, Richard B., Duke, John C.,Jr., and Green, Robert E.,Jr., "Early Detection of Fatigue Cracks in Aircraft Aluminum Alloy Sheets," Talk presented at National Fall Meeting of ASNT, Detroit (October 1977).

8. Duke, John C.,Jr., and Green, Robert E.,Jr., "Simultaneous Monitoring of Acoustic Emission and Ultrasonic Attenuation During Fatigue of 7075 Aluminum," Talk presented at National Spring Meeting of ASNT, New Orleans (April 1977).

9. Duke, John C.,Jr., "Nondestructive Investigation of the Mechanical Deformation of 7075 Aluminum," Ph.D. Dissertation, Department of Mechanics and Materials Science, The Johns Hopkins University, Baltimore, Maryland (1978).

10. Green, Robert E.,Jr. and Pond, Robert B.,Sr., "Ultrasonic and Acoustic Emission Detection of Fatigue Damage," Annual Report (1977-78), Air Force Office of Scientific Research AFOSR-TR-78-1284 (1978).

11. Duke, John C.,Jr., and Green, Robert E.,Jr., "Capability of Determining Fatigue Mechanisms in 7075 Aluminum by Combining Ultrasonic Attenuation and Acoustic Emission Monitoring," Paper presented and published in Proceedings of ARPA/AFML Review of Progress in Quantitative NDE Meeting, La Jolla, California (July 1978), AFML-TR-78-205 (January 1979).

12. Green, Robert E.,Jr., "Non-Destructive Methods for the Early Detection of Fatigue Damage in Aircraft Components," Lecture Series No. 103 Non-Destructive Inspection Methods for Propulsion Systems and Components, London, England and Milan, Italy (April 1979), AGARD-LS-103, Paper No. 6 (1979).

13. Green, Robert E.,Jr., and Duke, John C.,Jr., "Ultrasonic and Acoustic Emission Detection of Fatigue Damange," International Advances in Nondestructive Testing 6, pp.125-177, Gordon and Breach, New York (1979).

14. Buxbaum, S. R., Friant, C.L., Fick, S.E., and Green, Robert E.,Jr., "Ultrasonic and Acoustic Emission Detection of Fatigue Damage," Annual Report (1978-1979), Air Force Office of Scientific Research AFOSR-TR-79-1287 (1979).

15. Duke, John C.,Jr., and Green, Robert E.,Jr., "Simultaneous Monitoring of Acoustic Emission and Ultrasonic Attenuation During Fatigue of 7075 Aluminum," International J. Fatigue 1, pp.125-132 (1979).

16. Mignogna, Richard B., Duke, John C.,Jr., and Green, Robert E.,Jr., "Early Detection of Fatigue Cracks in Aircraft Aluminum Alloy Sheets," Materials Evaluation 38, No.3, pp.37-42 (March 1980).

17. Fick, Steven E. and Green, Robert E.,Jr., "Specialized Instrumentation and Procedures for Improved Acoustic Emission and Ultrasonic Attenuation Monitoring of Fatigue Damange," Talk presented at National Spring Meeting of ASNT, Philadelphia (April 1980).

18. Friant, C. L., Buxbaum, S.R., Fick, S.E., and Green, R. E., Jr., "Fatigue Damage Evaluation by Combination of Acoustic Emission, Ultrasonic and Eddy Current Monitoring," Talk presented at National Spring Meeting of ASNT, Philadelphia (April 1980).

19. Buxbaum, S. R., Friant, C. L., Fick, S.E., Green, R. E., Jr., "Acquisition and Reduction of Acoustic Emission Data from Fatigue Tests," Talk presented at National Spring Meeting of ASNT, Philadelphia (April 1980).

PROFESSIONAL PERSONNEL

In addition to the Principal Investigators, Professor Robert E. Green, Jr., and Professor Robert B. Pond, Sr., the following persons have been engaged with various aspects of the research program during the past four years:

Dr. John C. Duke, Jr. (Postdoctoral Research Associate)

Dr. Steven E. Fick (Postdoctoral Research Associate)

Mr. Carl Lee Friant (Graduate Student)

Mr. Sanford R. Buxbaum (Graduate Student)

Mr. Richard B. Weisinger (Graduate Student)

Mr. Richard B. Mignogna (Graduate Student)